#12

ISSUE A

SPAR-R.664

(2)

TECHNOLOGY SURVEY

OF

ATTITUDE CONTROL TECHNIQUES

Indus
LI

P
91
C655
S723
1975

SPAR

P
91
C655
S723
1975

SPAR-R.664

SPAR LIBRARY
COPY NUMBER........3

ISSUE A

SPAR-R.664

TECHNOLOGY SURVEY OF ATTITUDE CONTROL TECHNIQUES

COMMUNICATIONS CANADA
JUIL JULY 1984
LIBRARY – BIBLIOTHÈQUE

Industry Canada
LIBRARY
JUIL JUL 2 0 1998
BIBLIOTHÈQUE
Industrie Canada

PREPARED BY J.A. Harrison
J.A. Harrison
Control System Dynamics
Consultant - Hughes Aircraft

PREPARED BY D.A. Staley
D.A. Staley
Group Leader, Control Systems

APPROVED BY

APPROVED BY Howard S Kerr
H.S. Kerr
Technical Director

REASON FOR REISSUE

DATE April, 1975

AMENDMENTS			
NUMBER	REASON FOR AMENDMENT	SIGNATURE	DATE

SPAR FORM 2249 A

SPAR aerospace products ltd.
825 Caledonia Rd.
Toronto, Ontario
Canada M6B 3X8

P
91
C655
S723
1975

DD4633847
DL4633866

In the course of this program and in the preparation of this report, extensive use has been made of SPAR Aerospace Products Limited's background data and material. In order to protect SPAR Aerospace Products Limited's commercial position, it is respectfully requested that the Government of Canada take this into consideration in dissemination of this report.

SUMMARY

This report, prepared under contract for the Department of Communications, presents a review of three axis attitude control systems. The dynamic features of "biased momentum" systems in a number of configurations is discussed at some length. Reaction wheel and zero momentum systems are also considered. A system trade matrix applicable to the Multi-Purpose BUS Satellite shows that development of magnetic bearing wheels and the Micro-Wave Attitude Sensing System could result in a highly competitive attitude control system.

SURVEY OF ATTITUDE CONTROL TECHNIQUES

TABLE OF CONTENTS

7/CGC/01

TABLE OF CONTENTS (Cont'd) Page

TABLE OF CONTENTS - (Cont'd) Page

7/CGC/02A

1.0 INTRODUCTION

Orbiting earth satellites, in fact all spacecraft, are usually thought of as being either "3 axis" controlled or "Spin Stabilized". Such a classification is somewhat confusing, however, since most current satellites of both classes are controlled in three degrees of rotational freedom. Whatever confusion exists is probably due to the evolution of spacecraft in the last 15-20 years. The first artificial earth satellite, Sputnik 1, was launched in 1957 and had no attitude control system at all. The satellite body was spherical with whip antennas emanating all over the surface. The vehicle tumbled randomly without a preferred axis of rotation.

The first American satellite, Explorer 1, was designed to maintain one axis of the satellite fixed in inertial space. It was recognized that various external torques act in space and to resist these torques the satellite was to be spun about one axis. This would introduce "gyroscopic torques" about the two transverse axes which would tend to maintain the spin axis fixed in inertial space. This technique, which became known as "spin stablization" had been used for years in more earthbound applications such as the spinning bullet and spiraling football. We might more properly refer to this as "2 axis" control since restoring torques are applied to two vehicle axes. At the time of the Explorer 1 design phase, indeed even at the time of launch, the nature of spinning body motion was not completely understood and the Explorer 1 configuration proved to be an unstable one. This will be fully explained shortly, the intent here being to illustrate the control that was desired.

In the years following the time of Explorer 1, payloads were developed that required "3 axis" control, i.e., the ability to control attitude about three distinct vehicle axes. The Surveyor moon lander is an early example, using reaction

7/CGC/03

jets to impose control torques about any spacecraft axis. For longer life earth satellites, efforts were made to reduce the amount of attitude control fuel required by using other sources of external control torques. So called "gravity gradient" control was widely used in the 1960s to provide 2 axis (pitch-roll) control with gas jets to control yaw (motion about the satellite - earth line). The use of the gravity gradient was effective for pointing requirements on the order of a few degrees but as required accuracies became tighter this form of control ceased to be viable.

* The techniques of "spin stabilization", first introduced with Explorer 1, were then revived in the form of adding a spinning wheel to the main satellite body. The angular momentum stored in the wheel would render the axes transverse to the wheel axis "stiff" in response to external disturbances while satellite motion about the wheel axis could be controlled by changing the wheel speed, the combined effect being 3 axis control. External disturbance torques having secular components in inertial space will cause a secular change in the satellite's angular momentum magnitude and direction and therefore at periodic intervals an external control torque (e.g. magnetic or gas jets) must be employed to correct for this. It is the frequency of correction that characterizes two very important classes of satellite stabilization schemes. We will refer to these using the terms "medium momentum" and "high momentum".

For medium momentum systems (commonly referred to as "Momentum Bias"), the wheel is small enough to be housed inside the main spacecraft body and is light enough so that it seldom needs to serve auxilliary functions to be weight effective. Typically the wheel will weigh considerably less than 100 lbs. (probably more like 20 lbs) with a momentum of less than 100 ft.lb.sec (probably on the order of 20 ft.lb.sec). The momentum correction interval might be minutes or hours, most likely requiring an autonomous system to do so.

The second class of systems containing a spinning wheel, those with high momentum, have a wheel that is very large compared to what was previously called the satellite main body. In such vehicles, referred to as "Dual-Spin" satellites, the wheel, now called a "rotor" is so large that it dominates the size and weight of the total vehicle.

To be weight effective most of the control fuel, electronics, solar cells, and apogee motor are mounted on the rotor whereas the other body, the "platform", often merely consists of the pointed payload. Dual-Spin satellites are characterized by angular momentum levels on the order of 1000's of ft.lb.sec and momentum correction intervals on the order of days or weeks. For such long intervals this is usually done by ground command.

Two final classes of attitude control systems are the zero and low momentum systems. In both of these no reliance is made on gyroscopic torques for control. The former technique uses thrusters, e.g. gas jets to apply control torques on three distinct vehicle axes. In the latter the torques are a result of accelerating small reaction wheels, their gyroscopic influence being negligible.

This study will only consider zero, low and medium momentum systems, the high momentum designs being excluded. In these introductory remarks an attempt has been made to show that the medium and high momentum designs have much in common from a theoretical point of view, the differences being in size and weight of the components. In particular it has been shown that all of these systems are really 3 axis controlled although the period of correction on certain axes may be much longer for some systems than for others. In the following section we examine some characteristics of the attitude motion of spinning bodies or bodies with a single fixed wheel. This is necessary in order to establish definitions of terms which will pervade future discussions.

7/CGC/05

2.0 MOTION OF SPINNING BODIES AND BODIES CONTAINING A SINGLE FIXED WHEEL

2.1 Nutation, Precession and Wobble

2.1.1 Nutation

Figure 2.1.1-1 illustrates the types of medium and high momentum systems that have been discussed.

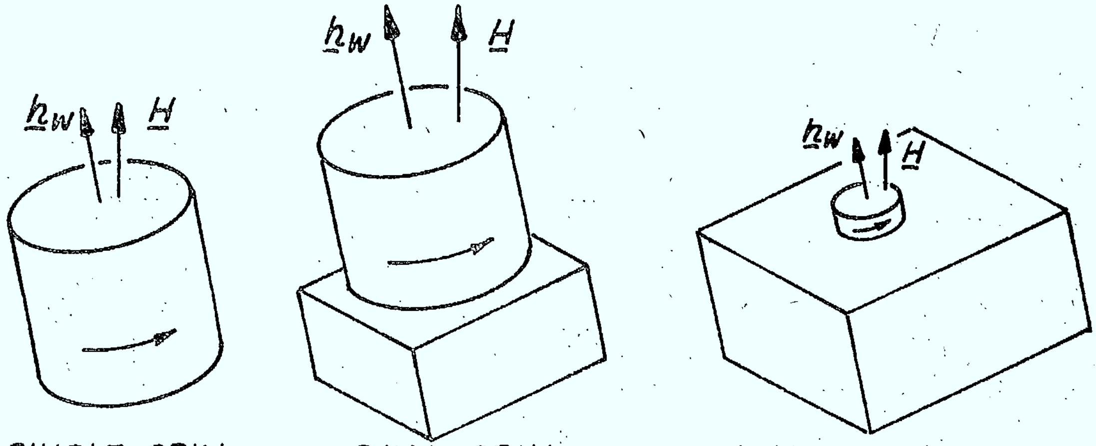

FIGURE 2.1.1-1 - CLASSES OF MEDIUM AND HIGH MOMENTUM SYSTEMS

In the Dual-Spin and Momentum Bias systems the wheel's momentum, $\underline{h}_W$, comprises nearly all of the total vehicle's momentum, $\underline{H}$, since the other body is assumed to rotate very slowly in space. Let us first consider the case in which no external torques act on the systems. Then, by conservation of angular momentum, $\underline{H}$ is fixed in inertial space. Let us also assume for the moment that the wheel is balanced, i.e., that its spin axis is a principal axis for its center of mass. The desired motion of most satellites is one in which $\underline{h}_W$ and H are parallel. This will occur only if there are no rates on "transverse" axes, i.e., axes normal to the spin axis. In general there are such rates, due to initial conditions and external torques, and these will cause $\underline{h}_W$ to cone around $\underline{H}$ as shown in Figure 2.1.1-2.

7/CGC/06 *

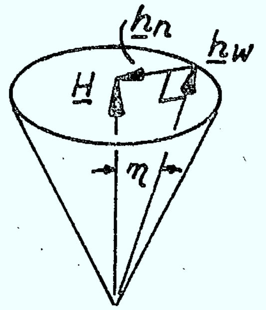

FIGURE 2.1.1-2 - NUTATIONAL MOTION

This motion is commonly referred to as "nutation". The "nutation angle" η is the cone half angle. If $\underline{h}_n$ is the angular momentum caused by the transverse rate, then

$$\underline{H} = \underline{h}_w + \underline{h}_n$$

and the nutation angle is given by

$$\eta = \tan^{-1} \frac{|\underline{h}_n|}{|\underline{H}|} \text{ radians}$$

The frequency with which $\underline{h}_w$ cones around $\underline{H}$ is called the "nutation frequency", ω. If the system is nutationally stable, a concept to be discussed shortly, $\underline{h}_w$ will cone around $\underline{H}$ at constant frequency but decreasing angle, until $\underline{h}_w$ and $\underline{H}$ are coincident. If unstable, the coning motion will grow.

The nutation frequency is an important parameter for both Momentum Bias and Dual-Spin systems. An appendage attached to the main body will be excited at this frequency. To avoid structural interaction problems the natural frequencies of such an appendage should be far removed from the nutation frequency. As will be discussed shortly, a passive damper can be mounted on the main body to damp nutation and for optimum performance it should be tuned to the nutation frequency. As will be discussed in Section 4.3, certain Momentum Bias systems will limit cycle, resulting in thruster activity that is proportional to the nutation frequency.

To develop an expression for the nutation frequency consider the system shown in Figure 2.1.1-3. This can represent any of those considered earlier by

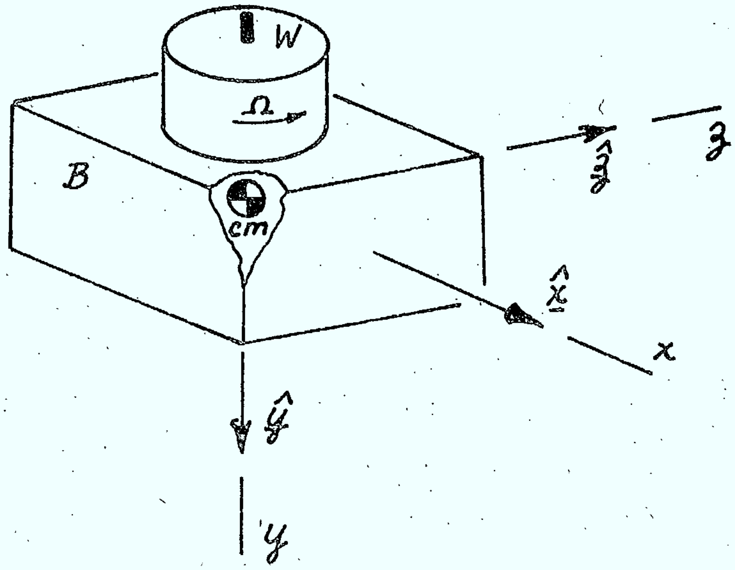

FIGURE 2.1.1-3 - GENERIC SPINNING WHEEL SYSTEM

changing the mass and inertia of the two bodies and the wheel speed Ω. Write the total inertial angular momentum of the system for its center of mass (cm):

$$\underline{H} = I_x\omega_x\,\hat{\underline{x}} + (I_y\omega_y - J\Omega)\,\hat{\underline{y}} + I_z\omega_z\,\hat{\underline{z}}$$

where J is the wheel moment of inertia, the I's are the total system principal moments of inertia for the cm, the ω's are the inertial angular velocity components of B for the x,y,z axes, Ω is the constant relative wheel speed, and $\hat{\underline{x}},\hat{\underline{y}},\hat{\underline{z}}$ are unit vectors parallel to the respective x,y,z axes. Differentiating $\underline{H}$ in inertial space, dropping second order terms in the ω's and equating this to the external torque, gives a form of Euler's equations for this system:

$$I_x\dot{\omega}_x + J\Omega\omega_z = T_x$$

$$I_y\dot{\omega}_y = T_y$$

$$I_z\dot{\omega}_z - J\Omega\omega_x = T_z$$

where the T's are the x,y,z components of the external torque.

These equations apply for small main body rates which is usually the case of interest. The first and third equations define the nutational motion. These can be differentiated and written as

$$\ddot{\omega}_x + \frac{(J\Omega)^2}{I_x I_z}\omega_x = 0$$

$$\ddot{\omega}_z + \frac{(J\Omega)^2}{I_x I_z}\omega_z = 0$$

and are in the form of an oscillator whose frequency (nutation frequency) is

$$\omega = \frac{J\Omega}{\sqrt{I_x I_z}}$$

Note that the nutation frequency is proportional to the wheel angular momentum, $J\Omega$. Also note that for a synmmetric spacecraft ($I_x = I_z = I$), the nutation frequency is greater than the spin speed for "oblate" systems (spin inertia greater than transverse inertia) and less than the spin speed for "prolate" systems (spin inertia less than transverse inertia).

2.1.2 Nutational Stability

Prior to the launch of Explorer 1 it was felt that a single spinning rigid, or almost rigid, body is stable about either the maximum or minimum moment of inertia axis. The instability of Explorer 1, designed to spin about its minimum axis, led to a more thorough understanding of spinning body motion. In particular it became apparent that the only stable motion of a spinning body with internal energy dissipation, i.e., a physical body, is about its axis of maximum inertia. The following heuristic analysis demonstrates this. Consider that a body is spinning about one of its principal axes, of moment of inertia I, with a rate Ω. It then possesses an angular momentum with a magnitude

$$H = I\Omega$$

and a kinetic energy of

$$K.E. = \frac{1}{2} I\Omega^2$$

Substitution of the first relation into the second gives

$$K.E. = \frac{1}{2} \frac{H^2}{I}$$

Now in the presence of no external torques H is constant and this last equation shows that the lowest energy state occurs for spin about the largest inertia axis. Assuming that internal energy dissipation can change the kinetic energy into heat energy and that the system will seek its lowest energy state, the only stable motion is spin about the maximum axis of inertia. This result has become to be known as the "maximum axis" rule. If one designs an effective dissipator for an oblate spinning body, for example using a spring-mass-dashpot tuned to nutation frequency, then the device is called a nutation damper. This can be passive, as in the example given, or active using sensors and thrusters or reaction devices.

It should be emphasized that an unstable system may be a very satisfactory design for time periods which are short in comparison to the divergence rate of the unstable motion. The previously mentioned spinning bullet and football are examples of unstable (minimum axis spin) designs which perform successfully for short time periods. In satellite applications the spinning apogee boost of a prolate spacecraft can be successful if the nutation grows slowly. The key to such a design is estimating the energy dissipation rate and ensuring that it is low enough to satisfy the mission requirements. This is often a very difficult task since the predominant dissipation mechanism is often difficult to analyze or test, such as fluid in tanks or pipes.

7/CGC/10

The stability analysis of Dual-Spin or Momentum Bias systems is greatly complicated due to the presence of two bodies. The complicating factors are the effects of the wheel motor, bearing friction, and the necessity for considering dissipation on both bodies. The latter introduces time varying coefficients in the equations of motion. A complete discussion of this subject is beyond the scope of this report and we will summarize the facts, specialized to the case of a non-rotating or slowly rotating main body:

- Energy dissipation on the main body is always stabilizing.

- Energy dissipation on the wheel is stabilizing if the wheel spin moment of inertia is greater than the entire satellite transverse moment of inertia for its cm, otherwise it is destabilizing (this is the maximum axis rule for wheel systems).

- From the previous two points it is apparent that one can design a stable satellite whose wheel spin inertia is less than the vehicle transverse inertia by installing a suitably effective passive nutation damper on the main body. The difficulty here though is the estimation of the (destabilizing) dissipation on the wheel, especially when this occurs as fuel slosh.

- If the wheel axis is not a principal axis of the main body the wheel speed control system may cause nutational instability even if the above criteria are satisfied. This phenomenon is analyzable and can easily be avoided.

Some high momentum (Dual-Spin) satellites are designed with a "stable" inertia ratio so as to eliminate possible nutational instability, e.g., the Orbiting Solar Observatory (OSO) series. For

7/CGC/11

systems with an "unstable inertia ratio", i.e., long and slender, careful estimation of the rotor dissipation is required. Such satellites are examples of the Hughes "Gyrostat" design and are represented by the TACSAT and INTELSAT IV series. It should be pointed out that Momentum Bias systems usually fall into the "unstable inertia ratio" class since the wheel spin inertia is much less than the satellite transverse inertia. For the systems proposed to date (<100 ft.lb.sec) this has not been a matter of great concern, although it is not completely clear that it shouldn't be. For these systems the presumption is usually made that the wheel is so small that very little destabilizing influence can result. However, for large Momentum Bias satellites (small dual-spinners) one may have to carefully analyze the energy dissipation properties of the wheel and bearings.

2.1.3 Precession

It is a widespread convention in the aerospace industry to use the term precession to describe the motion of the system angular momentum vector in response to an external torque. In classical mechanics treatises precession is used to denote the coning of the spin axis around the angular momentum vector, i.e., what we have called nutation. This is a perfectly acceptable terminology except that they had no term to describe the motion due to external torques.

When an external torque $\underline{T}$ acts on a system whose inertial angular momentum for its cm is $\underline{H}$ then the angular momentum principle, which is derivable from Newton's Second Law, gives the result

$$\frac{{}^N d}{dt} \underline{H} = \underline{T}$$

where ${}^N d/dt$ denotes time differentiation in an inertial (Newtonian) reference frame N. Integrating this expression gives the change in angular momentum, $\Delta \underline{H}$, due to the torque acting for Δt seconds:

$$\Delta H = \int_t^{t+\Delta t} \underline{T}\, d\tau$$

7/CGC/12

For example in Figure 2.1.3-1 if the system at time t has an angular momentum $\underline{H}(t)$ and it is acted upon for Δt seconds by an inertially fixed torque $\underline{T}$ then at $t+\Delta t$ the system has an angular momentum $\underline{H}(t+\Delta t)$ given by

$$\underline{H}\ (t + \Delta t) = \underline{H}(t) + \Delta \underline{H}$$

where

$$\Delta \underline{H} = \underline{T}\ \Delta t$$

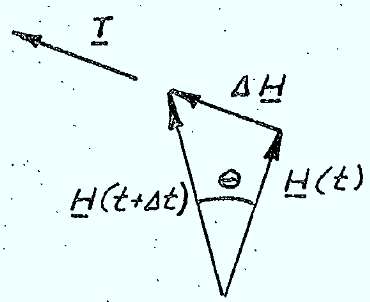

FIGURE 2.1.3-1 - PRECESSION

Note that the torque component parallel to $\underline{H}(t)$ tends to increase the momentum magnitude, i.e., spin up the wheel. The torque component normal to $\underline{H}(t)$ tends to precess the momentum vector through the angle θ. Therefore for small angles the precession angle θ is given by

$$\theta = \frac{T\,\Delta t}{H} \text{ radians}$$

where T is the torque component normal to $\underline{H}$ and $H = |\underline{H}|$.

7/CGC/13

2.1.4 Nutation and Precession Simultaneously

Usually we are interested in the motion of a body fixed wheel axis, not just the system angular momentum vector $\underline{H}$. The external torque $\underline{T}$, along with precessing $\overline{H}$, introduces nutation about $\underline{H}$ and to define the body motion we must determine the combined effects of nutation and precession. Consider a system with symmetric transverse inertias $I_x = I_z = I$ with a wheel of momentum $h_w = J\Omega$ on the y axis. Figure 2.1.4-1 shows three such systems acted upon by an inertially fixed torque $\underline{T}$ in the nominal x direction. In A the wheel has zero momentum, in B it has low momentum, and in C a much larger momentum. We will now consider wheel axis motion due to the torque. In A the torque simply rotates

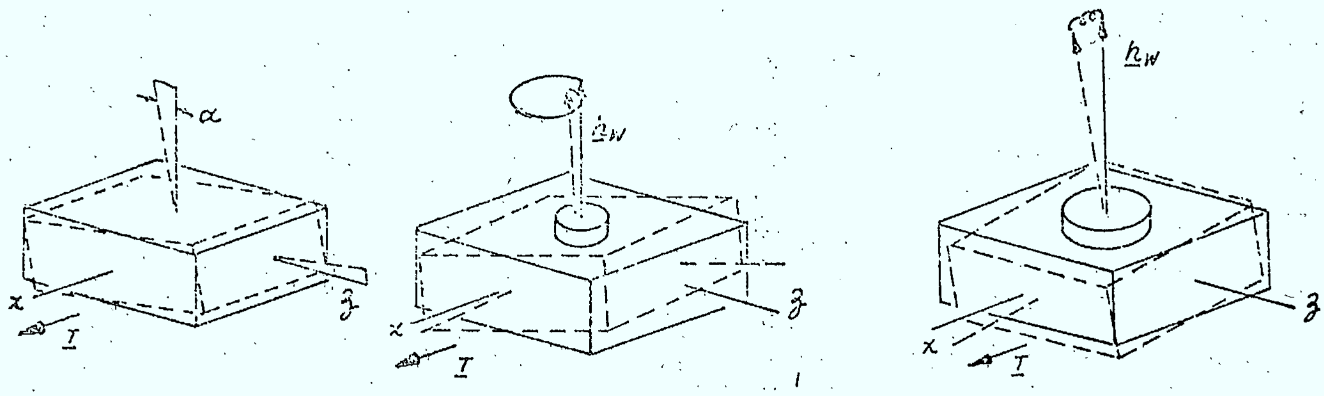

A — Zero Momentum B — Low Momentum C — High Momentum

FIGURE 2.1.4-1 - NUTATION AND PRECESSION MOTION

the body about the x axis an amount α, where

$$\ddot{\alpha} = \frac{T}{I} \qquad 2.1.4\text{-}1$$

or

$$\alpha = \frac{1}{2}\,\frac{T}{I}\,t^2 \qquad 2.1.4\text{-}2$$

for zero initial conditions. This motion could be considered as a pure nutation (with a 90 degree nutation angle). In B the wheel axis nutates with a smaller angle and precesses in the direction of $\underline{T}$. In C the nutation is quite small, the dominant effect being precession.

A quantitative determination of the precession and nutation angles caused by such a torque can be made using the Euler Equations derived in Section 2.1.1 with $I_x = I_z = I$, $h_w = J\Omega$

and $T_y = T_z = 0$, $T = T_x$:

$$\dot{\omega}_x + \frac{h_w}{I}\omega_z = T \qquad 2.1.4\text{-}3$$

$$\dot{\omega}_z - \frac{h_w}{I}\omega_x = 0 \qquad 2.1.4\text{-}4$$

Solving these for initial conditions $\omega_x(0) = \omega_z(0) = 0$ gives

$$\omega_x = \frac{T}{h_w} \sin \omega t \qquad 2.1.4\text{-}5$$

$$\omega_z = \frac{T}{h_w} (1-\cos\omega t) \qquad 2.1.4\text{-}6$$

where

$$\omega = \frac{h_w}{I} = \text{nutation frequency}$$

The transverse rate $\frac{T}{h_w}$ introduces a transverse momentum component $\frac{TI}{h_w}$ which represents nutation. The nutation angle is therefore

$$\eta \approx \frac{TI}{h_w^2} \qquad 2.1.4\text{-}7$$

(See Figure 2.1.4-2)

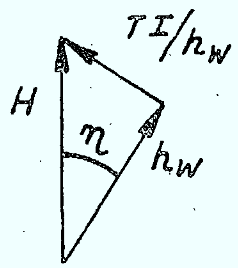

FIGURE 2.1.4-2 - TRANSVERSE MOMENTUM AND NUTATION ANGLE

The torque precesses the angular momentum vector an amount ΔH where

$$\Delta H = T\Delta t \qquad 2.1.4\text{-}8$$

The precession angle θ is therefore

$$\theta \approx \frac{\Delta H}{H} \qquad 2.1.4\text{-}9$$

(See Figure 2.1.4-3)

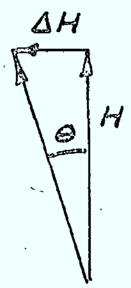

FIGURE 2.1.4-3 - PRECESSION

7/CGC/16

The precession rate is calculated as follows:

$$\dot{\theta} \approx \frac{\Delta\theta}{\Delta t} = \frac{\Delta H/H}{\Delta t} = \frac{T\,\Delta t}{H\,\Delta t} = \frac{T}{H} \qquad 2.1.4\text{-}10$$

This rate can be identified as the secular component of ω_z in Equation 2.1.4-6 since $H \approx h_w$. The precession angle is therefore

$$\theta \approx \frac{Tt}{h_w} \qquad 2.1.4\text{-}11$$

2.1.5 Wobble

Wobble is the term commonly used to describe the satellite motion resulting from an unbalanced spinning section. Figure 2.1.5-1 illustrates the general case with a statically and dynamically unbalanced wheel.

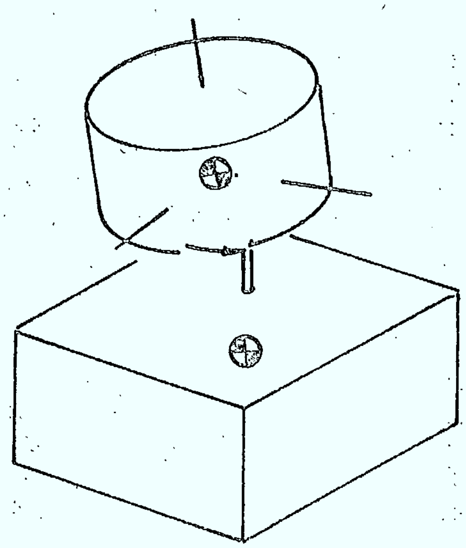

FIGURE 2.1.5-1 - SATELLITE WITH UNBALANCED WHEEL

The cm of the wheel is offset from the spin axis causing a static unbalance. Also, no principal axis of the wheel for its cm is parallel to the spin axis - this causes a dynamic unbalance.

For low and medium momentum systems unbalance is seldom important since the wheel is small and rigid. For large spinners or Dual-Spin satellites such is not the case. The spinning body is so large that it is difficult to accurately balance. Furthermore the presence of fuel and movable elements on the rotor alter the balance during the mission. Although high momentum systems will not be considered in detail in this study we include a brief discussion of wobble for completeness.

Consider first the case of the single spinning body (see Figure 2.1.5-2). The wobble motion

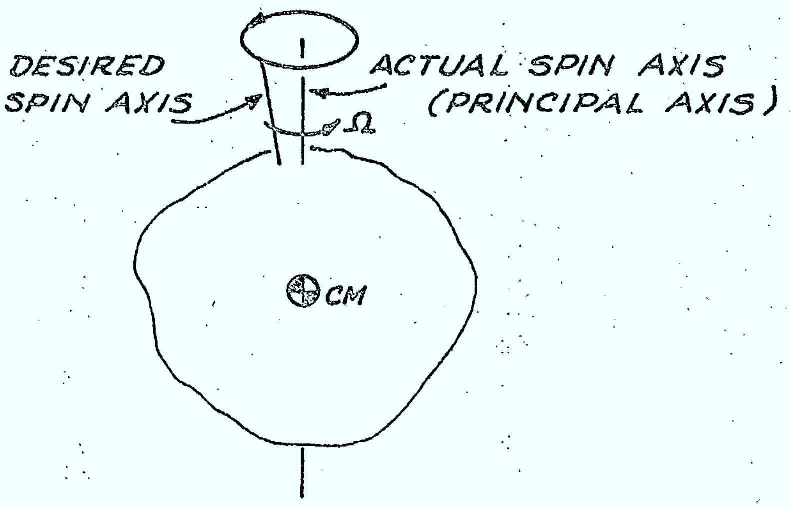

FIGURE 2.1.5-2 - WOBBLING OF A SINGLE SPINNING BODY

is spin about one of the principal axes for the cm, this axis being fixed in inertial space. As discussed earlier the only stable such motion is

7/CGC/18

about the axis of greatest inertia. Generally, one body fixed axis is a desired spin axis and if this is not parallel to the actual spin axis (principal axis) the former will cone around the latter at constant amplitude.

Now let us consider the wobble motion of a body with a single fixed unbalanced wheel, i.e., the system shown in Figure 2.1.5-1. This is a complicated problem in general and we will consider only the case of a symmetric, non-spinning main body. For this case the wobble motion is very similar to that of a single spinning body. The wheel spins about an axis fixed in it and in inertial space (see Figure 2.1.5-3). This axis is

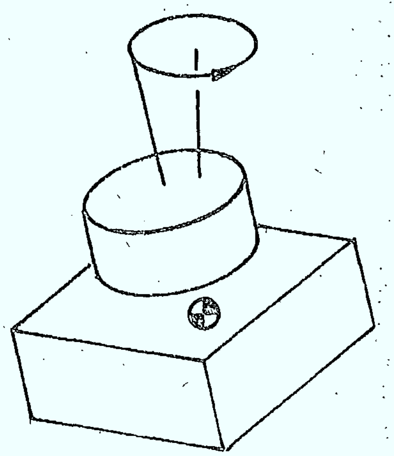

FIGURE 2.1.5-3 - WOBBLING OF A BODY WITH A SINGLE FIXED WHEEL

the centroidal principal axis of the entire system except that the moment of inertia of the main body about the wheel axis is neglected.

7/CGC/19

In general the motion is a combination of nutation, precession, and wobble, although in many practical cases at least one of the contributions will be negligible. The separate motions can be identified by their characteristic frequencies. For example, nutation occurs at nutation frequency and wobble at spin frequency. Precession occurs at the frequency of the external torque, usually either zero or a multiple of orbit rate.

3.0 COMPENSATION OF EXTERNAL TORQUES

3.1 External Torques - Their Impact on Spacecraft Design

For satellites with payloads which are not actively slewed relative to the main body, external torques represent the prime disturbance which the attitude control system must overcome. Theoretically, from Newton's first law, once a desired attitude is achieved no control system at all is required to maintain this attitude if no external torques exist. Practically, some finite torques will always exist and minimizing these results in lower spacecraft weight for two reasons. First, when gas jet thrusters are used as either the prime control or for momentum dumping, the amount of on-board fuel required increases as the external torque increases. Therefore, from fuel weight considerations it is important to minimize the external torque. Assuming that the control system does not limit cycle, the yearly fuel usage is

$$W = \frac{4 \times 10^7}{I_{sp} l} T_D \quad \frac{lb}{yr}$$

for a fixed momentum wheel system and

$$W = \frac{3.14 \times 10^7}{I_{sp} l} T_D \quad \frac{lb}{yr}$$

for systems with momentum storage such as a double gimballed wheel or three reaction wheel system, where

I_{sp} = propellant specific impulse (sec)

l = thruster lever arm (ft)

T_D = disturbance torque (ft.lb)

For typical parameter values of Isp = 100 sec, l = 2 ft, and $T = 10^{-5}$ ft.lb, we obtain a yearly fuel usage of 2 lb and 1.57 lbs for the respective systems.

7/CGC/21

The second reason that spacecraft weight is reduced by minimizing external torques is related to the pointing accuracy that is required from the attitude control system. Before proceeding further it is necessary to define a rotating coordinate system X,Y,Z as shown in Figure 3.1-1.

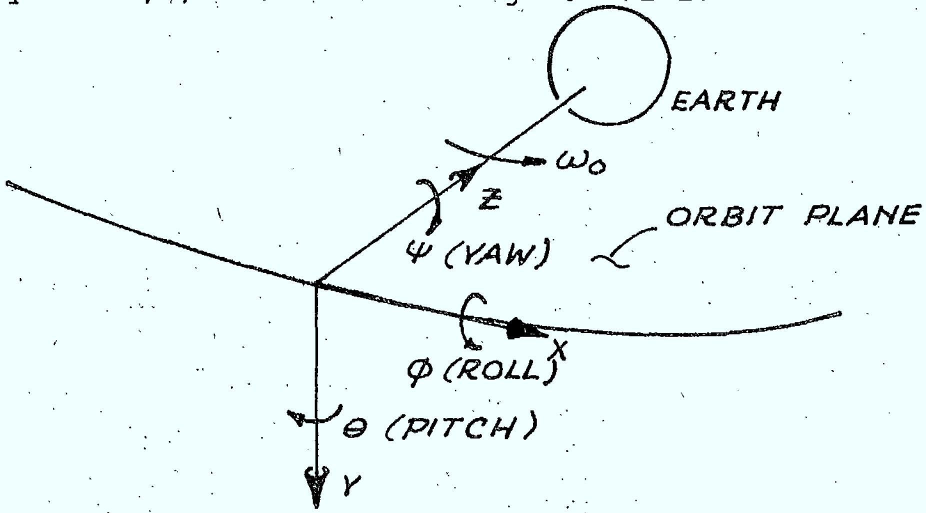

FIGURE 3.1-1 - ORBITING COORDINATE SYSTEM DEFINITION OF PITCH, ROLL, YAW

The Z axis points from the satellite to the center of the earth, X points in the direction of the satellite linear velocity, and Y is normal to the orbit plane. These axes rotate relative to inertial space at a rate ω_o and define the orbiting coordinate system. Satellite attitude is measured relative to this frame by the angles ϕ, θ, ψ (roll, pitch, yaw) about the respective axes X, Y, Z. Pitch and roll attitude is easily determined using horizon sensors whereas yaw measurement is more complicated. For most earth pointing missions the yaw pointing requirement is not as stringent as for pitch and roll. For missions which require accurate yaw measurement a gyro is often used. To compensate for drift, updates are usually made by a star tracker or sun sensor. It is clear that, especially when redundancy is desired, yaw sensing introduces considerable weight and complexity to the overall system and is therefore to be avoided if at all possible.

7/CGC/22 *

The most widely used alternative to direct yaw sensing is the technique of "gyrocompassing" which forms the basis for all of the momentum bias systems to be discussed. Gyrocompassing will be described in more detail in the next section but simply stated it relies on the fact that, since the momentum wheel tends to remain fixed in inertial space, yaw errors become roll errors as a result of the orbital motion. The error is then sensed by the roll horizon sensor and removed via the roll control system. Whereas pitch and roll torques produce errors which are quickly sensed and removed, a yaw torque can result in a significant error before it is detected and controlled using gyrocompassing. Therefore, even if the yaw pointing requirement is less than pitch and roll, a yaw torque is usually the most critical and is the factor that determines the amount of angular momentum required in the wheel. Reference 1 contains an approximate relationship for the peak yaw error resulting from a constant yaw torque T:

$$\psi \approx 57.3 \frac{T}{\omega_o h_w} \text{ degrees}$$

where T is in ft-lbs, ω_o is the orbital angular velocity ($\omega_o = 7.29 \times 10^{-5}$ rad/sec at synchronous altitude), and h_w is the wheel angular momentum in ft.lb.sec. To get a feeling for the magnitudes involved, a yaw bounded at 0.5 deg and an angular momentum of 10 ft.lb.sec requires a maximum yaw torque of 6.35×10^{-6} ft.lb.

The dominant external torque at synchronous altitude is due to solar pressure acting on the satellite. When the center of pressure (cp) of this force is not identical to the satellite center of mass (cm) a torque results. Every attempt is made to design a configuration in which the cp-cm offset is minimal but several factors contribute to increase this offset. The theoretical determination of the cp is a difficult task since shading must be determined, spacecraft thermal distortion accounted for, and assumptions made regarding the shear forces and reflective parameters. Furthermore,

7/CGC/23

even if the cp location were known precisely, the cm location is not. Even after assembly of the spacecraft an uncertainty in the cm location exists, and due to fuel usage and other effects it will not remain fixed while on orbit. If left uncompensated the resulting solar torque will cause a large number of control thruster firings and degrade the yaw pointing of a momentum bias satellite. We now discuss some techniques for compensating the solar torque.

3.2 Magnetic Compensation

The most commonly proposed technique of opposing the solar torque is the use of an electromagnet or a coil to produce a torque as a result of interaction with the earth's magnetic field. The device is often mounted on the sun tracking solar panels in an effort to produce an inertially fixed control torque. Ground estimation of the solar torque can be made after several orbits of data collection and an appropriate coil current can be commanded. The main disadvantage of magnetic torquing is due to the behavior of the earth's field at synchronous altitude. The field changes drastically and during periods of solar storms the field may actually reverse, rendering the magnetic torquer system unsatisfactory. This technique has not been used to date at synchronous altitude; however, its use has been recently proposed for a major communications satellite program.

3.3 Solar Pressure Trim Tab Compensation

An alternative method of solar torque compensation is to alter the location of either the cm or the cp by some mechanical means. For example a louver arrangement, mounted on the solar array, would alter the cp in the y direction (See Figure 3.3-1)

*

7/CGC/24

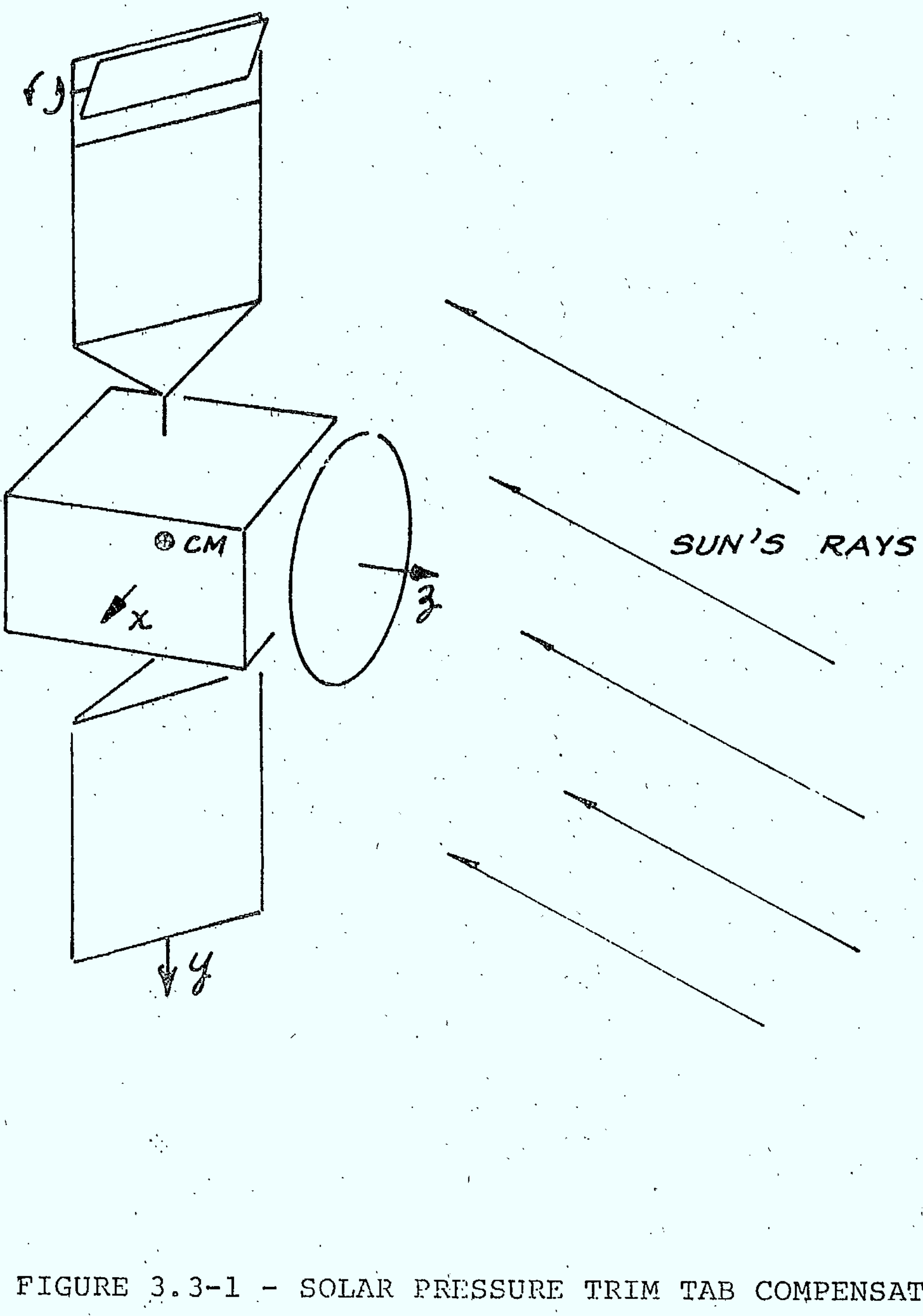

FIGURE 3.3-1 - SOLAR PRESSURE TRIM TAB COMPENSATOR

3.4 Mass Balance Compensation

An equivalent result could be obtained by moving the cm location in the y direction. A small weight commanded to move on a track would accomplish this (See Figure 3.4-1). To be weight effective the length of the track should be as long as possible with as much of the mechanism weight as possible in the moveable part.

*

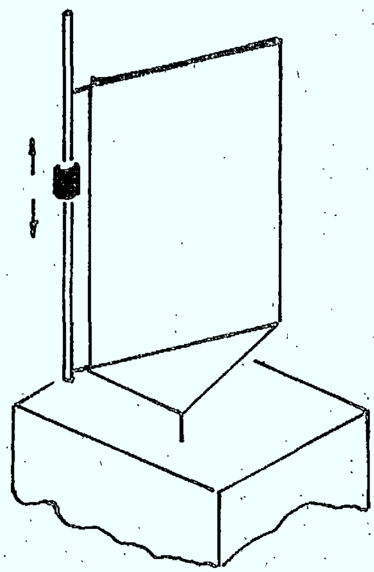

FIGURE 3.4-1 - MASS BALANCE COMPENSATOR

Both of these systems permit elimination of the cp-cm offset in the y direction which greatly minimizes the roll and yaw torque. By careful propellant management of the fuel in tanks located in the x-z plane one can, in principle, eliminate the offset completely. It should be pointed out that the cp will move somewhat on a daily basis and may change abruptly due to shadowing so it may be desirable to frequently control these mechanisms to counter the resulting torque.

On the other hand an acceptably low torque may be achievable by a very few number of corrections, possibly every month or so to account for seasonal (sun declination) variations. As far as is known the technique of altering the cp or cm has not been flown or even widely proposed. It appears that such a device may be attractive for long life, weight critical designs.

4.0 MOMENTUM BIAS OPTIONS

The heart of all of the systems to be discussed in this chapter is a single momentum wheel that nominally spins about an axis normal to the orbit plane as shown in Figure 4.0-1.

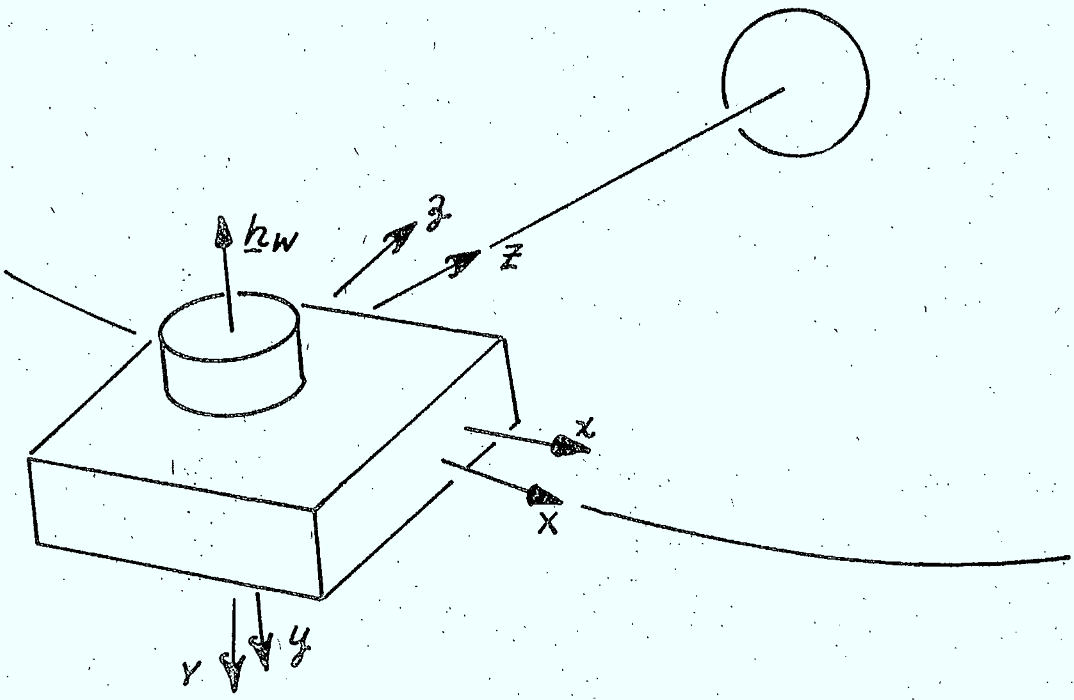

FIGURE 4.0-1 - MOMENTUM BIAS SYSTEM

The term "momentum wheel" will refer to a wheel whose momentum is sufficiently high to cause significant gyroscopic torques. "Reaction wheels" on the other hand are designed to provide a reaction torque on the satellite, the gyroscopic torques being an undesirable feature.

In Figure 4.0-1 the X, Y, Z axes define the orbiting coordinate system and x,y,z are spacecraft fixed axes nominally aligned with the orbiting axes. Roll, pitch, yaw (ϕ,θ,ψ) angles define the relative orientation of the two sets of axes. For small angles these represent rotations about the respective x,y,z axes. The wheel angular momentum $\underline{h}_W$ is nominally along the -y axis. In all systems to be discussed, pitch attitude is controlled by operating the momentum wheel in a "reaction wheel" mode, i.e., accelerating the wheel in one direction causing the body to rotate in the opposite direction. A secular torque on the pitch axis will cause the wheel speed to eventually increase or decrease to an unacceptably high or low level. The wheel must therefore be torqued back to nominal speed at periodic intervals while applying an external torque to control the body. This operation, called "momentum dumping", is usually accomplished using gas jet thrusters or magnetic torquers.

The gyroscopic torques resulting from the momentum wheel are used to control roll and yaw. In addition some systems contain reaction wheels or gimbals on the main wheel to give auxilliary roll or yaw control. A prime attribute of momentum bias systems is that the yaw error can be controlled without the need for sensing yaw attitude. The manner in which this is accomplished is the subject of the next section.

4.1 Gyrocompassing

The fact that the wheel posseses appreciable angular momentum has little significance to the pitch control but is inherent to control of the roll and yaw motion. Whereas the pitch axis is nominally fixed in inertial space, the roll and yaw axes are constantly rotating and in fact the two axes interchange every 90 degrees of orbit position. This fact, together with the fact that detection of pitch and roll errors is relatively easy using earth horizon sensors forms the basis of the "gyrocompassing" technique of yaw attitude

7/CGC/28

detection. Any system that does not involve direct yaw measurement, i.e., a yaw sensor, must indirectly sense yaw by gyrocompassing.

Gyrocompassing relies on the fact that a yaw error turns into a roll error due to the fact that the wheel axis tends to remain fixed in inertial space while the satellite traverses the orbit. Consider a satellite with a single fixed momentum wheel as it travels around the orbit at a rate ω_o (see Figure 4.1-1). At time t_1 a pure yaw error (ψ) exists. If no external torques are applied the wheel axis will remain fixed in inertial space. At time t_2, a quarter of an orbit later, the wheel is in the same orientation as it was at t_1 but the body axes are not. By applying reaction torques to the wheel the pitch control system has kept the z axis nominally pointed toward the earth. The vehicle axes therefore rotate around the wheel axis and at time t_2 all of the original yaw error has turned into a roll error (ϕ). This error can be detected by the roll horizon sensor. The essence of gyrocompassing is as follows. At any particular time the yaw attitude is not known, but the roll error is. Furthermore, if there are no external torques and the roll error is

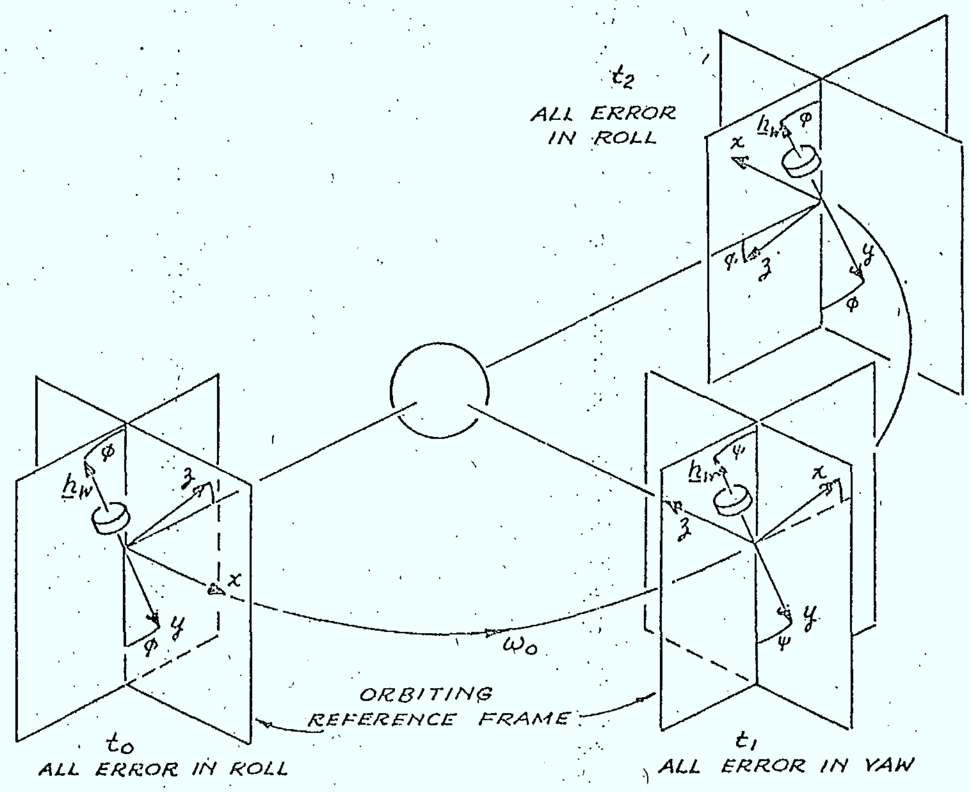

FIGURE 4.1-1 - ILLUSTRATION OF GYROCOMPASSING

7/CGC/29

changing then there must be a yaw error present. We are therefore able to infer yaw attitude by observing the roll behavior.

For the analysis to follow it will be useful to consider the vehicle attitude motion relative to the orbiting reference (Figure 4.1-1) rather than an inertial frame. Figure 4.1-2 shows the roll-yaw motion previously described as it appears in the orbiting

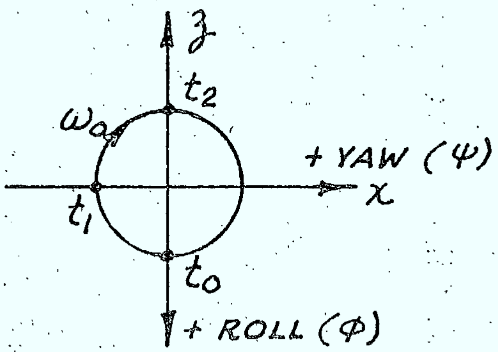

FIGURE 4.1-2 - EFFECT OF ORBIT MOTION IN ORBITING REFERENCE FRAME

reference frame. The times t_0, t_1, t_2 refer to Figure 4.1-1.

7/CGC/30

Gyrocompassing enables one to design a system to control yaw without direct yaw sensing. This forms the basis for all of the momentum bias systems to be considered. The one that results in the simplest, and probably the lightest, control system involves ground commanded corrections to vehicle attitude. This will be discussed in the next section.

4.2 Fixed Momentum Wheel - Ground Command Correction

Figure 4.2.-1 illustrates a fixed momentum wheel system in which all of the control functions are handled on the ground. The satellite contains the pitch and roll horizon sensors, the control thrusters, and the momentum wheel. A block diagram of the control system is given in Figure 4.2-2.

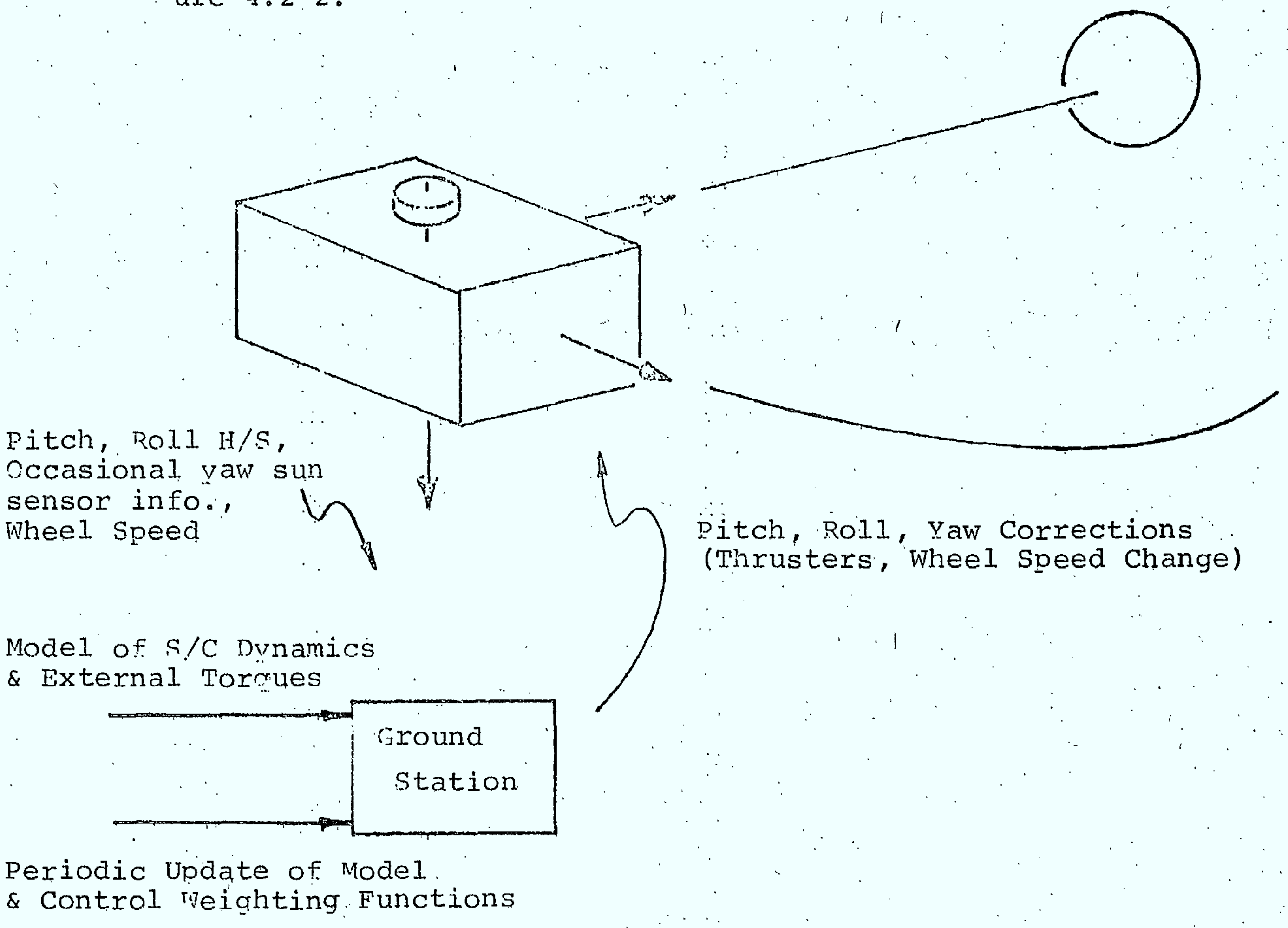

FIGURE 4.2-1 - FIXED MOMENTUM WHEEL - GROUND COMMAND CORRECTION

7/CGC/31

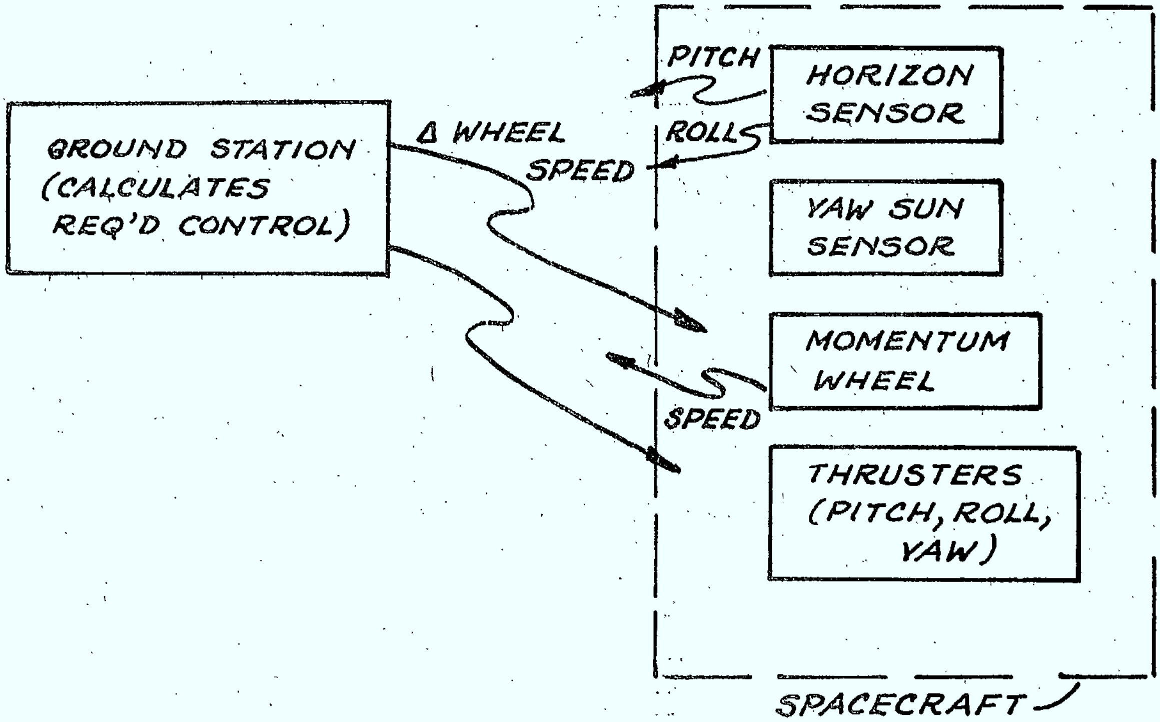
GROUND STATION
(CALCULATES
REQ'D CONTROL)
Δ WHEEL
SPEED
PITCH
ROLL
HORIZON
SENSOR
YAW SUN
SENSOR
MOMENTUM
WHEEL
SPEED
THRUSTERS
(PITCH, ROLL,
YAW)
SPACECRAFT

FIGURE 4.2-2

Pitch and roll horizon sensor signals and wheel speed are continuously transmitted to the ground station. The output of a yaw sun sensor could also be continuously sent, but for much of the day this signal would not accurately represent yaw attitude due to an unfavorable sun direction. For those periods in which an accurate measurement of yaw is available, this information could be used to improve the yaw estimate. Using a high speed digital computer at the ground station, a detailed model of the spacecraft dynamics, including appendage flexibility and external torques, could be implemented. Solution of the equations of motion should give an accurate, continuous estimate of vehicle rates and yaw attitude. The computer could simultaneously be used to solve sophisticated optimal control equations to obtain the desired control strategy to be sent to the satellite. This optimization could be weighted heavily toward minimizing fuel usage, response time, or pointing error, the weighting functions changeable depending on current requirements.

The on-board equipment consists of the momentum wheel, horizon sensors, and control thrusters. The sun sensor could probably be eliminated for the normal mode but since it is needed for stationkeeping its output might as well be used, when available, to update the yaw estimation. It is difficult to estimate the size of momentum wheel required for this system without performing a detailed simulation of the spacecraft dynamics, ground control law, and external torques. However, it would appear probable that a wheel with between 5 and 10 ft.lb.sec would suffice although some type of solar torque compensation may be necessary. Figure 4.2-3 shows how the weight of the wheels vary with angular momentum. Also shown is the total control system weight. The horizon sensor package, with redundancy, weighs about 15 lbs and the sun sensor about 1 lb. with electronics.

7/CGC/32

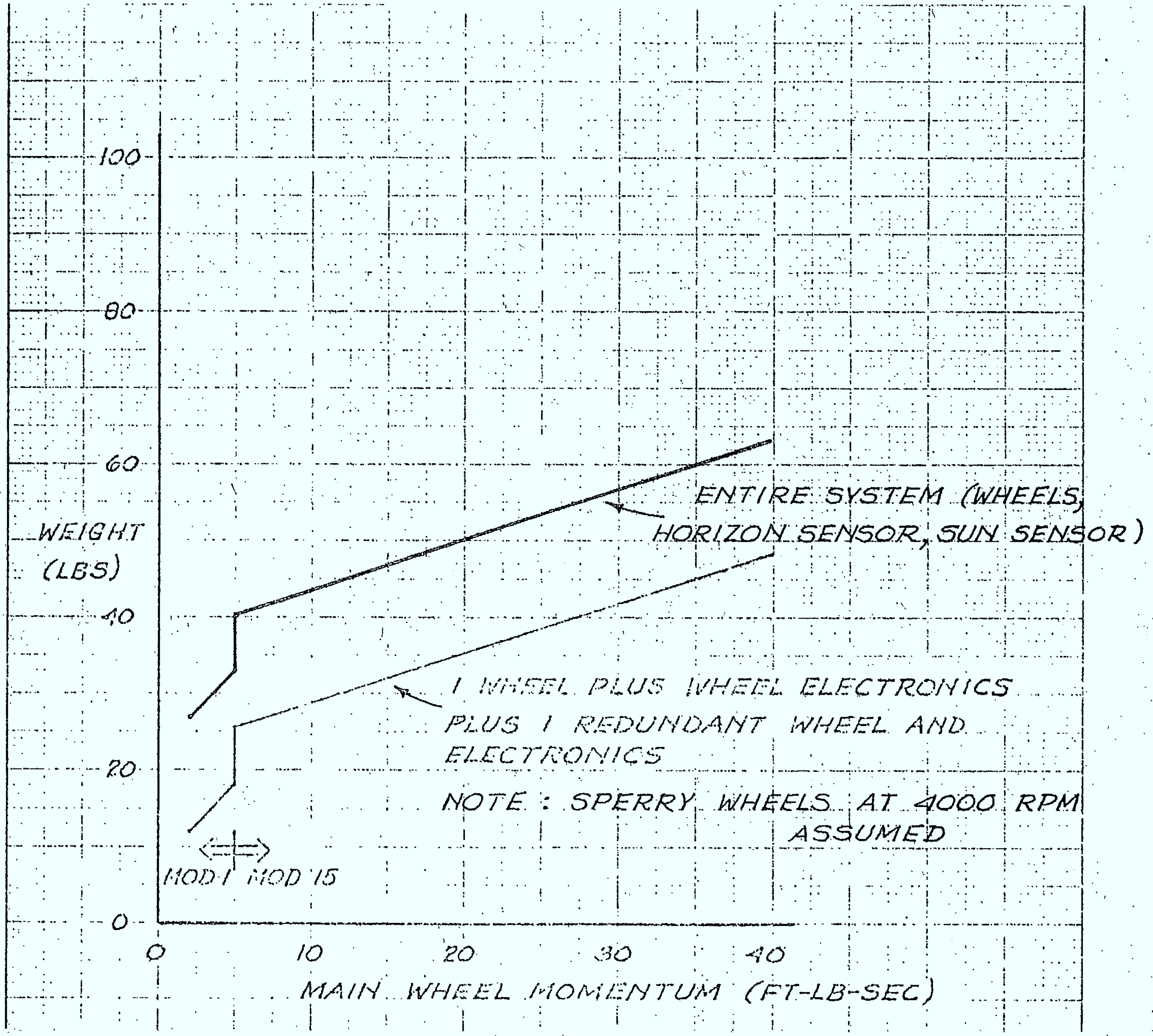

FIGURE 4.2-3 - WEIGHT OF GROUND CONTROLLED SYSTEM VS. ANGULAR MOMENTUM

A system such as this, where so many of the control functions are placed on the ground, has received little attention in the past. Part of the reason for this has probably been the usual requirement for autonomous operation for reasonably long time intervals. However, it would seem that the ground in the loop system could be automated to the extent that essentially autonomous control would result. The system has the obvious advantage of a minimal amount of on-board hardware which results in low weight and high reliability. Also, probably the ultimate in sophisticated control techniques is possible using the powerful computation capability available on the ground. The main disadvantage of this system is the difficulty in which off axis pointing and rapid three axis control can be accomplished.

4.3 Fixed Momentum Wheel - Offset Jets (WHECON)

WHECON (WHEel CONtrol) is a Lockheed developed control concept incorporating a single fixed momentum wheel. Gyrocompassing is used to transfer yaw errors into roll errors where they are detected by the roll axis horizon sensor. The unique feature of the WHECON system is that, instead of a pure roll correction, a combined roll and yaw motion is created by thrusters which are offset from the vehicle axes as shown in Figure 4.3-1.

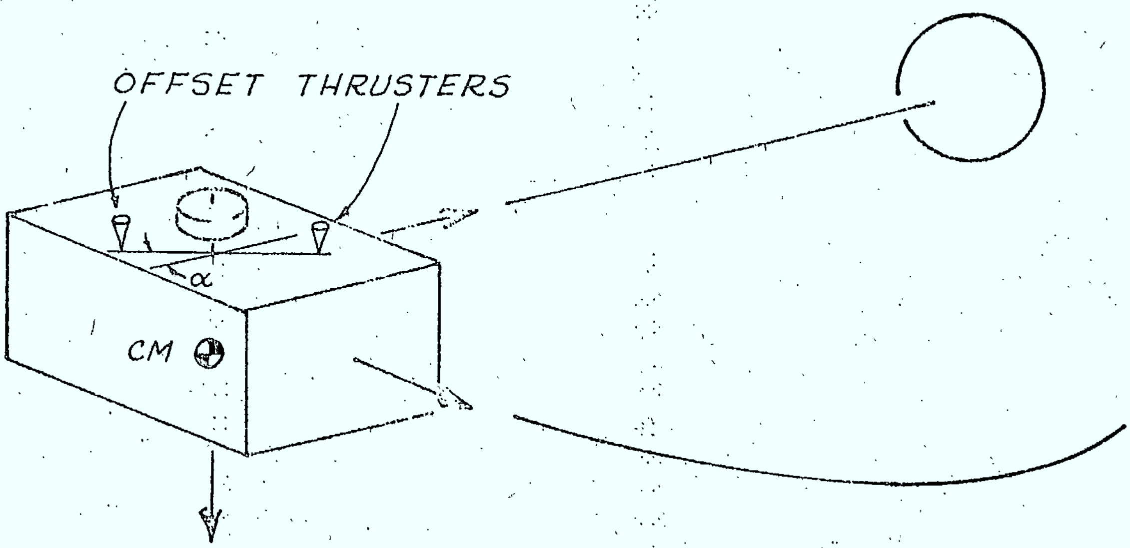

FIGURE 4.3-1 - WHECON SYSTEM

The block diagram of the system is shown in Figure 4.3-2. It has been shown through extensive

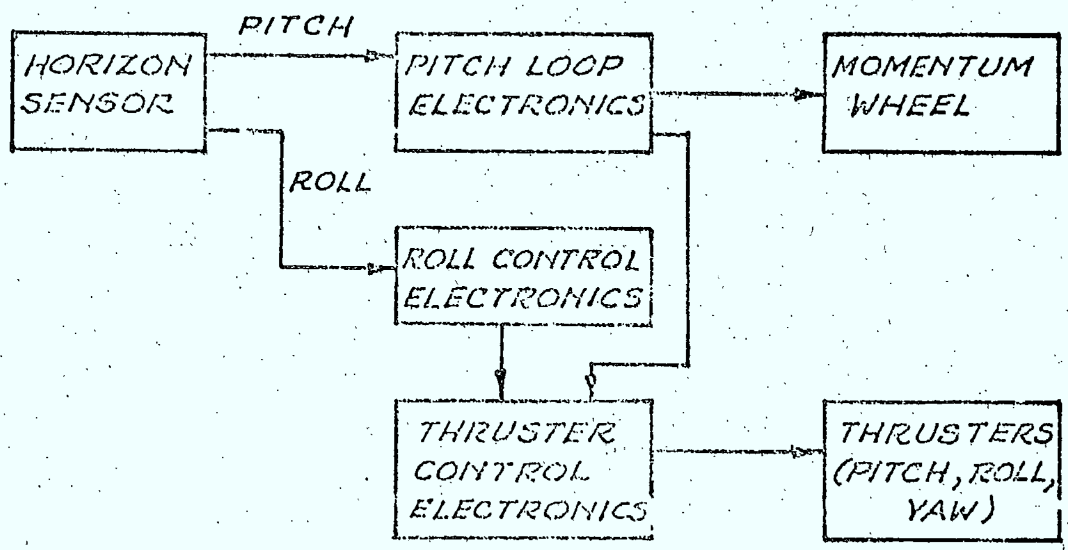

FIGURE 4.3-2

analysis (See Reference 2) that the offset jets can reduce the yaw response time to significantly less than one quarter of an orbit period, and also introduce damping in yaw. The roll response is damped by electronically filtering the roll horizon sensor signal to introduce rate compensation.

7/CGC/34

Firing one of the offset thrusters produces a torque about the vehicle cm as shown in Figure 4.3-3. This is a top view of the system - looking

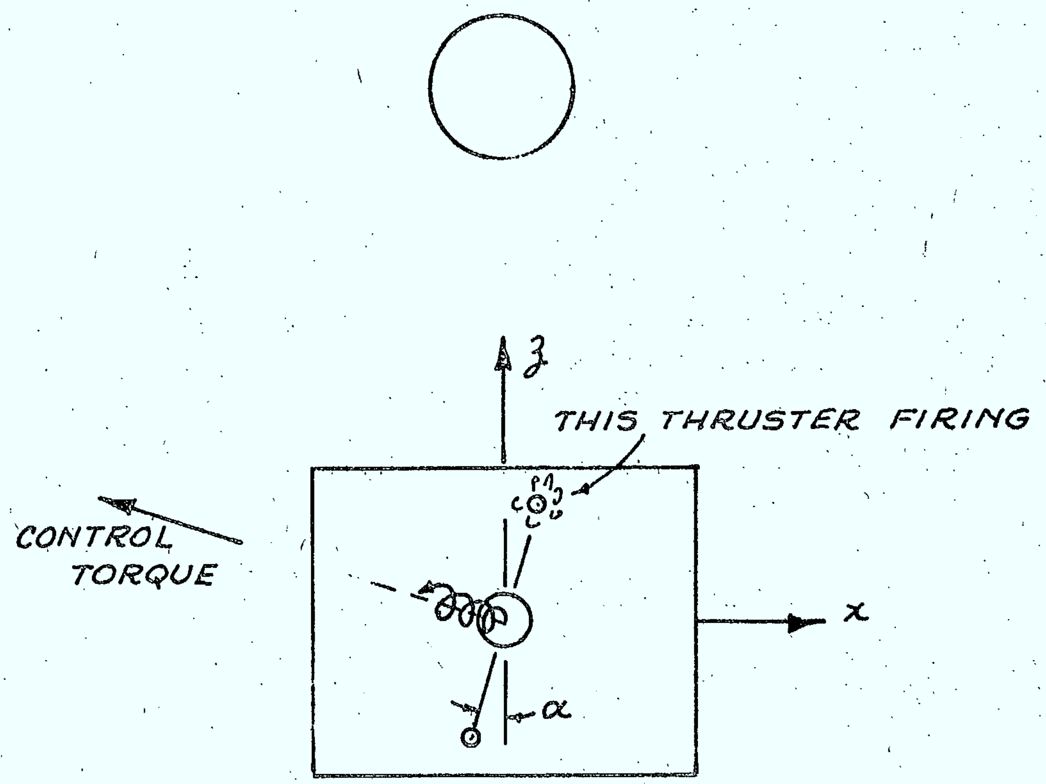

FIGURE 4.3-3 - WHEEL PRECESSION IN ROLL AND YAW DUE TO OFFSET THRUSTER

down on the orbit plane. Assuming that the torque is small relative to the wheel momentum, the wheel axis will precess in the direction of the torque with small nutation (see Section 2.1.4 for a review of nutation and precession motion). It has

7/CGC/35

been determined analytically, and can be demonstrated intuitively, that optimum system performance requires a small offset angle α. This causes a large yaw motion, as shown in Figure 4.3-3. It may seem strange that when the horizon sensor detects a roll error the control system responds by creating a large yaw excursion. We will now demonstrate that this is necessary in order to effectively control and damp yaw errors without using a yaw sensor.

Suppose that we did command a pure roll correction. Figure 4.3-4 shows the attitude motion that would result, observed in the orbiting reference frame and neglecting nutation. A roll deadband is

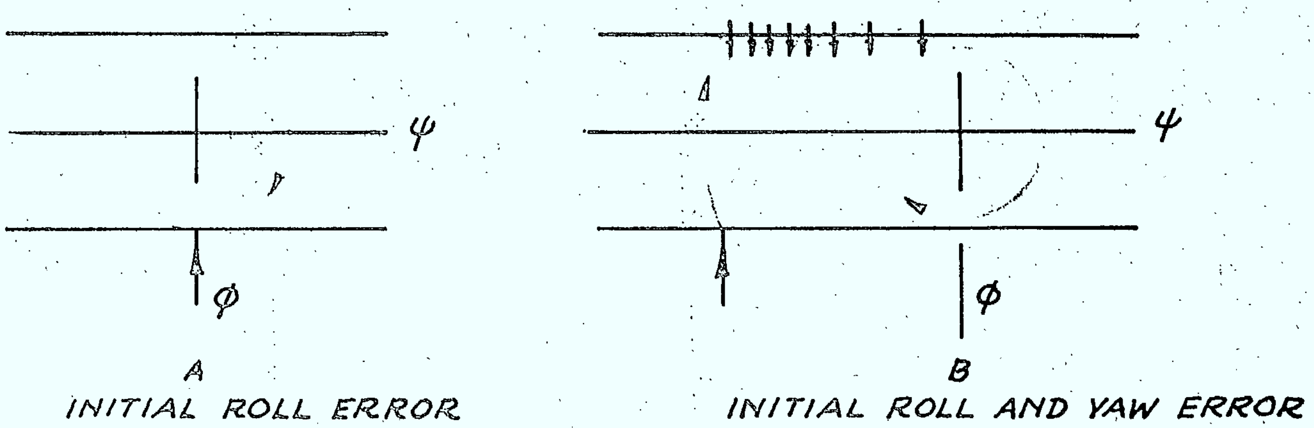

FIGURE 4.3-4 - PURE ROLL CORRECTION (α= 90°)

included so that no control thruster firing occurs when the roll error is less than a certain value. Orbit motion, as discussed in Section 4.1, causes the circular paths inside the deadband. The dark lines indicate intervals of thruster firing. In A the response from an initial pure roll error (no

7/CGC/36

yaw) is shown. The thruster fires continuously until the roll is inside the deadband, whereupon it ceases. The orbit motion then transfers the remaining error back and forth between roll and yaw. This is an acceptable transient response. Now suppose that along with an initial roll error a yaw error also is present. This case is shown in B. As before, the thruster fires until roll is within the deadband. However, this time the orbit motion causes the opposite roll deadband to be exceeded, resulting in the series of thruster pulses shown. Eventually the yaw error is nulled but since the correction is due to the slow orbit motion the yaw response time is very long.

To speed up the yaw response we need the thruster to cause precession in the yaw direction. This is precisely what a small offset angle accomplishes. The response of the system from an initial roll and yaw error using a small offset angle is shown in Figure 4.3-5.

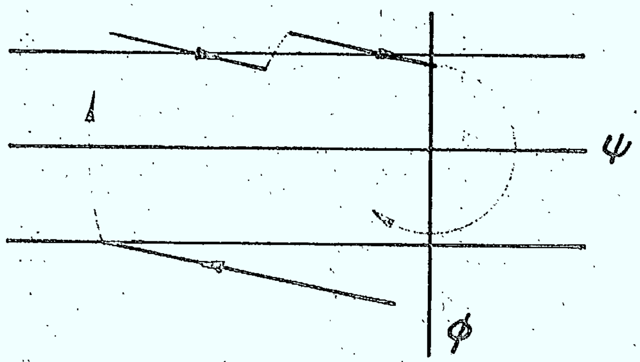

FIGURE 4.3-5 - ROLL-YAW CORRECTION (α SMALL)

Note that initially the yaw attitude grows, until roll is within the deadband. This situation, in which yaw is driven the wrong way, is not desirable but cannot be avoided without yaw sensing. After the deadband is crossed, however, the real advantage of the small offset angle becomes apparent. The control pulses now act in a direction to quickly null the yaw error. Thus, with a

7/CGC/37

small offset angle, the yaw error is removed much more rapidly, even though a large transient error is created. It should be pointed out that the case we have just considered represents a worst case initial error. For positive roll and yaw errors the control torque will initially null both, as shown in Figure 4.3-6.

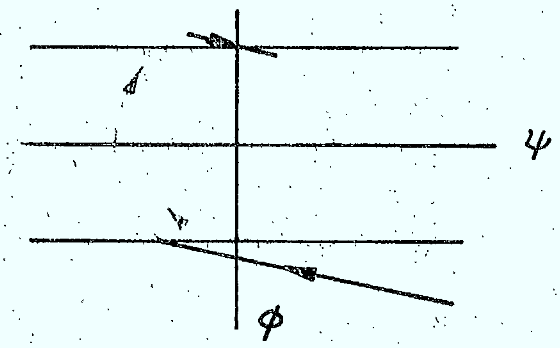

FIGURE 4.3-6 - ROLL-YAW CORRECTION (α SMALL)

To simplify the preceeding discussion the nutation caused by the thruster firings has been neglected. As discussed in Section 2.1.4 when a torque is applied to a body containing a momentum wheel the total angular momentum vector precesses in the direction of the torque while the wheel axis nutates around this vector. The trajectories in the orbiting reference frame that have been discussed in this section actually represent motion of the total angular momentum vector. The wheel

7/CGC/38

axis, to which the roll and yaw angles are referenced, nutates around it. Thus, the path of the wheel axis for the case shown in Figure 4.3-6 might appear as in Figure 4.3-7. Usually the nutation

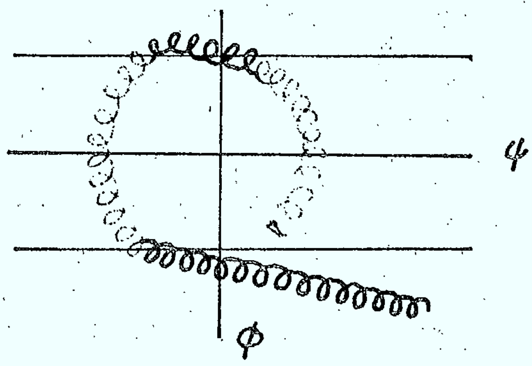

FIGURE 4.3-7 - ROLL-YAW CORRECTION INCLUDING NUTATION

induced by one thruster firing is small but a sequence of pulses can be phased to either build up or reduce the nutation. Consider

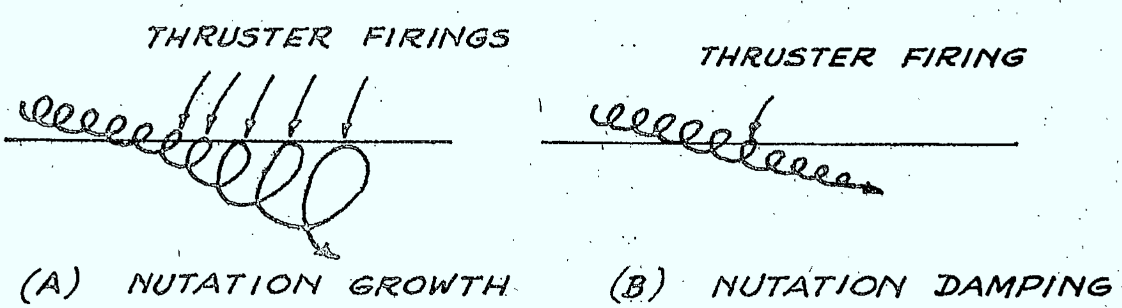

FIGURE 4.3-8 - NUTATION CAUSED BY THRUSTER FIRING

the trajectories entering the deadband as illustrated in Figure 4.3-8. In A the thruster firings happen to occur at just the right times to build up nutation. Therefore even after the momentum vector has precessed well inside the deadband there is still thruster activity and in fact an unstable situation may result in which the nutation continually grows. In contrast, the pulses in B occur at the appropriate times to damp nutation and as a result once the deadband is entered very few thruster pulses are commanded.

It is very important for long life missions to ensure adequate nutation damping as this will ensure that only the minimum number of thruster firings occur. As a result less control fuel is required and longer thruster life is realized. Since the original Lockheed design various techniques have been proposed for increasing the nutation damping and reducing excess thruster firing by timing the pulses appropriately. This is the function of the "augmented pseudo-rate modulator" in the CTS design. TRW uses a timing mechanism to accomplish the same thing for FLEET-SAT-COM. With such a modification WHECON is a viable long life control system.

The WHECON system weight, as a function of angular momentum is given in Figure 4.3-9. This is similar to the previous ground controlled system with the exception of 18 lbs of additional weight due to the on board attitude control electronics.

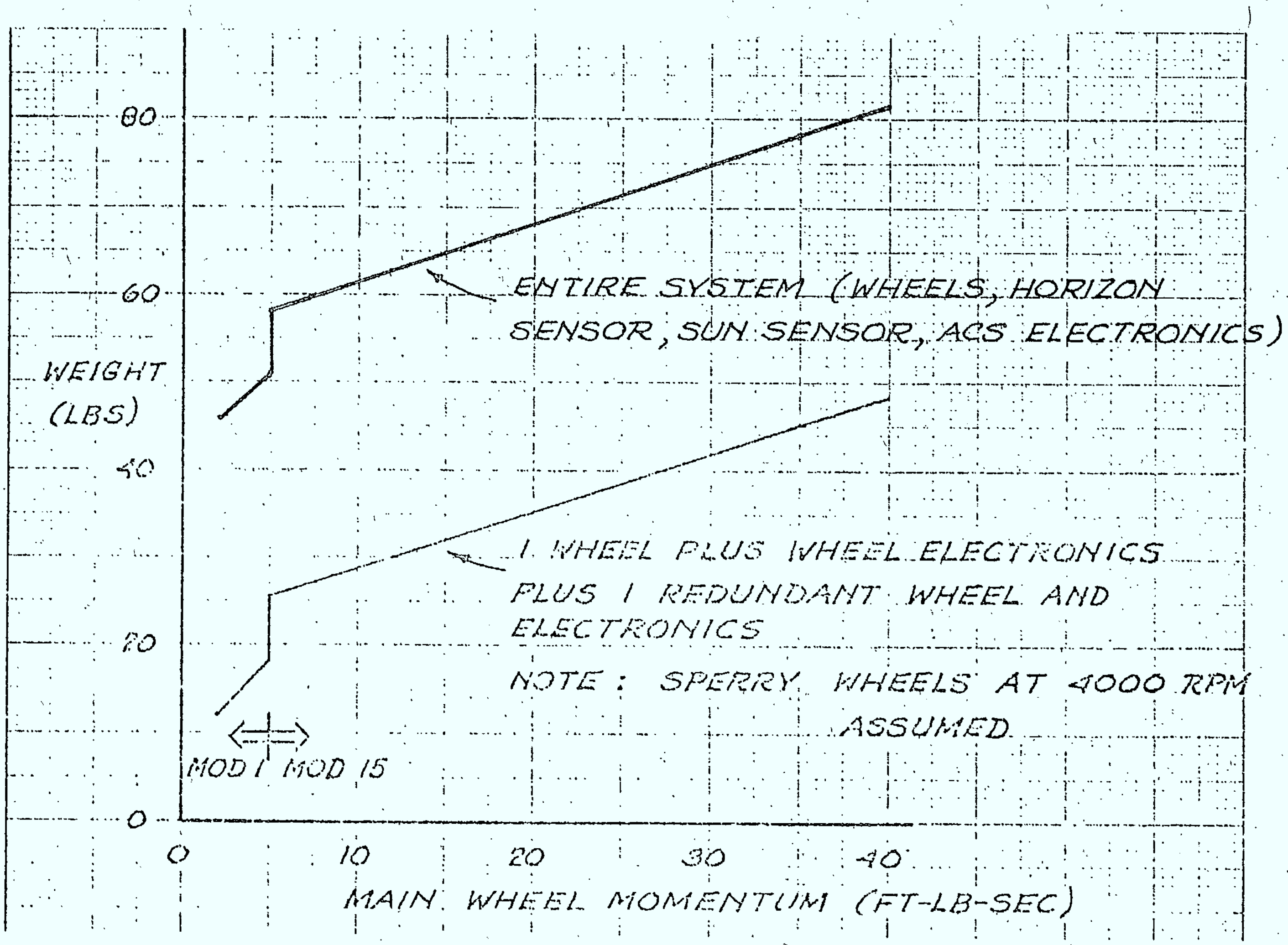

FIGURE 4.3-9 - WEIGHT OF WHECON SYSTEM VS. ANGULAR MOMENTUM

As discussed in Section 3.1, an approximate relationship exists between angular momentum and external torque, for a specified maximum yaw angle and orbital rate ($h_W \approx 57.3 \frac{T}{\omega_o \psi}$). This relationship applies for systems, such as WHECON, that bound yaw errors by controlling roll. Using this relationship together with the data given in Figure 4.3-9 we can determine how the WHECON system weight varies with the yaw external torque. These results are shown in Figure 4.3-10 for a maximum yaw error of 0.5 degrees at synchronous altitude.

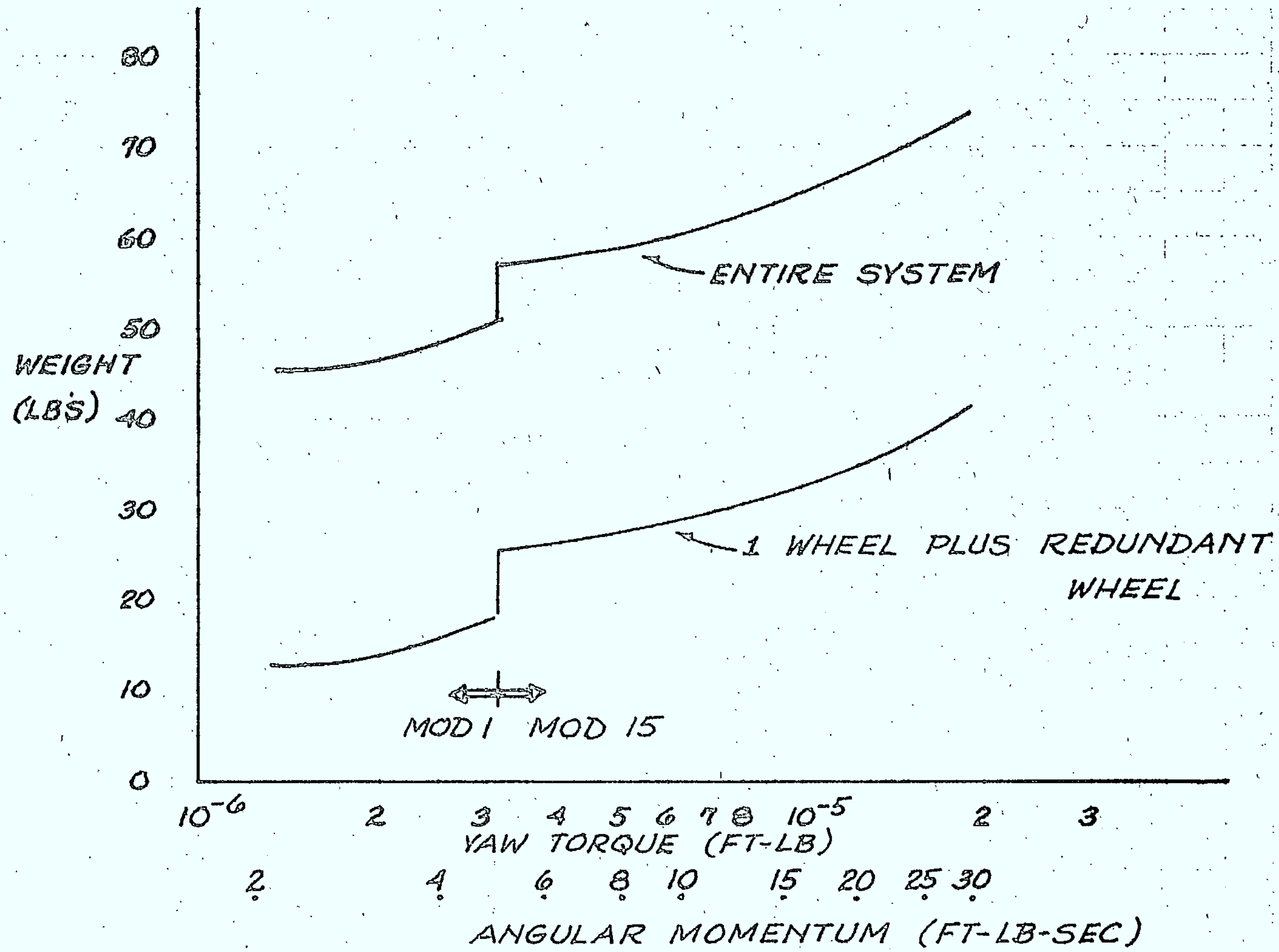

FIGURE 4.3-10 - WEIGHT OF WHECON SYSTEM VS. YAW TORQUE AND ANGULAR MOMENTUM

The WHECON design represents the most highly favoured attitude control system at the present time for missions for which it is compatible.

Formally presented by Lockheed in 1968 (reference 2), although not so stated, it has presumably been used for several years in classified missions. These were probably of short life times since the original design did not include modifications to limit thruster activity. With such modifications the system has been chosen for the CTS, the TRW Fleet Sat-Com, the RCA Satcom, and the Hughes 3 Axis research and development satellite. As with the system discussed in the previous section WHECON is not suited for missions in which off axis pointing is required or where rapid 3 Axis control is necessary.

The WHECON system and the ground control system discussed in the last section are the only ones containing a single fixed momentum wheel that will be considered. The remainder of the report deals with designs incorporating something other than a single fixed momentum wheel for attitude control.

4.4 Fixed Momentum Wheel Plus Roll Axis Reaction Wheel

The system shown in Figure 4.4-1 has, in addition to the main momentum wheel, a small reaction wheel which spins about the vehicle roll axis. This wheel provides a source of reaction torque, as well as momentum storage, on the roll axis.

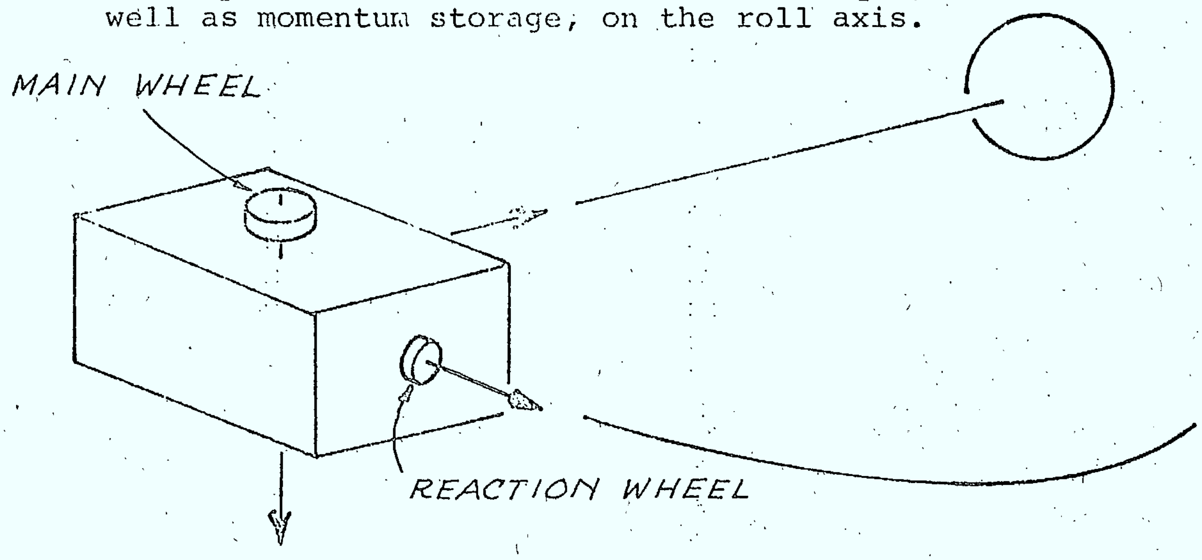

FIGURE 4.4-1 - FIXED MOMENTUM WHEEL PLUS ROLL AXIS REACTION WHEEL

7/CGC/42

Yaw is controlled in a gyrocompassing or WHECON mode using the thrusters to unload the wheel. A block diagram of the control system is given in Figure 4.4-2.

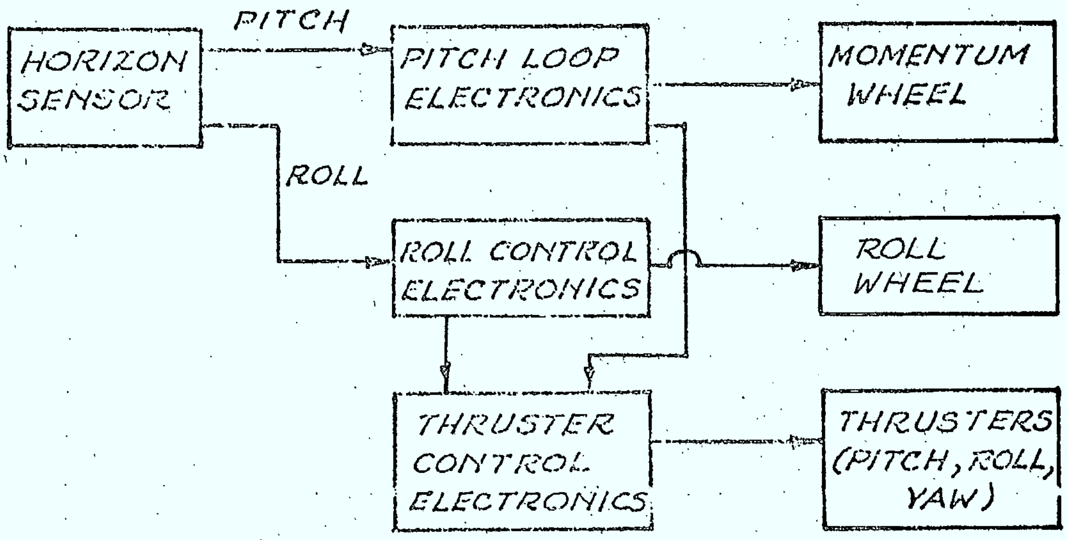

FIGURE 4.4-2

Whereas thrusters have a minimum torque impulse associated with them the reaction wheel, for all practical purposes, does not. Therefore very fine linear control results and thus serves to efficiently damp nutation and eliminate limit cycling due to overcorrecting. The capability of the wheel to store a small amount of momentum allows it to compensate for a roll external torque. This compensation is only temporary, however, since the orbital rotation would require precessing the roll wheel angular momentum. Therefore the wheel must be periodically unloaded using thrusters or some other source of external torque, e.g. magnetic. Momentum storage in the reaction wheel also allows offset pointing in yaw which may be desirable for some missions. We will now discuss the operation of this system in more detail.

7/CGC/43

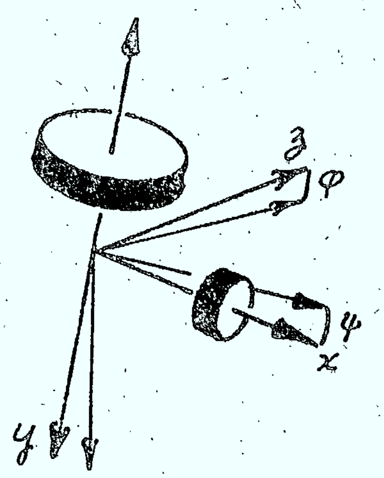

FIGURE 4.4-3 - SYSTEM WITH NON-ZERO ROLL AND YAW ANGLES

Figure 4.4-3 illustrates the system with small roll and yaw errors (ϕ, ψ). In order to determine analytically how these angles vary as a result of accelerating the reaction wheel the equations of motion will be derived and then solved. The development will be very similar to that of Sections 2.1.1 and 2.1.4 which was for a single momentum wheel system acted upon by an external torque. In the present analysis we will proceed one step further than before and actually solve for the attitude angles ϕ and ψ as a function of time. The inertial angular momentum of the system is

$$\underline{H} = (I_x \omega_x + h_x)\ \hat{\underline{x}} + (I_y \omega_y - h_w)\ \hat{\underline{y}} + I_z \omega_z\ \hat{\underline{z}} \qquad 4.4\text{-}1$$

where the I's are moments of inertia of the system for its cm, the ω's are the inertial angular velocity components, h_w is the momentum wheel angular momentum (assumed constant), and h_x is the reaction wheel momentum, i.e.,

$$h_x = J_R \Omega_R \qquad 4.4\text{-}2$$

7/CGC/44

where J_R is its moment of inertia and Ω_R its spin speed. Differentiating $\underline{H}$ in inertial space and setting the result to zero (zero external torque assumed) gives

$$I_x \dot{\omega}_x + h_w \omega_z + \dot{h}_x = 0$$

$$I_y \dot{\omega}_y = 0 \qquad 4.4\text{-}3$$

$$I_z \dot{\omega}_z - h_w \omega_x = 0$$

where second order terms in the ω's and h_x are neglected since these are assumed small. Rewriting these equations and noting that for small angles $\dot{\phi} \approx \omega_x$, $\dot{\psi} \approx \omega_z$ where the orbit rate ω_o is ignored for the moment, we obtain

$$\dot{\phi} = - \frac{\dot{h}_x}{I_x \omega_n} \sin \omega_n t$$

$$4.4\text{-}4$$

$$\dot{\psi} = - \frac{\dot{h}_x}{h_w} (1 - \cos \omega_n t)$$

where the nutation frequency ω_n is

$$\omega_n = \frac{h_w}{\sqrt{I_x I_z}} \qquad 4.4\text{-}5$$

and it is assumed that $\dot{\phi}(0) = \dot{\psi}(0) = 0$.

For the case in which the reaction wheel is accelerated at a constant rate $\dot{h}_x$ is constant and Equations 4.4-4 can be integrated to yield

$$\phi = - \frac{\dot{h}_x}{h_w^2} I_z (1 - \cos \omega_n t)$$

$$4.4\text{-}6$$

$$\psi = \frac{\dot{h}_x}{h_w^2} \sqrt{I_x I_z} \sin \omega_n t - \frac{\dot{h}_x}{h_w} t$$

7/CGC/45

FIGURE 4.4-4

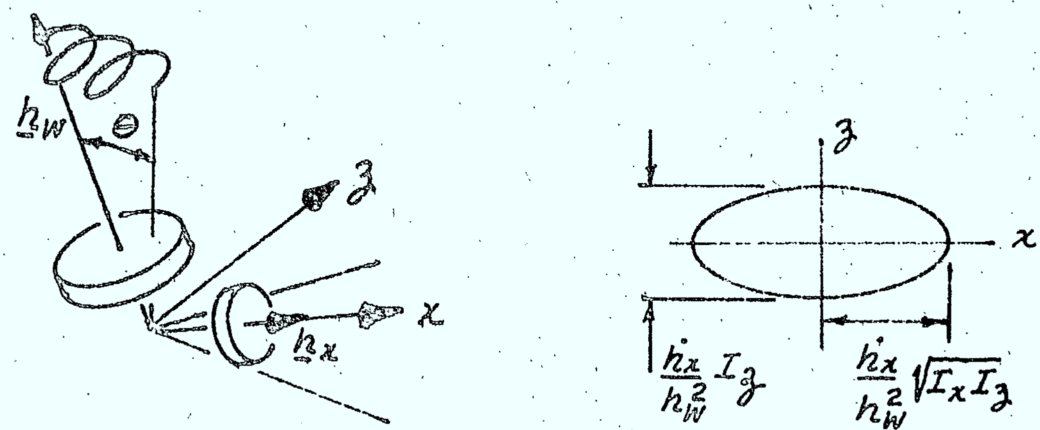

ATTITUDE MOTION

NUTATION ELLIPSE

The motion indicated by these expressions is illustrated in Figure 4.4-4. The secular component represents the precession angle θ of the angular momentum vector, i.e., $\theta = \frac{\dot{h}_x t}{h_w}$, and the sinusoidal components represent nutation of the wheel axis around the momentum vector. If the inertias I_x and I_z are not equal the nutation cone is actually an ellipse as shown in Figure 4.4-4. It is interesting to compare these results with those obtained in Section 2.1.4 for an external torque T acting on the x axis and no reaction wheel. In that analysis the assumption is made that $I_x = I_z = I$ and for this case Equations 4.4-6 become

7/CGC/46 *

$$\phi = -\frac{\mathring{h}_x I}{h_w^{\,2}} (1 - \cos \omega_n t)$$

$$\psi = \frac{\mathring{h}_x I}{h_w^{\,2}} \sin \omega_n t - \frac{\mathring{h}_x}{h_w} t \qquad 4.4\text{-}7$$

The nutation cone is now an ellipse with half angle $\eta = \frac{\mathring{h}_x I}{h_w^{\,2}}$. These results are identical to those obtained in Section 2.1.4 where $T = \mathring{h}_x$. Therefore the reaction wheel can be thought of as applying an external torque to the rest of the system.

Another way of analyzing this motion is through conservation of angular momentum. Consider Figure 4.4-5. In the first picture the attitude errors are all zero, all of the momentum in the momentum wheel, this being normal to the orbit plane. As the reaction wheel is spun up it develops some momentum h_x of its own on the x axis. Now if no external torques are present the total momentum $\underline{H}$, which is the vector sum of $\underline{h}_w$ and $\underline{h}_x$, must remain fixed. The only way this can happen is if the vehicle yaws through an angle ψ where

$$\psi = \tan^{-1} \frac{h_x}{h_w}$$

If the wheel's acceleration is a constant then its momentum is $h_x = \mathring{h}_x t$ and therefore, for small angles, we obtain

$$\psi \approx \frac{\mathring{h}_x t}{h_w}$$

This is the same expression previously obtained by solving the equations of motion (Equations 4.4-7).

7/CGC/47

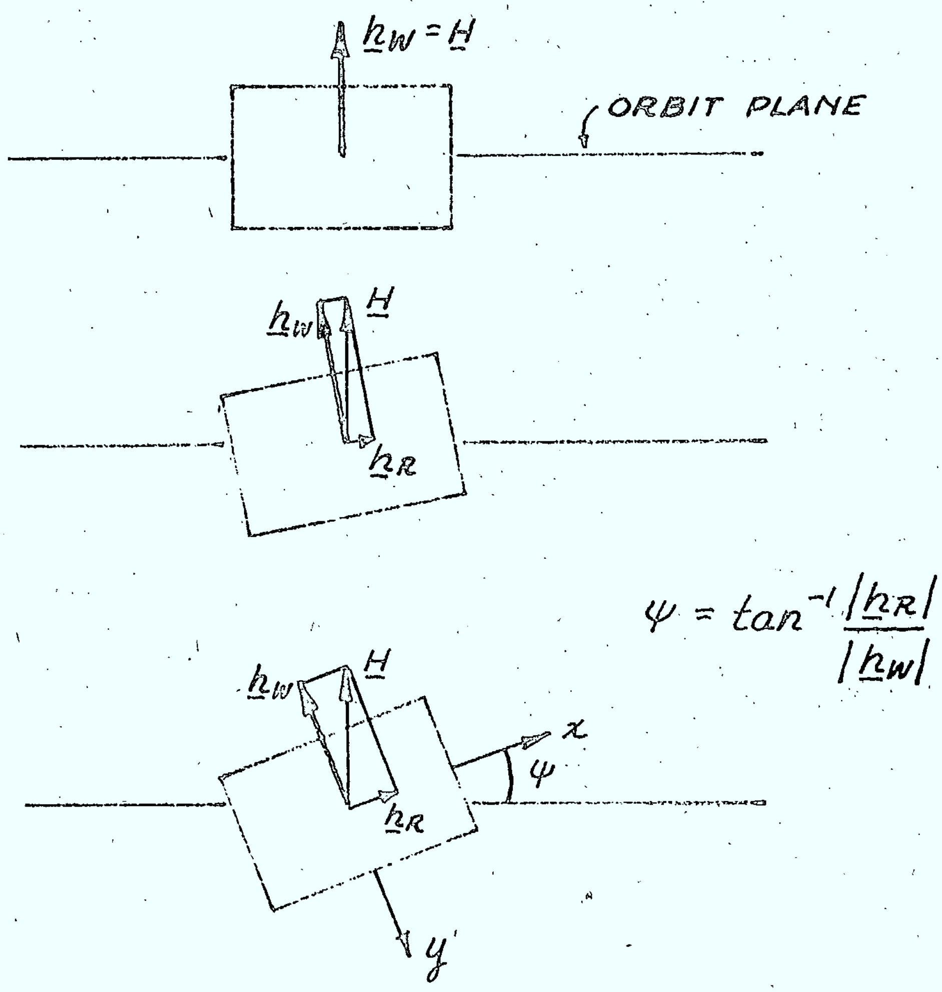

FIGURE 4.4-5 - YAW MOTION DUE TO CONSERVATION OF ANGULAR MOMENTUM DURING REACTION WHEEL ACCELERATION

We have seen that yaw motion is induced by accelerating the reaction wheel. If the acceleration is removed, the wheel will be left with a constant value of momentum and an offset yaw attitude will remain. If the total angular momentum vector was normal to the orbit plane before the manoeuver then it will also be afterwards. The vehicle can therefore proceed along the orbit with a constant yaw offset without external torques applied as would be the case with a single fixed wheel system. The yaw offset bias resulting from the reaction wheel does not turn into a roll error in a gyrocompassing fashion. This system would, therefore, be ideally suited to missions which require offset pointing in yaw for extended periods.

The effect of external torques, which represent a major source of attitude perturbation, will now be discussed. In the case of a single fixed wheel system an external roll or yaw torque causes precession and nutation and the corresponding corrective thruster activity. If a reaction wheel is added, then the component of the torque impulse along the wheel axis can be absorbed as angular momentum in the wheel. The body attitude is not perturbed and no thruster activity results until such time as the wheel speed reaches unacceptable levels. Moreover for periodic torques of a low enough level no thruster activity may ever be required since the external torque itself serves to dump the wheel momentum. Figure 4.4-6

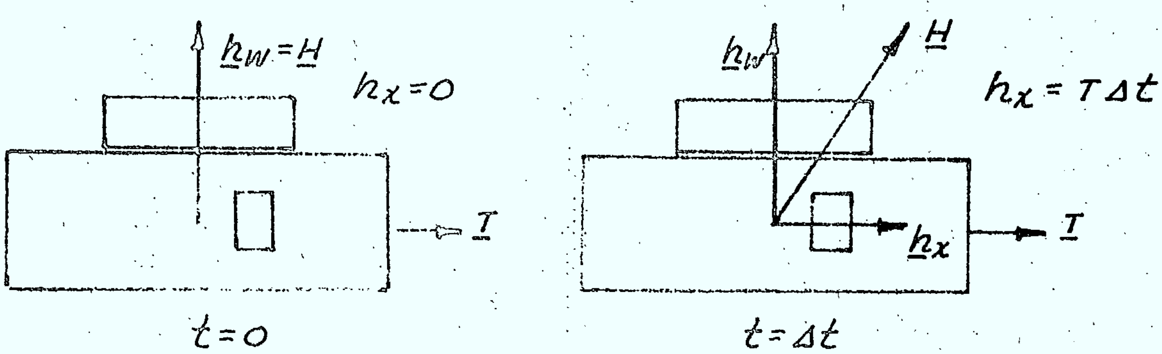

FIGURE 4.4-6 - SYSTEM RESPONSE TO EXTERNAL TORQUE

7/CGC/48

illustrates the effect of an x axis external torque. At t = 0 the reaction wheel is assumed stationary and the torque is applied. The vehicle will develop a rate in reaction to the torque which can be sensed and used to command the reaction wheel to spin up. At a time Δt seconds later the wheel momentum will be $h_x = T\Delta t$ with the vehicle unperturbed.

A single reaction wheel system can only give such performance if the torque is directed along the wheel axis and even then only for relatively short periods of time. Torques along the z axis will cause the usual precession common to single fixed wheel systems. Moreover, as is seen in Figure 4.4-6, the reaction wheel spinup causes the total momentum vector $\underline{H}$ to not be normal to the orbit plane. After the torque ceases, or changes direction, $\underline{H}$ will remain fixed in space which results in roll and yaw errors due to orbit rotation. It is therefore imperative that a desaturating mechanism be built into the control system to dump wheel momentum before these errors result. Typically thrusters or magnetic devices are proposed for this.

As has been pointed out, the added reaction wheel creates the ability to do offset yaw pointing and results in reduced thruster activity due to external torques. However, probably the greatest attribute of this system is the rapid nutation damping that can result by torquing the wheel in opposition to the nutational motion. Figure 4.4-7 illustrates part of the nutation coning that was shown in Figure 4.4-4.

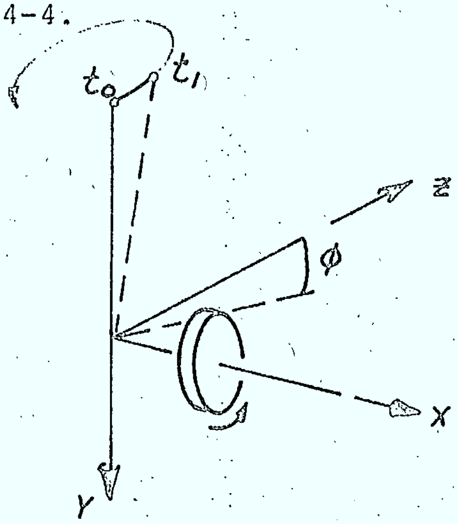

FIGURE 4.4-7 - ILLUSTRATION OF NUTATION DAMPING

7/CGC/49

Between times t_0 and t_1 the nutation causes the vehicle to rotate such that a roll error ϕ develops. A reaction torque applied by accelerating the wheel as shown would oppose this nutational motion and therefore damp it. The wheel can be made to respond very quickly to this motion using the roll horizon sensor signal to drive it.

For purposes of determining the amount of momentum wheel angular momentum that is required, the same criteria based on yaw excursions as used for the WHECON system is applicable. Regarding the roll reaction wheel, for any expected external disturbance torque and a maximum offset pointing requirement in yaw of only a few degrees, a 1 ft.lb.sec. wheel should be satisfactory. Probably, a significantly lower momentum would suffice for many applications but there is very little to be gained from a weight or power standpoint. Using a weight of 6 lb. for a 1 ft.lb.sec. wheel, which is representative of both Sperry and Bendix wheels, (12 lb. for a redundant system) we obtain the ACS weight versus momentum wheel angular momentum as shown in Figure 4.4-8.

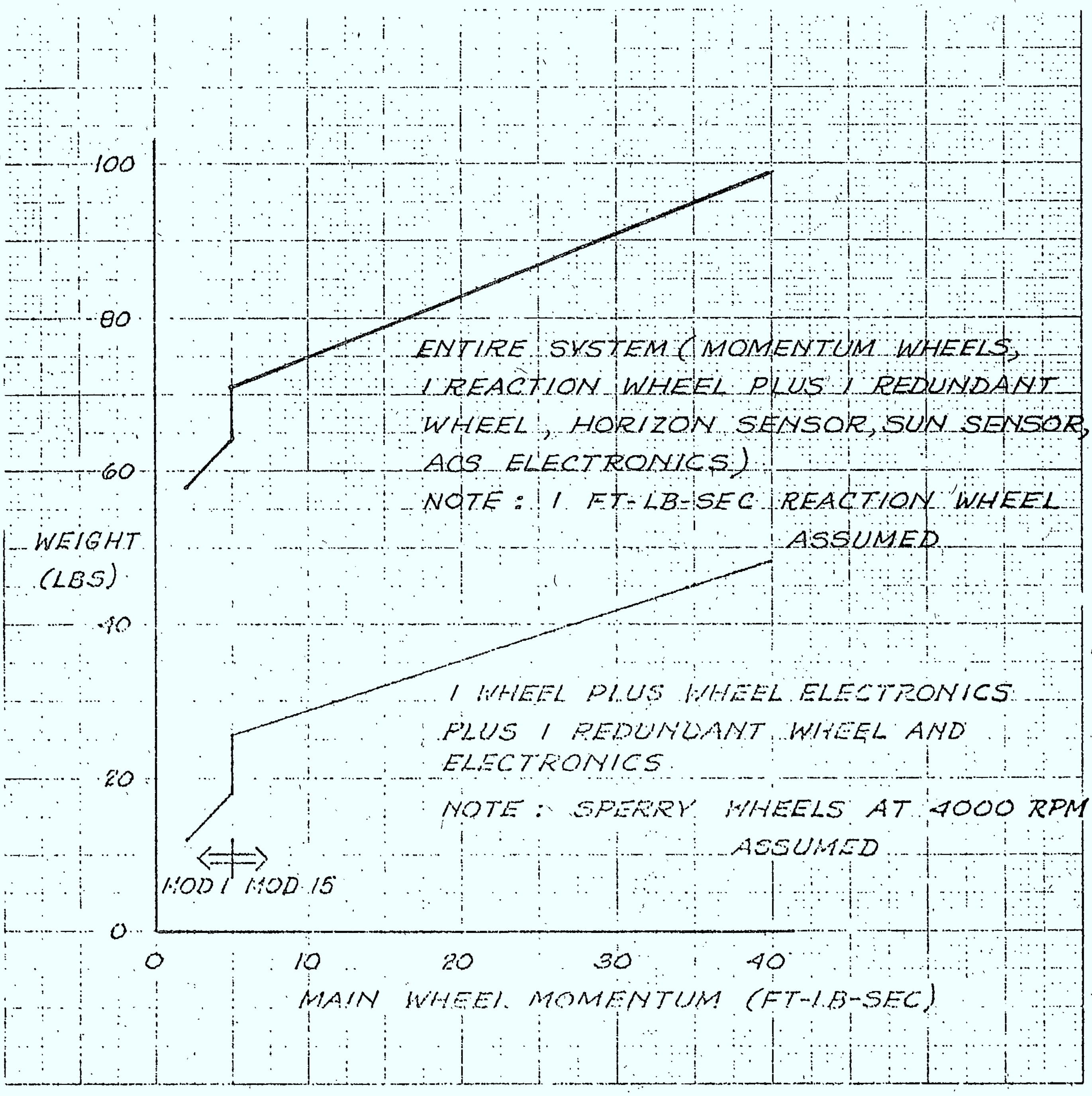

FIGURE 4.4-8 - WEIGHT OF FIXED MOMENTUM WHEEL PLUS ROLL REACTION WHEEL SYSTEM VS. ANGULAR MOMENTUM

In summary, the advantages of the momentum wheel plus roll reaction wheel system over the basic WHECON system are reduced thruster activity due to external torques, rapid nutation damping, and the capability of offset pointing in yaw. As discussed in Section 4.3 modifications can be made to the basic WHECON system to reduce thruster activity and therefore the first stated advantage disappears. For most missions offset yaw pointing is not a requirement and, except for those for which it is, the third advantage disappears also. Rapid nutation damping is usually desirable but in light of the added weight and complexity, the nutation damping afforded by the normal WHECON mode may be acceptable. It therefore appears that the arguments for adding the roll wheel are somewhat weak while the following arguments against it are strong: The added weight of 12 lb (with redundancy) is significant; the reliability, even with one backup wheel, is certainly less than for the WHECON system; finally there is no known record of on-orbit experience with such a system nor has it been chosen for any future design.

4.5 Yaw Gimballed Momentum Wheel

The system discussed in the previous section incorporated an extra wheel on the roll axis to create roll reaction torque and momentum storage. Virtually the same results can be achieved by gimballing the main momentum wheel, the gimbal being aligned with the yaw axis. (See Figure 4.5-1)

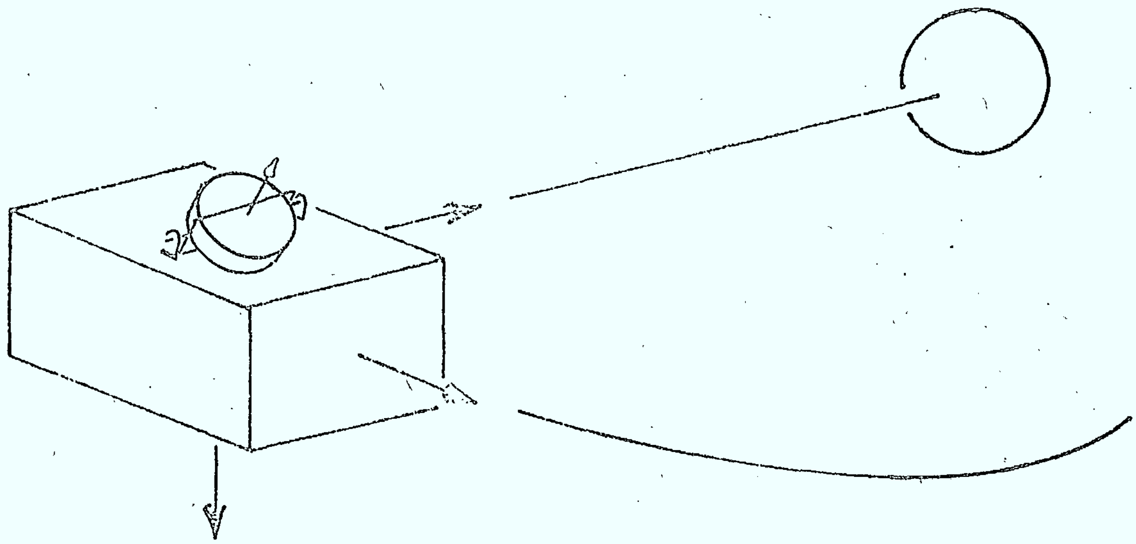

FIGURE 4.5-1 - YAW GIMBALLED MOMENTUM WHEEL SYSTEM

7/CGC/51

As the gimbal is rotated, a component of the wheel momentum is placed on the roll axis giving almost the identical results as accelerating a roll wheel. Figure 4.5-2 illustrates the similarity. The x axis momentum induced by a wheel is $h_x = J_R\Omega_R$ where J_R is its moment of inertia and Ω_R is the spin speed. For the gimballed wheel the transverse momentum is $h_W \sin\gamma$, where h_W is the angular momentum of the main wheel and γ is the gimbal angle.

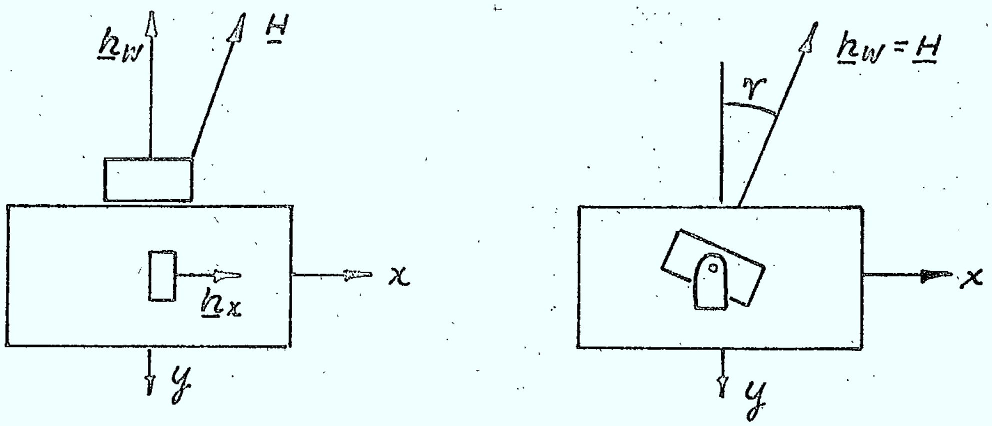

FIG. 4.5-2 EQUIVALENCE OF A WHEEL AND GIMBAL

The same transverse momentum is obtained if

$$\sin\gamma = \frac{J_R}{h_W}\Omega_R$$

Usually only small gimbal angles are required and therefore the following linear relationship between wheel speed and gimbal angle applies:

$$\gamma \approx \frac{J_R}{h_W}\Omega_R = \frac{h_x}{h_W} \qquad 4.5\text{-}1$$

The only theoretical difference between the two systems is that a small reaction torque is induced about the gimbal axis due to the small but finite gimbal and transverse wheel axis inertia. This torque, not present in the reaction wheel system, is usually completely negligible. The control system block diagrams for both systems are therefore identical, wheel speed being replaced by gimbal angle and a gain change (see equation 4.5-1). The block diagram, shown in Figure 4.5-3, is therefore virtually identical to that of the reaction wheel system.

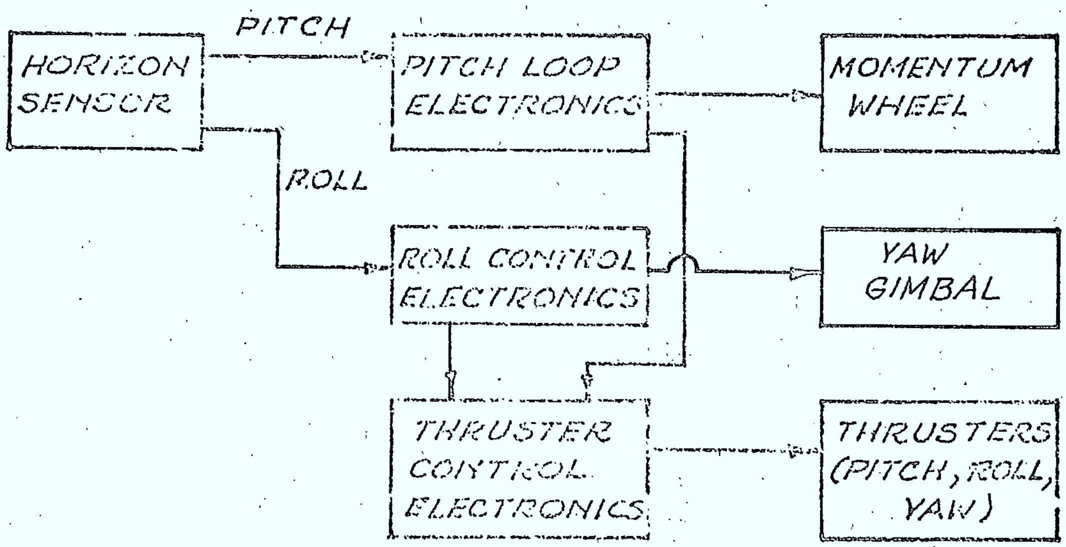

FIG. 4.5-3 YAW GIMBALLED MOMENTUM WHEEL CONTROL SYSTEM BLOCK DIAGRAM

6/CHW/2

The equations describing the attitude motion of a gimballed wheel system are identical to those previously derived for the reaction wheel system (Equations 4.4-6). The physical interpretation of these equations is somewhat different however. The equations describe the body axis motion and this is identical in both cases but the motion of the momentum wheel is not. Consider first a yaw maneuver in the presence of zero external torques. Figure 4.5-4 shows the situation after completion of such a maneuver.

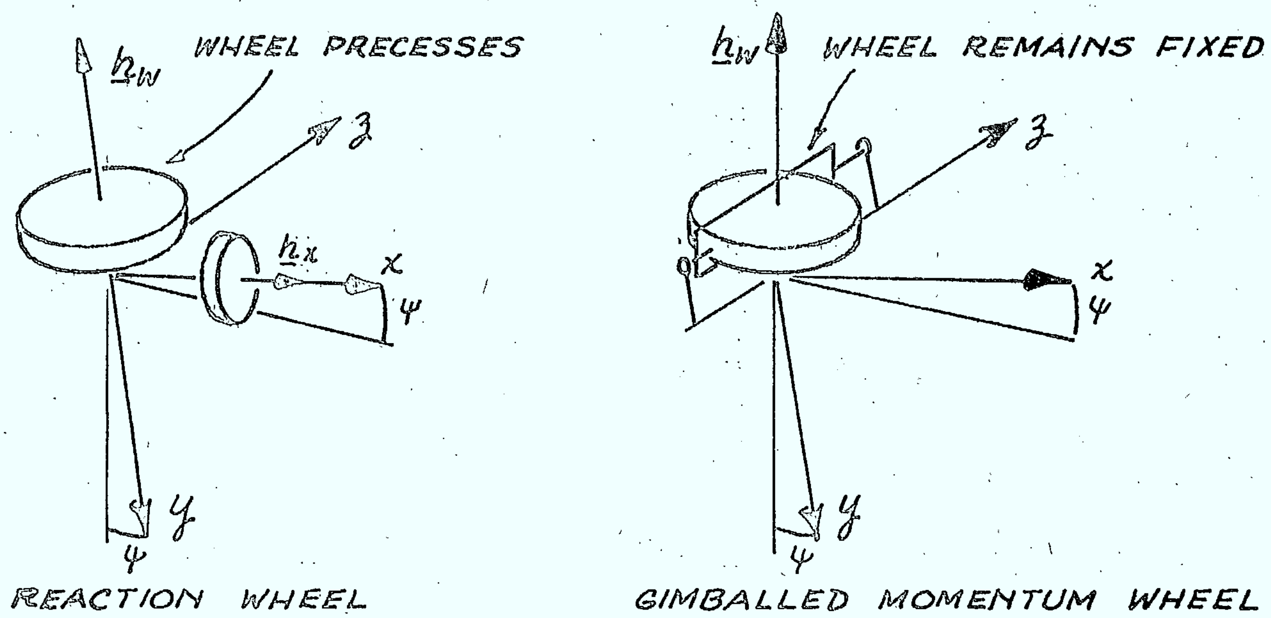

FIG. 4.5-4 YAW MANEUVER

In both cases the total angular momentum remains fixed in inertial space. For the reaction wheel system the momentum is distributed between the two wheels and the main wheel precesses through the yaw angle. In the gimballed wheel system all of the momentum is in the wheel and therefore it remains fixed in space. In this case the momentum

6/CHW/3

wheel acts as an "anchor" about which the body is torqued. Both systems will exhibit nutation which causes the wheel axes and the body axes to cone. This will be a small motion in comparison to the secular yaw motion if the command torque on the reaction wheel or gimbal is small.

The motion of the momentum wheel is also different in both systems when an external torque is applied although in both cases the body axes remain fixed. In the case of two wheels the reaction wheel absorbs the effect of the torque impulse while the momentum wheel does not move. For the gimballed wheel system the torque causes the wheel to precess while the body remains fixed. This is illustrated in Figure 4.5-5.

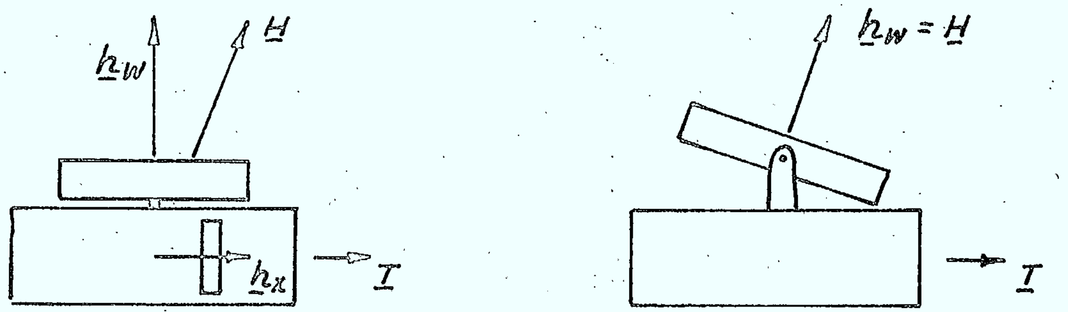

FIG. 4.5-5 EXTERNAL TORQUE RESPONSE

In spite of the fact that the momentum wheel response is different for both systems, the body axis motion is the same and this is the only characteristic that matters. From a theoretical standpoint the systems are virtually equivalent. The weights for both are also very nearly equal. There appears to be a small weight advantage for the gimbal for momentum under 10 ft.lb.sec. and a small penalty above this level. Sperry

6/CHW/4

indicates that the MODEL 1 momentum wheel weight increases by about 5 lb. when a gimbal is added and 7 lb. for the larger MODEL 15. Figure 4.5-6 gives the weights as a function of angular momentum.

In terms of reliability the reaction wheel system would seem to have the advantage since there is an independent backup for each device with moving parts. Therefore, if a reaction wheel fails the backup wheel can be used, while using the original momentum wheel. A backup momentum wheel is still available for use at a later time.

A similar redundancy situation may also be obtained with the gimballed wheel by mounting redundant wheels on a platform which in turn is driven with series gimballs.

4.6 Fixed Momentum Wheel Plus Yaw Axis Reaction Wheel

In this section we present a system with a single fixed momentum wheel and a small reaction wheel mounted on the yaw axis as shown in Figure 4.6-1. The principals of operation are identical to those discussed in Section 4.4 for the roll axis wheel. Also, the control system block diagram is, to the level of this presentation, unaltered and will not be repeated here. The operational differences are due simply to the fact that the wheel is mounted on the yaw axis instead of the roll. As a result, accelerating the wheel in this case causes a roll attitude change as shown in Figure 4.6-2. Therefore, the capability exists with this system to do offset roll pointing, which is usually much more desirable than offset yaw pointing.

Whereas the roll axis wheel performs well as a nutation damper, the yaw axis wheel does not. This is due to the fact that the yaw wheel reaction torque causes an initial nutational motion which cannot be detected by the roll horizon sensor. By appropriately filtering the horizon sensor output,

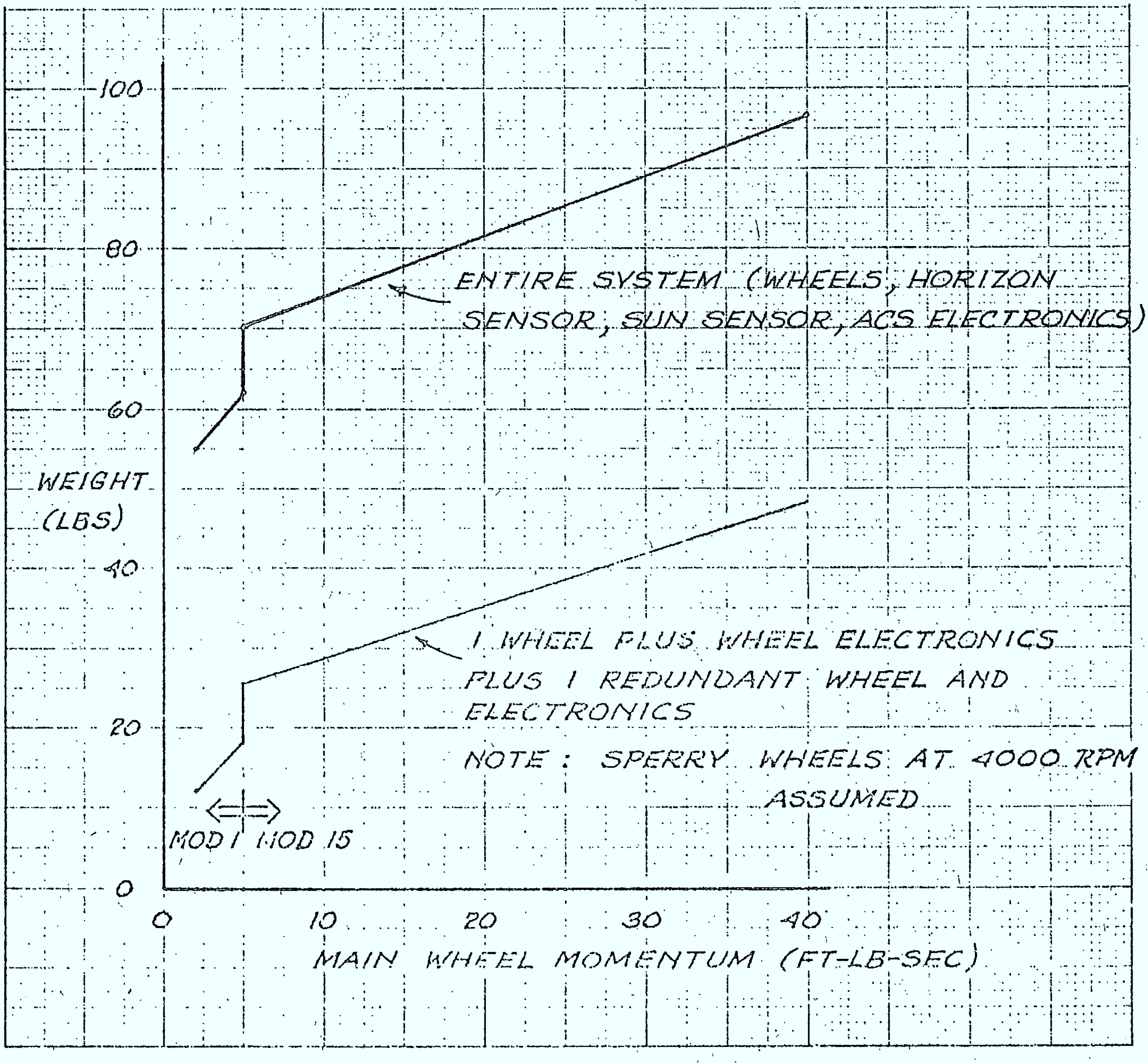

WEIGHT OF SINGLE GIMBALLED WHEEL SYSTEM VS. ANGULAR MOMENTUM

FIG. 4.5-6

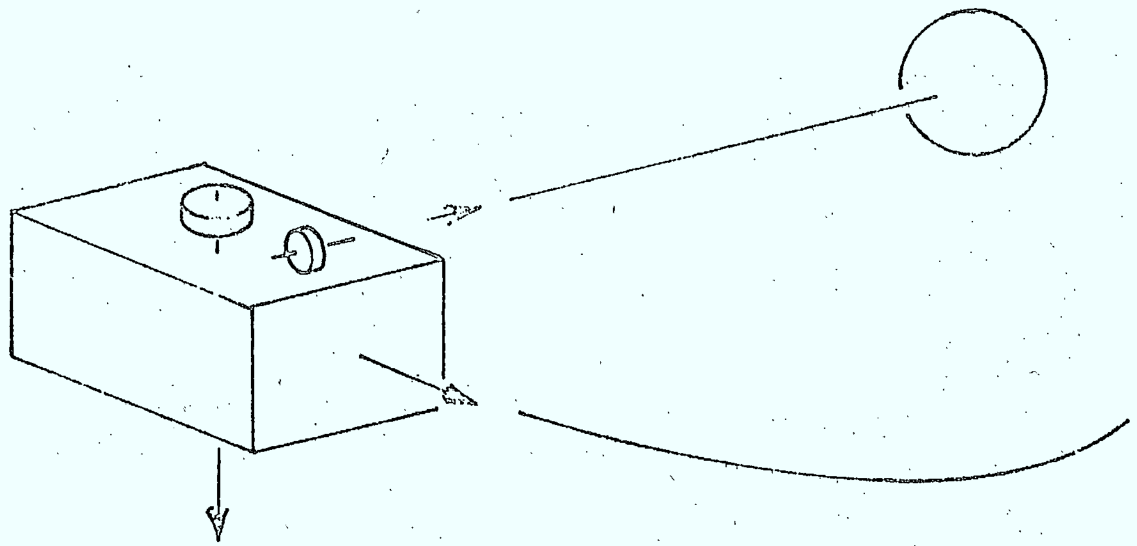

FIG. 4.6-1 FIXED MOMENTUM WHEEL PLUS YAW REACTION WHEEL

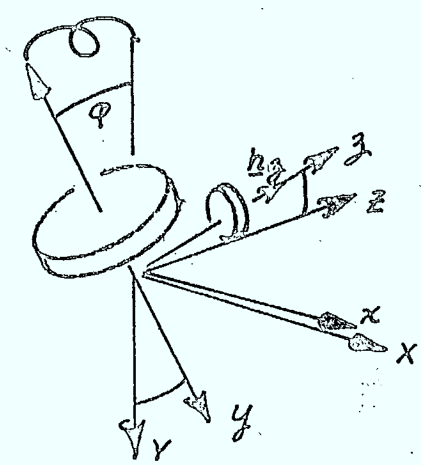

FIG. 4.6-2 ROLL ATTITUDE CHANGE DUE TO YAW AXIS WHEEL

however, a control signal can be obtained to drive the reaction wheel in opposition to nutation. Therefore a weak, but for some missions acceptable, nutation damping results.

The yaw wheel performs similarly to the roll wheel in absorbing the effects of (yaw) external torques for short periods of time. As with the former system, the wheel must be periodically unloaded to prevent roll-yaw errors due to orbit motion. The same hardware is assumed for the yaw wheel system as for the roll wheel system and therefore the weight data of Section 4.4 applies here.

4.7 Roll Gimballed Momentum Wheel

Performance which is virtually identical to the yaw axis wheel system can be obtained by gimballing the momentum wheel about the roll axis. (See Figure 4.7-1) The principles of operation of gimballed wheels were presented in Section 4.5 and will not be repeated here. The weight data and the reliability discussion in that section apply also to this system.

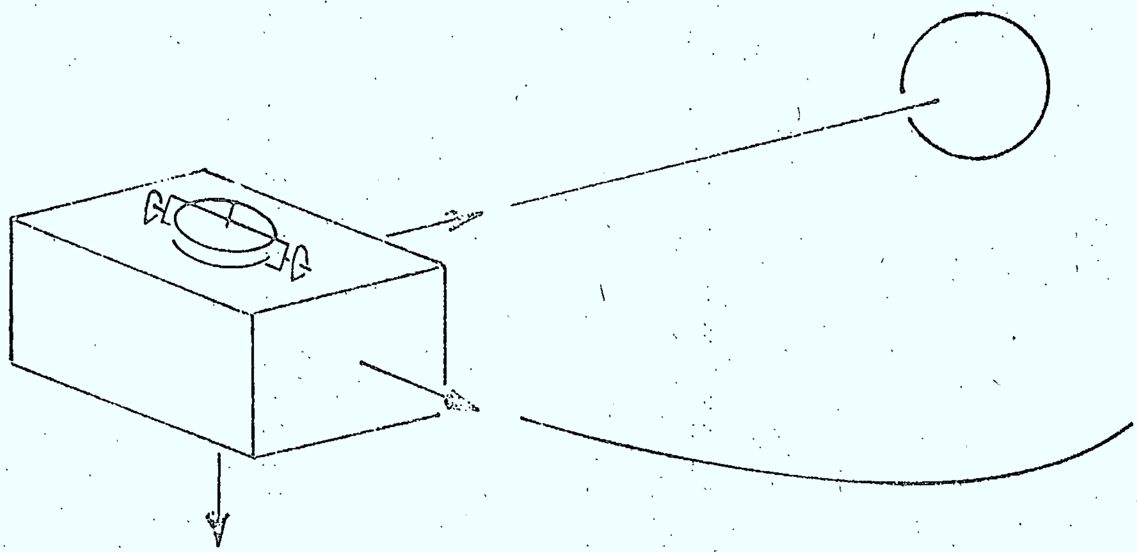

FIG. 4.7-1 ROLL GIMBALLED MOMENTUM WHEEL

6/CHW/6

4.8 Fixed Momentum Wheel Plus Roll and Yaw Reaction Wheels

It has been pointed out that there are certain advantages to be gained from adding a reaction wheel to the roll or yaw axis of a fixed momentum wheel system. The roll axis wheel is an efficient nutation damper, provides offset yaw pointing, and temporarily compensates for roll axis external torques.

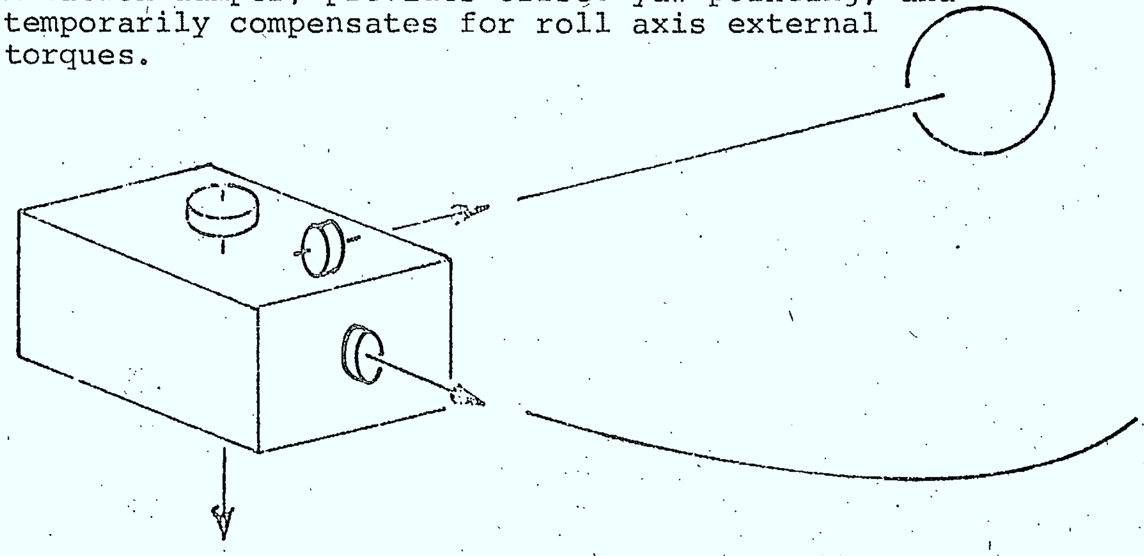

FIGURE 4.8-1 - FIXED MOMENTUM WHEEL PLUS ROLL AND YAW REACTION WHEELS

With a reaction wheel on the yaw axis offset roll pointing and temporary compensation of roll external torques can be accomplished. The system considered in this section, illustrated in Figure 4.8-1, utilizes both a roll and yaw axis reaction wheel. The obvious advantage of such a design is to incorporate the best features of each of the single wheel systems in one package, i.e., offset roll and yaw pointing and efficient nutation damping. What is not so obvious is the improved performance obtained by "orbit decoupling" and "nutation decoupling", two forms of control which require momentum storage on both the roll and yaw axes. We will now discuss these two techniques starting with orbit decoupling.

5/CS/1

When a roll or yaw external torque acts on the vehicle for a period of time an inertially fixed component of the total angular momentum will lie in the orbit plane. If this angular momentum is initially stored internally in a momentum wheel the vehicle attitude can remain unperturbed for a short period of time. However, as the earth pointing orientation is maintained the orbit plane component of momentum alternately appears on different vehicle axes. Figure 4.8-2 illustrates the vehicle motion relative to the momentum component $\underline{H}_T$, where we have assumed that initially all the transverse momentum is along x. If there is no capability for changing the stored angular momentum the vehicle will develop a rate about the body axis that is instantaneously aligned with $\underline{H}_T$, resulting in attitude errors. The single reaction wheel systems previously discussed can store momentum on only one axis and therefore cannot compensate for these orbit motion induced errors. As was mentioned, these systems must be unloaded to prevent the attitude errors from growing. However, with wheels on two different axes the inertially fixed momentum can be exchanged back and forth between the wheels while the vehicle attitude is unperturbed.

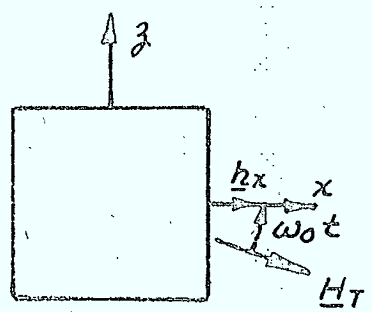

FIGURE 4.8-2 - VEHICLE ROTATION RELATIVE TO INDUCED COMPONENT OF MOMENTUM

5/CS/2

To determine the wheel commands necessary to accomplish this, consider the following. The vehicle angular momentum in body coordinates is:

$$\underline{H} = (I_x \omega_x + h_x)\hat{\underline{x}} + (I_y \omega_y - h_W)\hat{\underline{y}} + (I_z \omega_z + h_z)\hat{\underline{z}}$$

where h_x and h_z are the x and z axis wheel momentum. For zero attitude errors we can also write:

$$\underline{H} = H_T(\cos \omega_o t \; \hat{\underline{x}} - \sin \omega_o t \; \hat{\underline{z}}) - h_W \hat{\underline{y}}$$

(See Figure 4.8-2). Equating these two expressions gives:

$$I_x \omega_x + h_x = H_T \cos \omega_o t$$

$$I_y \omega_y - h_W = - h_W \quad \Longrightarrow \quad \omega_y = 0$$

$$I_z \omega_z + h_z = - H_T \sin \omega_o t$$

To eliminate vehicle attitude errors we require $\omega_x = \omega_y = \omega_z = 0$ and therefore the wheels must be controlled as follows:

$$h_x = H_T \cos \omega_o t$$

$$h_z = - H_T \sin \omega_o t$$

When the wheels are driven in this manner the stored momentum is "decoupled" from the orbit motion and this technique is therefore called "orbit decoupling". By implementing this control the momentum dumping intervals can be greatly expanded since the only limiting factor is the momentum storage capacity of the wheel. If the wheels are sized to handle all of the cyclic torques then momentum dumping due to only the secular torques is required and a minimum amount of control fuel will be required. Typically, momentum dumping is handled automatically by firing a thruster when a wheel speed reaches an upper limit.

5/CS/3

When no yaw sensing is available the WHECON concept can be employed with this system to control yaw errors. This is accomplished by commanding a yaw motion whenever a roll correction is made. As was discussed in Section 4.3 the WHECON system using a single fixed momentum wheel had two disadvantages. First, in order to provide rapid yaw damping, large yaw errors could result from an initial roll error. Second, to eliminate large nutational motions the control torque cannot be very great and as a result roll errors cannot be removed rapidly. Both of these characteristics are due to the nutation that causes roll motion to turn into yaw motion. Using the technique of "nutation decoupling" the nutational motion can be partly or wholly eliminated. To make use of the WHECON concept, when no yaw sensing is desired, the nutational coupling that turns roll errors into yaw errors is eliminated but not vice versa. That is, yaw is necessarily still coupled into roll. When nutation is decoupled in this manner fast roll corrections are possible without causing large yaw errors. Consider the case of the basic WHECON design without nutation decoupling. A thruster torque $\underline{T}$, offset by an angle α, causes an initial motion which is mostly in roll. However, the gyroscopic torques turn this into a yaw motion and the large nutation results.

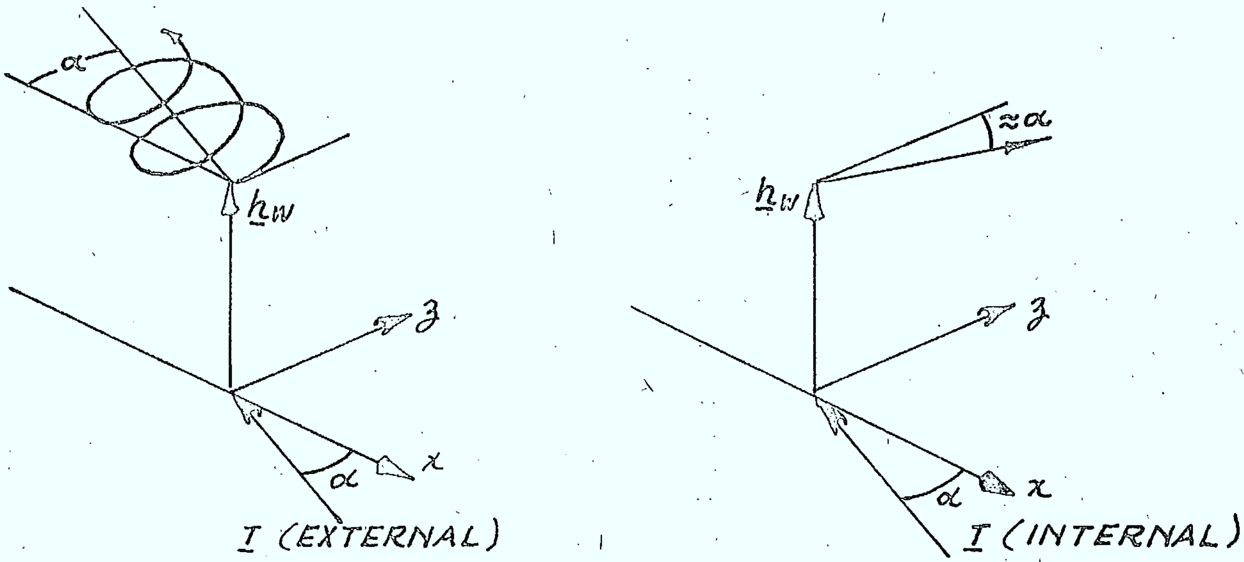

No Nutation Decoupling (WHECON with thrusters)

With Partial Nutation Decoupling (2 Reaction Wheels)

FIGURE 4.8-3

5/CS/4

The accompanying precession due to the external torque causes a large net yaw motion and a small net roll correction. Now consider the case of the two reaction wheel systems when the roll to yaw nutation is eliminated. The torque T is now an internal reaction torque and causes a roll motion without any nutation. The end result is that the path of the wheel axis is straight instead of coning and the resulting roll correction is rapid.

Now let us consider how yaw errors are damped out when nutation decoupling is employed. Figure 4.8-4 shows a correction from an initial pure roll error ϕ_o. A control torque drives roll quickly to the deadband edge where a small yaw error exists.

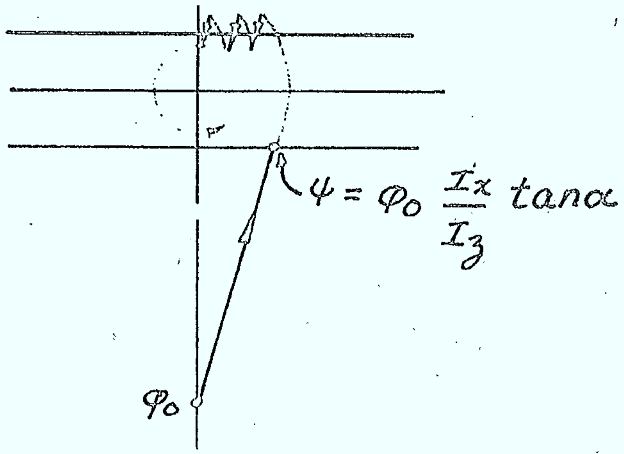

FIGURE 4.8-4 - CORRECTION FROM INITIAL ROLL ERROR AND YAW DAMPING

The nutation coupling still present from yaw to roll causes the opposite roll deadband to be exceeded and a control to be applied. The resulting motion quickly damps the yaw error. This damping is much faster than for the WHECON system since the rate induced by the reaction torque can be much larger than the thruster torque and the motion through the deadband is faster with the wheel system. This is due to the fact that in the case of WHECON the deadband motion occurred at

5/CS/5

orbit rate but with the reaction wheels it occurs at nutation frequency which is much higher. Finally, as the figure illustrates, an initial roll error ϕ_o produces a small maximum yaw error $(\psi = \phi_o \frac{I_x}{I_z} \tan\alpha)$, where α is usually small. Recall that for the WHECON system a large yaw error results $(\psi = -\phi_o \cot\alpha)$.

If yaw sensing is available the nutation can be completely decoupled. If this is done rapid yaw corrections can also be made and true three-axis control results. In such a mode the system behaves much like the low momentum all reaction wheel system discussed in Section 5.0.

As is the case for the three reaction wheel system discussed in Section 5.0 it is not necessary to have a separate backup reaction wheel for each of the two roll-yaw wheels, nor is it necessary that any wheel be mounted on either the roll or yaw axis. All that is required for the system to operate is the ability to create independent momentum components on the roll and yaw axes. This can be done, for example, by utilizing any two of the three skewed wheels shown in Figure 4.8-5.

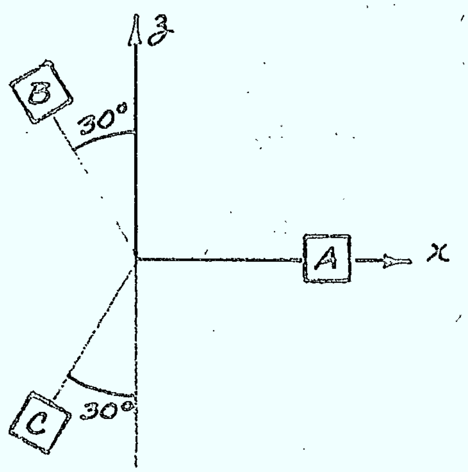

FIGURE 4.8-5 - REDUNDANT REACTION WHEELS

5/CS/6

The third wheel, that is initially not used, therefore acts as a backup for a failure of either of the primary wheels. To illustrate how two wheels can provide the desired roll-yaw momentum, consider Figure 4.8-6, which uses wheels A and B. A roll axis momentum is obtained simply by using wheel A. A yaw axis momentum h_z requires using both wheels, where the momentum in wheel A is

$h_A = \frac{1}{\sqrt{3}} h_z$ and the momentum in wheel B is

$h_B = \frac{2}{\sqrt{3}} h_z$. If wheel A failed, then we can use wheels B and C, as in Figure 4.8-7. For a roll momentum we have

$h_B = h_C = -h_x$ and for a yaw momentum

$h_B = -h_C = \frac{2}{\sqrt{3}} h_z$.

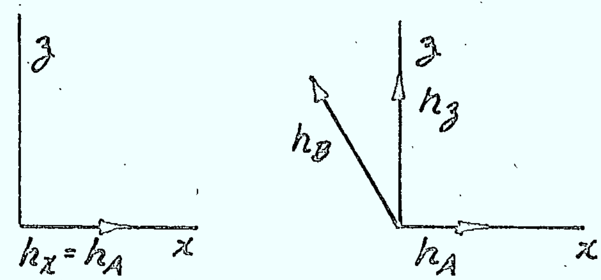

Pure Roll Momentum　　　Pure Yaw Momentum

FIGURE 4.8-6 - ROLL OR YAW AXIS MOMENTUM FROM WHEELS A AND B

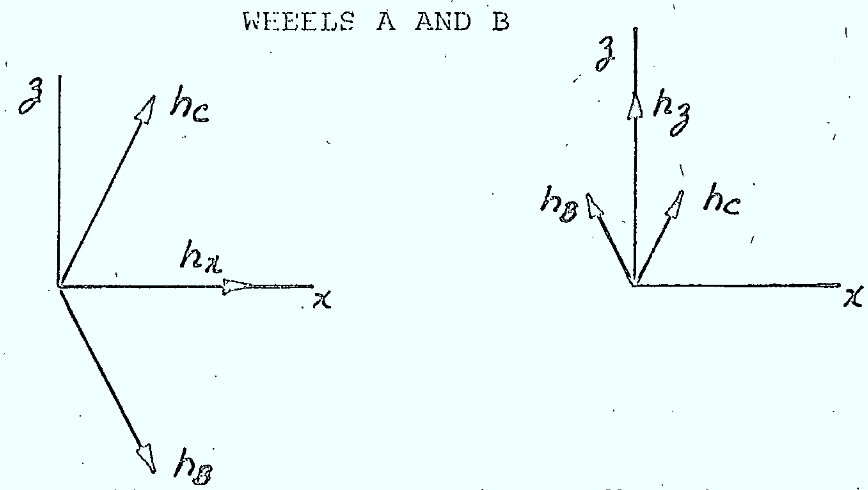

Pure Roll Momentum　　　Pure Yaw Momentum

FIGURE 4.8-7 - ROLL OR YAW AXIS MOMENTUM FROM WHEELS B AND C

In the case of the single reaction wheel systems discussed in Sections 4.4 and 4.6 a one ft.lb.sec. momentum capacity was rather arbitrarily assumed. Those systems lacked orbit decoupling and hence only a small amount of stored momentum could be tolerated. For the system discussed in this section the use of orbit decoupling allows the storage of a large amount of momentum and a more rational choice of reaction wheel capacity is necessary. In the following section the double gimballed momentum wheel will be discussed and a comparison of the relative advantages of the two systems will be made. To form a common basis for a weight comparison it is desirable to compare systems with the same main wheel momentum as well as roll-yaw momentum storage capacity. Typically double gimballed wheels have gimbal angle ranges of about 20 degrees and therefore the available momentum in either the roll or yaw axis is

$h_{R,Y} = h_W \sin 20° = 0.342\ h_W$. This relationship will be used to size the reaction wheels for the weight data presented in this section.

Curves of system weight versus main wheel angular momentum for the partially and fully redundant systems are presented in Figures 4.8-8 and 4.8-9.

To the author's knowledge this system has not been proposed for a satellite control system to date. The reason for this is probably that the extra advantages over the basic WHECON design, in terms of rapid roll and yaw corrections and offset pointing capability, have not been required for past missions. It seems quite likely that for future missions, involving steerable payloads and large flexible appendages that require rapid control, this system will be a prime candidate.

5/CS/8

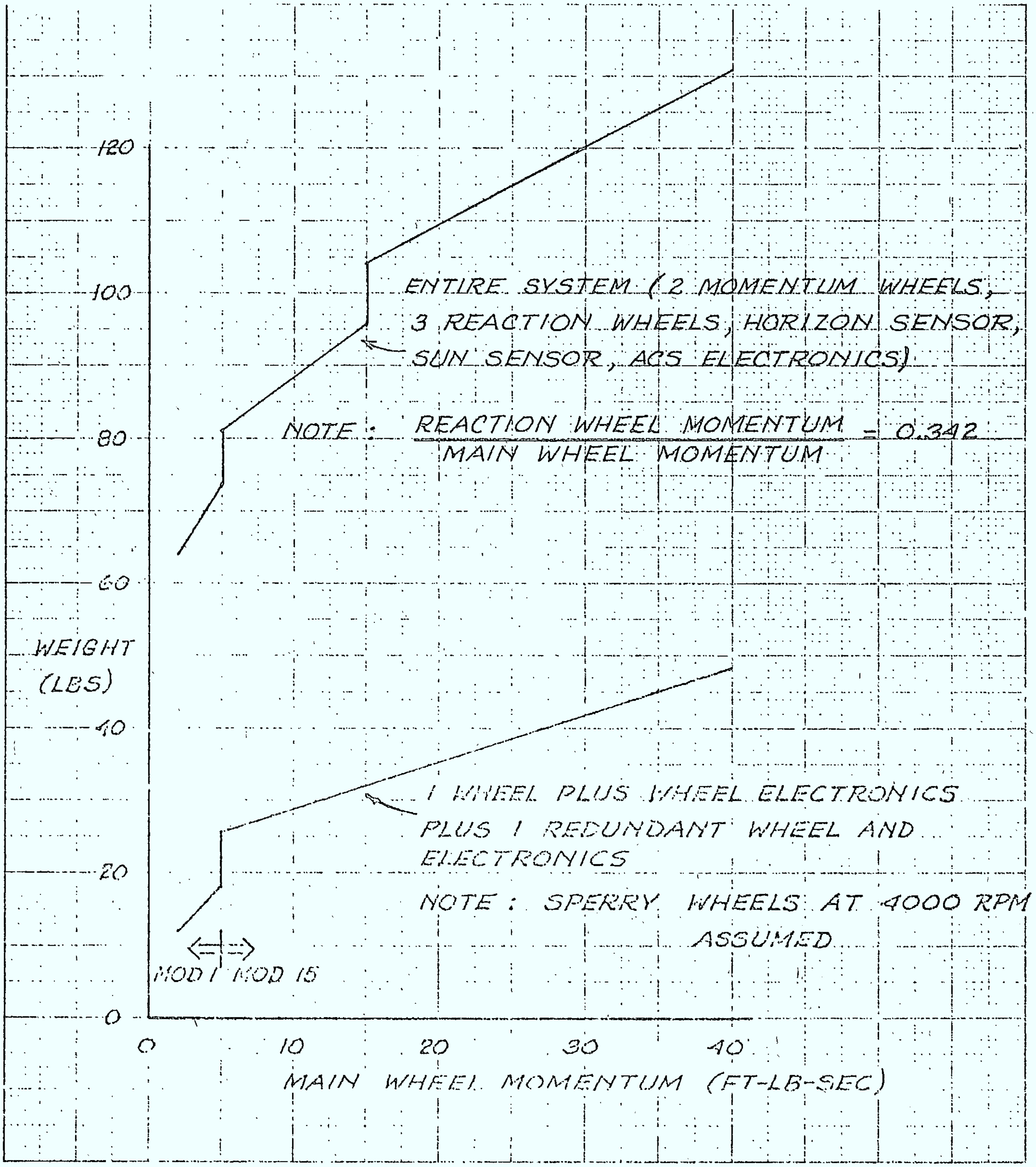

FIGURE 4.8-8 - WEIGHT OF FIXED MOMENTUM WHEEL PLUS ROLL AND YAW REACTION WHEEL SYSTEM VS. ANGULAR MOMENTUM (PARTIALLY REDUNDANT)

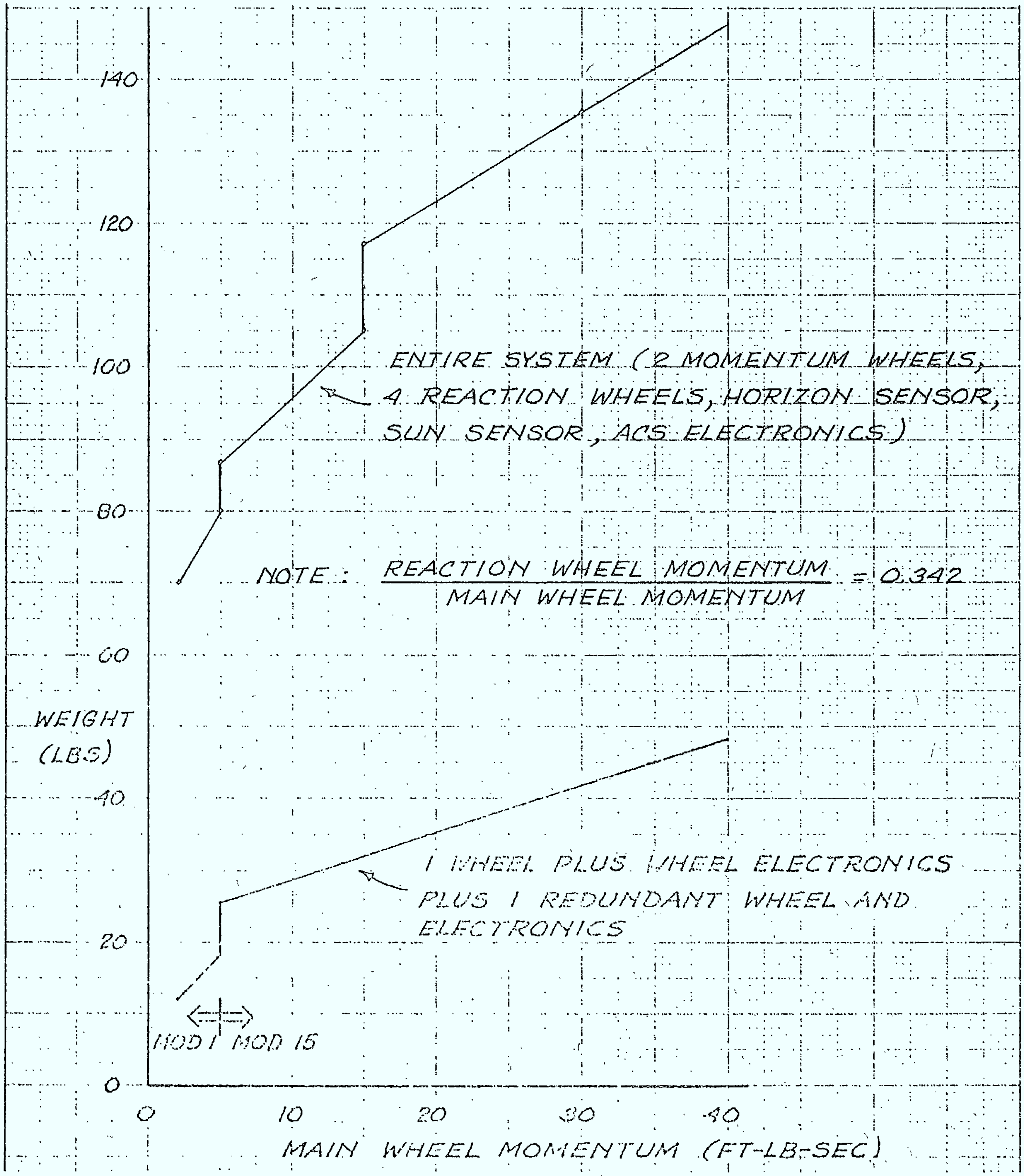

FIGURE 4.8-9 - WEIGHT OF FIXED MOMENTUM WHEEL PLUS ROLL AND YAW REACTION WHEEL SYSTEM VS. ANGULAR MOMENTUM (FULLY REDUNDANT)

4.9 Double Gimballed Momentum Wheel

In Section 4.5 the equivalence of a reaction wheel and a gimballed momentum wheel was discussed. Similarly, the two reaction wheel system discussed in the last section is equivalent to a momentum wheel mounted on two gimbals as shown in Figure 4.9-1. The preceeding analysis assumes that an x and z axis component of momentum, h_x and h_z, can be supplied by the controller, where

$h_x = J_x\Omega_x$, $h_z = J_z\Omega_z$, the J's being the wheel inertias and Ω's their spin rates. All of the discussions in the last section apply to the double gimballed wheel if one relates the momentum components to gimbal angles, i.e.,

$$h_x = h_w\gamma$$

$$h_z = -h_w\delta$$

for small angles. (See Figure 4.9-1).

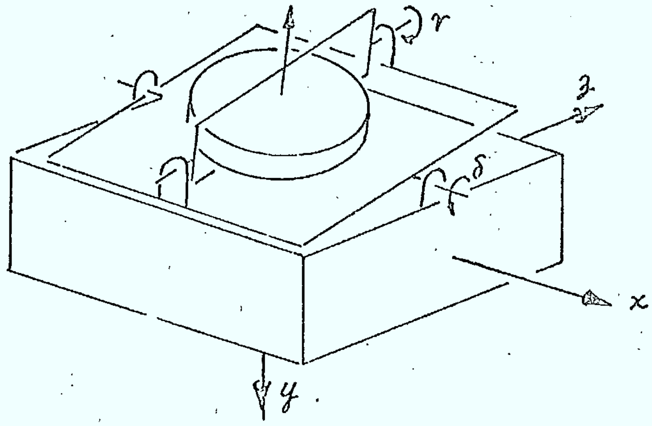

FIGURE 4.9-1 - DOUBLE GIMBALLED MOMENTUM WHEEL SYSTEM

The weight of a redundant double gimbal wheel system as a function of angular momentum is presented in Figure 4.9-2. As with the WHECON system, the ACS electronics weight is assumed to be 18 lb. and the horizon and sun sensor weight is 15 lb. A

5/CS/9

Sperry Model 30 wheel is assumed for prime and backup. By comparison with the reaction wheel system discussed in the previous section it is seen that the gimballed wheel design is somewhat lighter than the partially redundant and considerably lighter than the fully redundant system.

However, for the same reasons as mentioned in Section 4.5 for the single gimbal versus single reaction wheel comparison, the overall reliability of the redundant double gimbal system appears to be worse than if reaction wheels are used.

The double gimballed wheel has been given much attention in the open literature from Lockheed and TRW (See References 3 and 4). To the author's knowledge, however, the system has not been flown to date.

5/CS/10

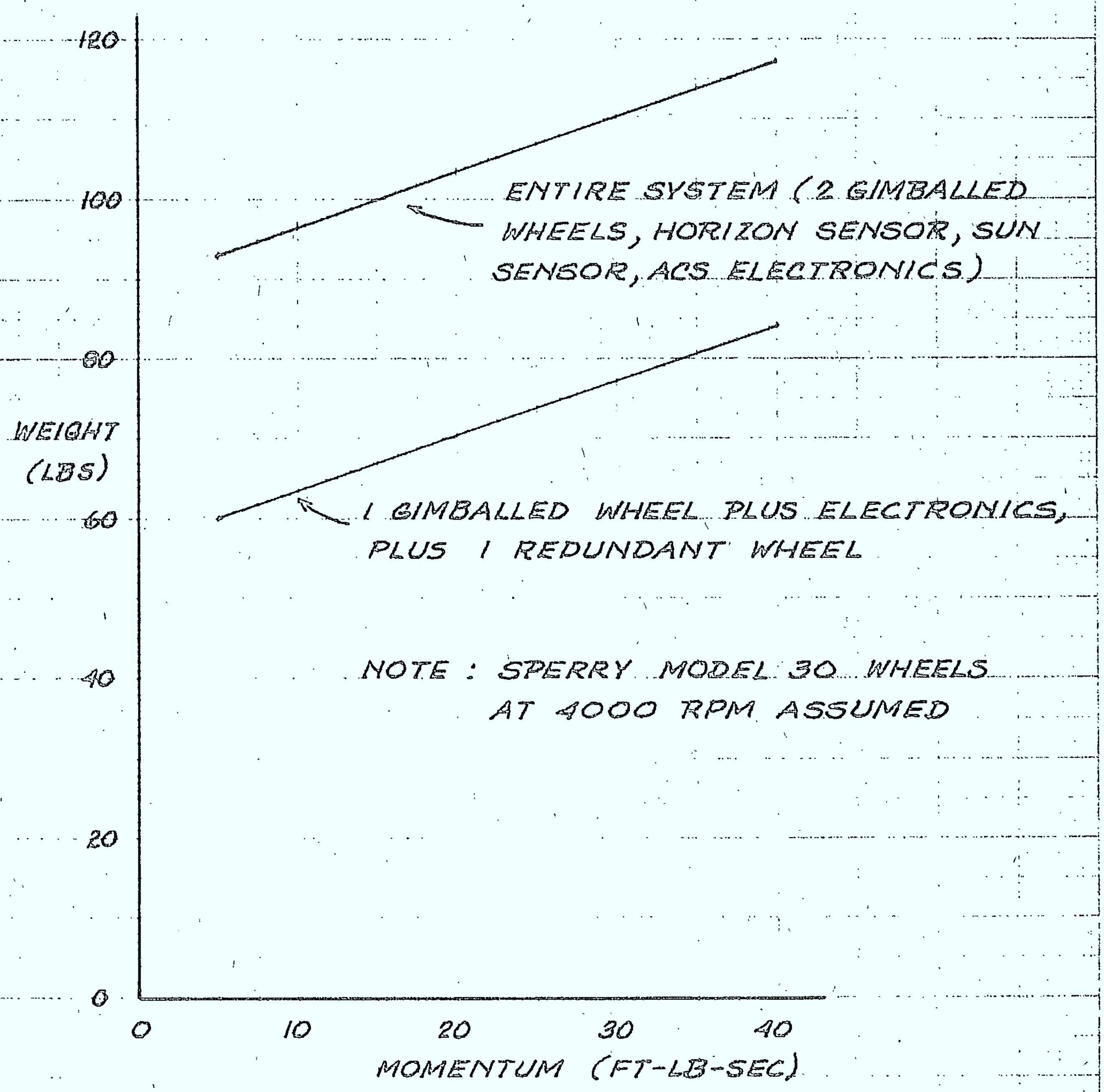

FIGURE 4.9-2 - WEIGHT OF DOUBLE GIMBALLED MOMENTUM WHEEL SYSTEM VS. ANGULAR MOMENTUM

4.10 Impact of Magnetic Bearing Wheels

The development of momentum and reaction wheels with bearings consisting of a magnetic suspension is currently being pursued by Sperry as well as other companies. The main advantage is high reliability which translates into weight savings due to elimination of redundant wheels. Furthermore, the possibility exists of using the wheel as a gyro by taking advantage of the bearing compliance. This feature would most likely be utilized for yaw sensing during stationkeeping manoeuvers.

Precise data is not available at this time on the weight of a magnetically supported wheel but it appears that it will be about the same as ball bearing wheels. Since it would seem that the development of a gimballed magnetic bearing wheel is not in the near future, the system using a fixed momentum wheel plus roll-yaw axis reaction wheels, all magnetically supported, would be a more viable option.

4.11 Summary

In this section we will summarize the main characteristics of the momentum bias systems discussed in this chapter. The weight of the various systems versus the momentum wheel angular momentum is presented in Figure 4.11-1. Data corresponding to magnetic bearing wheels is also presented, where it is assumed that a magnetic bearing wheel weighs the same as a ball bearing one and redundancy is eliminated. The performance characteristics are now reviewed:

Fixed Momentum Wheel-Ground Command Correction

- Minimum on-board hardware - high reliability
- Potential for high accuracy using sophisticated ground software
- No offset roll or yaw pointing

Fixed Momentum Wheel-Offset Jets (WHECON)

- Initial roll errors cause large yaw errors
- No offset roll or yaw pointing
- Proven system at low altitudes

Fixed Momentum Wheel Plus Roll Axis Reaction Wheel or Yaw Axis Gimbal

- Limited short term compensation of external torques
- Rapid nutation damping
- Offset yaw pointing
- Gimbal system less reliable than reaction wheel system and not compatible with magnetic bearings

5/CS/12

Fixed Momentum Wheel Plus Yaw Axis Reaction Wheel or Roll Axis Gimbal

- o Limited short term compensation of external torques
- o Limited nutation damping
- o Offset roll pointing
- o Gimbal system less reliable than reaction wheel system and not compatible with magnetic bearings

Fixed Momentum Wheel Plus Roll and Yaw Reaction Wheels or Double Gimballed Momentum Wheel

- o Long term external torque compensation using orbit decoupling
- o Rapid roll and yaw response using nutation decoupling
- o Initial roll errors do not introduce large yaw errors
- o Offset roll and yaw pointing
- o Gimbal system less reliable than reaction wheel system and not compatible with magnetic bearings
- o Superb three axis control using yaw sensing.

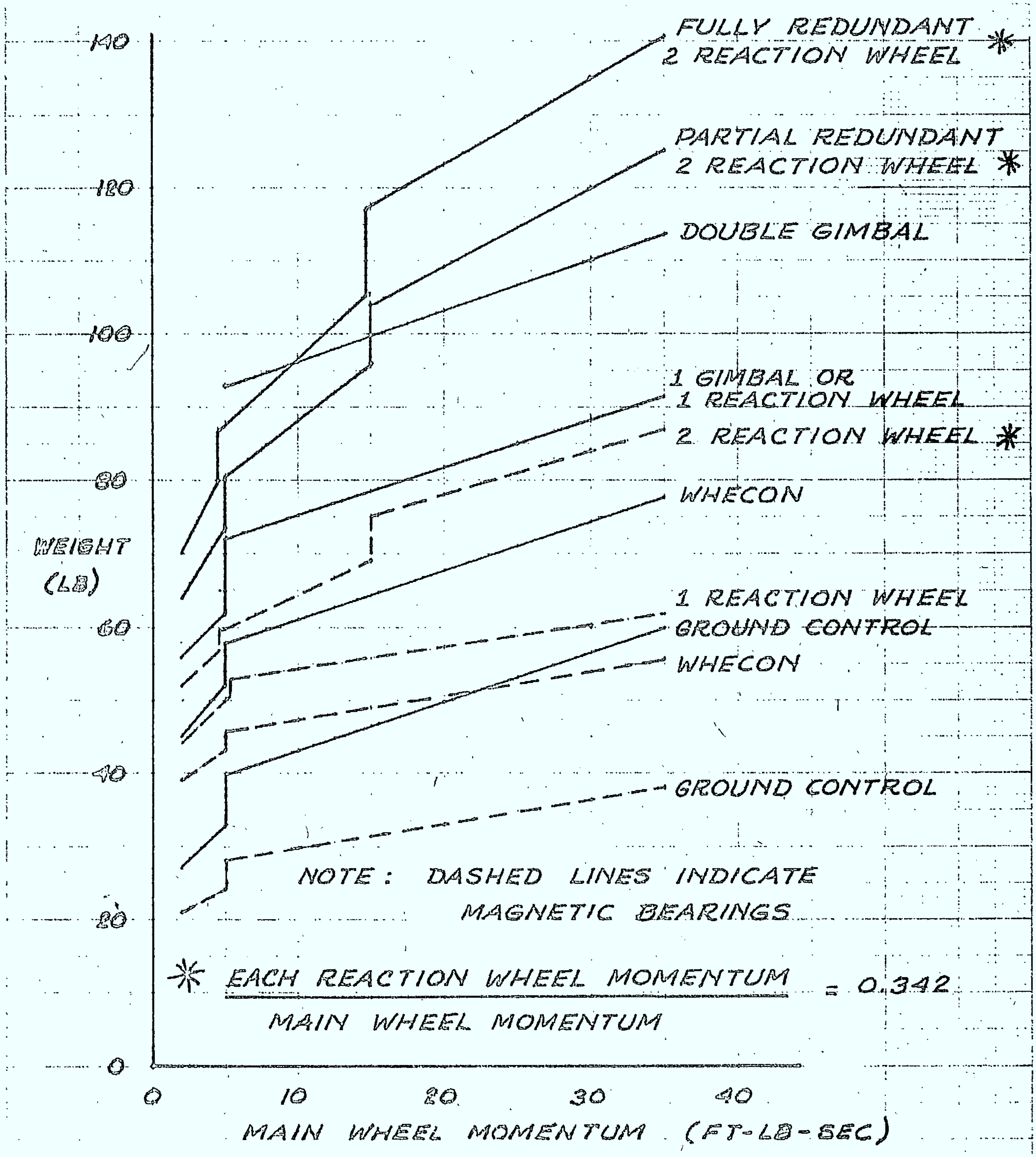

FIGURE 4.11-1 - WEIGHT OF MOMENTUM BIAS SYSTEMS VS. ANGULAR MOMENTUM

5.0 LOW MOMENTUM (REACTION WHEEL) ATTITUDE CONTROL SYSTEM

The low momentum or reaction wheel control system may be considered a degenerate form of the system discussed in Section 4.8 above, in which the pitch wheel is small with a nominal zero angular momentum. Systems with three wheels have been used on numerous flight spacecraft and systems employing four or more wheels in a skewed configuration have been considered.

5.1 Basic Three Wheel System

The basic three wheel system which is illustrated in Figure 5.1-1 is conceptually very simple. Correction torques are applied about each axis independently through the reactions resulting from a change of wheel speed. Due to the pitch orbit rate (ω_o), some gyroscopic coupling exists between the roll and yaw wheels, such that a periodic interchange of momentum takes place between these wheels. This interchange can be allowed to take place simply through completely independent control of each wheel. Alternatively, the orbit motion may be decoupled within the controller. In their simplest (approximate) form, the dynamic equations for the roll and yaw axes are:

$$I_x \ddot{\phi} = T_x - (\dot{h}_x - \omega_o h_z)$$

$$I_z \ddot{\psi} = T_z - (\dot{h}_z + \omega_o h_x)$$

Thus, if the change in angular momenta is:

$$h_x = T_x{}^c + \omega_o h_z$$

$$h_z = T_z{}^c - \omega_o h_x$$

With $T_x{}^c$ = required roll control torque

$T_z{}^c$ = required yaw control torque

the decoupling will occur. Figure 5.1-2 is a block diagram for such a configuration.

6/CHW/7

OSR

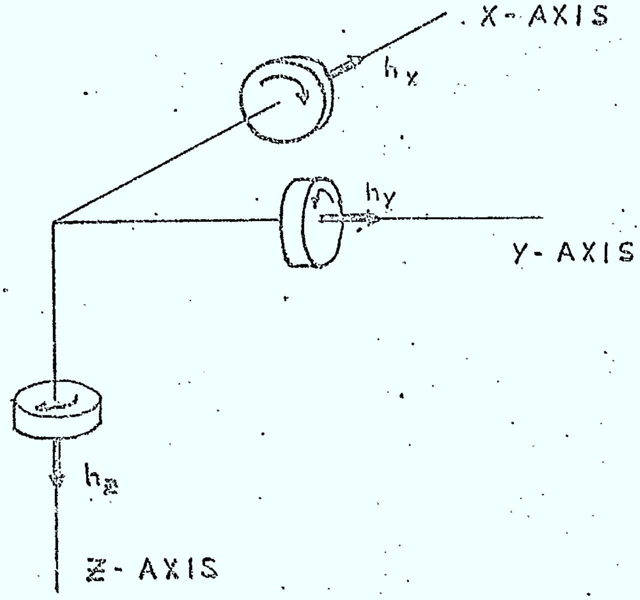

FIG. 5.1-1 BASIC THREE WHEEL CONFIGURATION

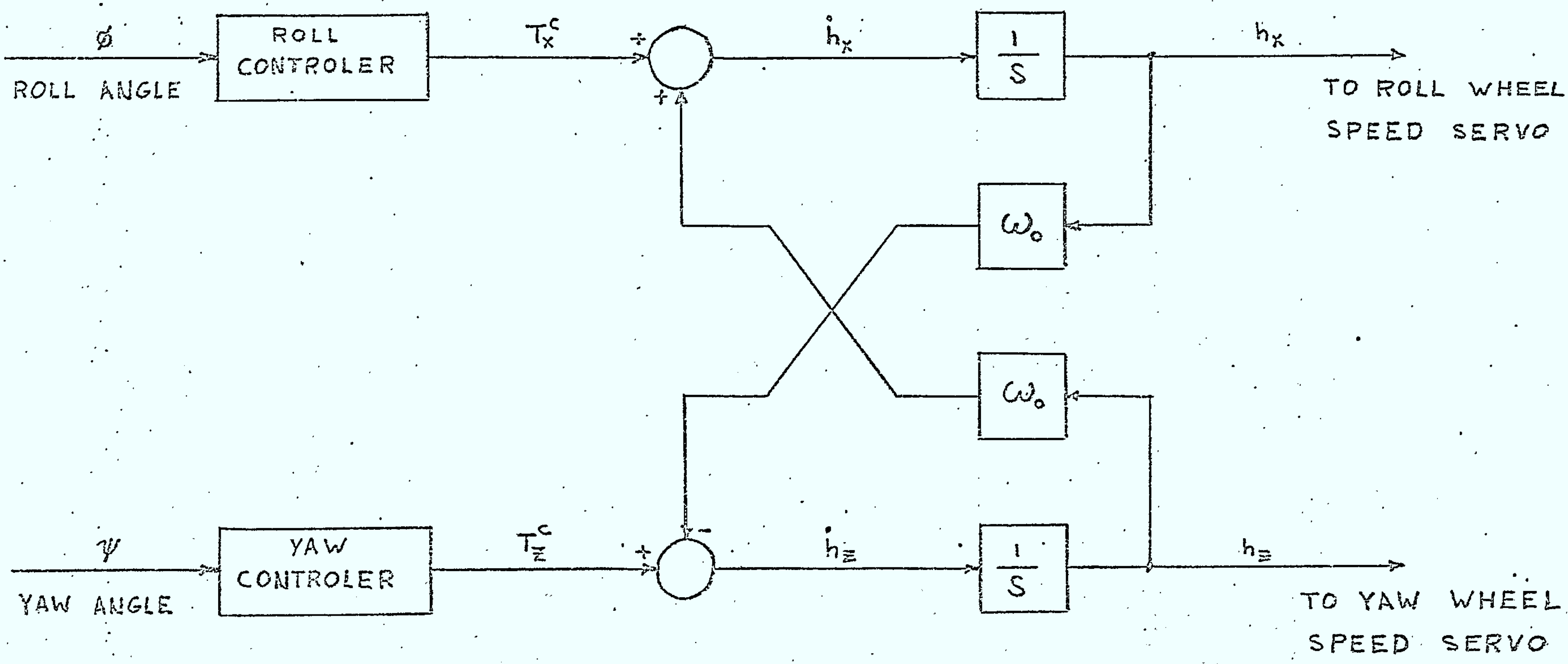

FIG 5.1-2 BLOCK DIAGRAM OF ROLL/YAW DECOUPLING

The normal function of the reaction wheel control system is to provide an accurate and smooth control as well as a temporary storage of angular momentum. At periodic intervals, the stored momentum may reach the wheel saturation limit, at which time momentum must be removed with thrusters. However, it is noteworthy that periodic disturbance torques will cause the wheels to store momentum for half the disturbance period, but then will remove this momentum during the subsequent half period. Thus, only the non-periodic (secular) components of the disturbance torque will result in the use of thruster fuel.

A distinct disadvantage of the reaction wheel control system is the necessity to sense all three attitude errors. Yaw sensing on a continuous basis is a particularly difficult problem.

5.2 Skewed Wheel Modifications

For long life spacecraft missions, a single wheel about each axis represents a potential single point failure. Complete redundancy could be assured by simply using two wheels about each axis, however this can impose a severe weight penalty. Alternately it is feasible to consider four wheels mounted along non-orthogonal axes. In this way, any three of the wheels would produce a resultant angular momentum about each of the three principle control axes. Operationally only three wheels would be used at any one time, with the fourth wheel retained in a non-running standby mode. At periodic intervals, the standby configuration would be permuted resulting in a uniform wheel usage.

Reliability can be further enhanced with five wheels in a skewed arrangement. Six skewed wheels could provide a very high degree of redundancy.

6/CHW/8

6.0 ZERO MOMENTUM (THRUSTER) ATTITUDE CONTROL SYSTEMS

The true zero momentum system includes no means for the temporary storage of externally applied angular momentum. All control is exercised through thrusters. This implies that even the periodic disturbance which can be readily absorbed with wheels, must be overcome through the thruster of a zero momentum system, with a fuel consumption penalty. Only where the fuel penalty is less than the weight of wheels, is the zero momentum system a practical alternative. However, this system does have the advantage of simplicity.

6.1 Mass Expulsion Limit Cycle Control Systems

All control axes are decoupled for the zero momentum system. It is therefore sufficient to consider the control of a single axis only.

The major parameter of interest for this configuration is the long term fuel consumption. Since all mass expulsion thrusters are capable of producing only a discrete minimum impulse, three types of steady limit cycle motions are possible as depicted in Figure 6.1-1. The limit cycle period and daily impulse expenditure for each case can be readily calculated, using the following parameters.

I = Moment of Inertia of the axis under consideration (slug ft.^{2})

D_b = Control deadband (deg.)

L = Thruster moment arm (ft.)

I_b = Thruster minimum impulse bit (lb. sec)

ω_o = Orbit rate (rad/sec)

T_d = Disturbance torque (ft. lb.)

Case (a)

$$\text{Period} = \frac{8\ I}{L\ I_b} \frac{(D_b)}{(57.3)} \text{ seconds}$$

6/CHW/9

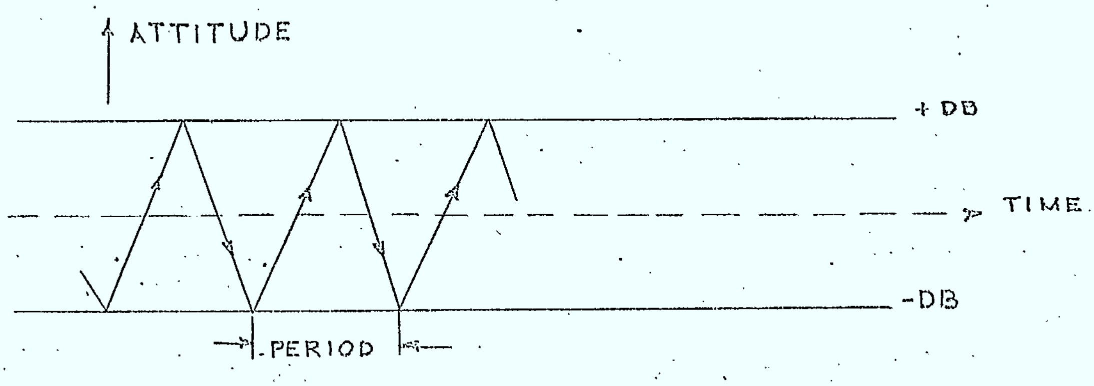

(a) TORQUE FREE LIMIT CYCLE MOTION

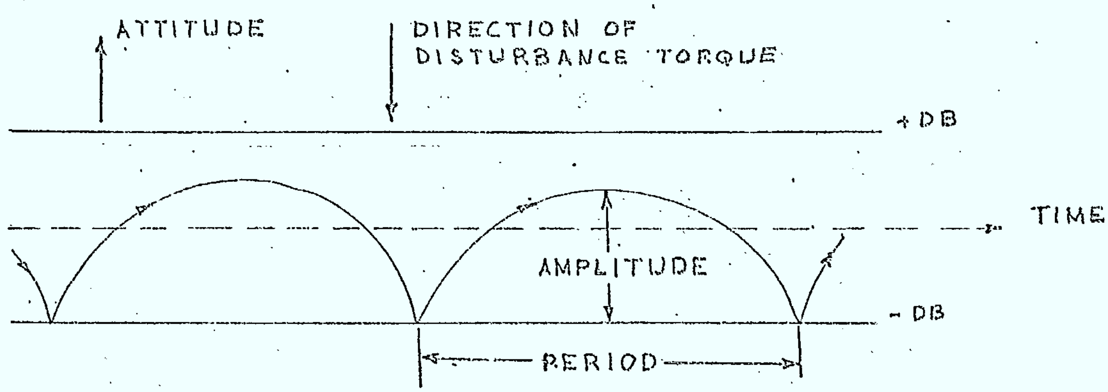

(b) SCALLOP MOTION WITH DISTURBANCE TORQUE

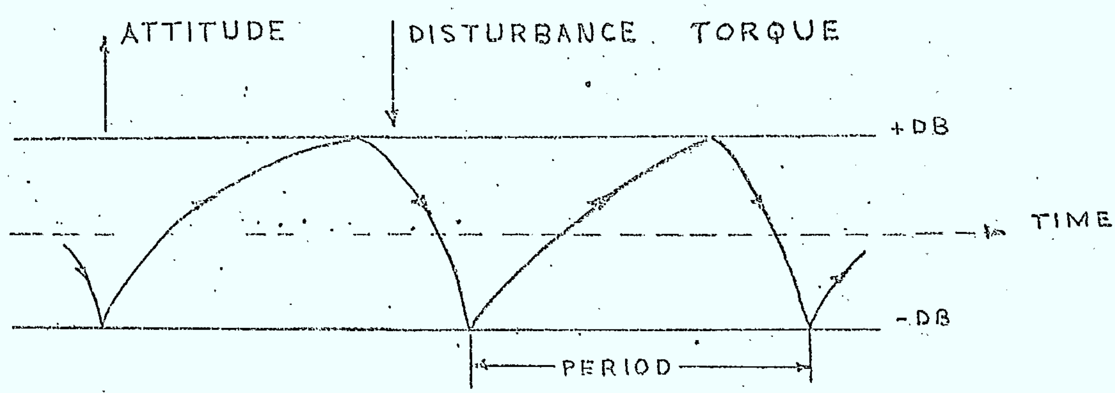

(c) LIMIT CYCLE MOTION WITH DISTURBANCE TORQUE

FIG 6.1-1 ZERO MOMENTUM LIMIT CYCLES

$$\text{Impulse Rate} = \frac{2\pi}{\omega_o} \; \frac{(57.3)}{(D_b)} \; \frac{L\,I_b^2}{4\,I} \quad \frac{\text{lb. sec}}{\text{day}}$$

Case (b)

$$\text{Amplitude} = \frac{57.3}{8} \; \frac{(I_b L)^2}{I\,T_d} \quad \text{deg.}$$

$$\text{Critical Torque } T_d^* = \frac{57.3}{D_b} \; \frac{(I_b\,L)^2}{16\,I}$$

$$\text{Period} = \frac{I_b\,L}{T_D} \quad \text{sec.}$$

$$\text{Impulse Rate} = \frac{2\pi}{\omega_o} \; \frac{T_D}{L} \quad \frac{\text{lb. sec.}}{\text{day}}$$

Case (c)

$$\text{Period} = \frac{L\,I_b}{2\,T_D}\left[\sqrt{1 + \frac{T_D}{T_D^*}} - \sqrt{1 - \frac{T_D}{T_D^*}}\right]$$

$$\text{Impulse Rate} = \frac{2\pi}{\omega_o} \; \frac{4\,T_D}{L\,I_b} \; \frac{1}{\sqrt{1 + \frac{T_D}{T_D^*}} - \sqrt{1 - \frac{T_D}{T_D^*}}}$$

It will be noted that the equations for case (a) are in fact the limiting forms of case (c) for $T_D \rightarrow 0$. Transistion from (b) to (c) occurs at T_D^*.

When the disturbance torque is slowly varying, periodic at orbit rate for example, the impulse rate must be obtained by integration.

A realistic example could be:

$I_b = 2 \times 10^{-3}$ lb. sec.
$L = 2$ ft.
$T_D = 10^{-5} \cos \omega_o t$ ft. lb.
$I = 800$ slug ft.
$D_b = 0.1$ deg.

In this case $T_D^* = 7.2 \times 10^{-7}$ ft. lb., so that T_D is less than T_D^* for only approximately 5% of the orbit. The daily impulse expenditure is then approximately 0.28 lb. sec. per day, which for a specific impulse of 100 sec. amounts to approximately 6 lbs. of fuel for a 6 year mission, quite competitive with a reaction wheel weight. This competitive position is highly dependent on the minimum impulse available from a thruster since the fuel consumption will grow approximately as the square of the minimum impulse.

6.2 Electric Propulsion (Low Thrust Level) Control Systems

The minimum impulse attainable with certain types of electric or ion propulsion systems can indeed be made quite small thus satisfying a basic requirement for a competitive zero momentum control system. Perhaps of greater interest is the fact that electric propulsion engines are vectorable, either electrostatically or mechanically. Thus, a north-south stationkeeping electric thruster could be vectored in such a manner that control torques as well as stationkeeping forces may be obtained. With the very large specific impulse inherent with electric propulsion, it is conceivable that a non-wheel control system could be feasible, at least for missions with stringent and long term station-keeping requirements which dictate the use of electric propulsion.

7.0 YAW SENSING AND STATIONKEEPING

7.1 The Yaw Sensing Problem

The majority of primary attitude sensors are optical, using visible or infra-red radiation from heavenly bodies for attitude reference. Earth orbiting satellites can readily measure roll and pitch angles through direct reference to the earth's infra-red horizon. However, since the yaw angle is a rotation about a line joining the earth and satellite, a yaw measurement cannot be performed with the earth as reference, at least not with optical sensors.

A number of alternate reference sources have been used or proposed for yaw measurement. At present, no "universally" accepted technique has been adopted for spacecraft control, and in fact, the biased momentum control systems have been specifically designed in order to circumvent the yaw sensing problem. However, even these systems require some form of yaw sensing during periods of orbit adjust thruster activity when perturbation torques can be substantial.

7.2 Continuous and Intermittent Yaw Sensing

Yaw sensing may be performed using the sun, a star, another spacecraft or other reference source. The sun is probably the simplest source to use though it cannot provide a continuous yaw reference directly. For biased momentum control systems this is often quite adequate. However, the zero and low momentum systems require continuous yaw sensing and where very tight tolerances are to be maintained on the orbital elements, even the biased momentum systems may require continuous yaw sensing.

7.2.1 Yaw Measurement With A Sun Sensor

The sun does provide a reference from which yaw angles may be measured. When the sun is near the dawn and evening terminators, a sun sensor can provide quite an accurate yaw measurement. In the noon and midnight orbit positions, particularly during the equinox seasons, the sun lies on the

6/CHW/12

yaw axis, and yaw angles cannot be measured. Between these two extremes, a yaw angle may be calculated using a sun sensor output, though the accuracy degrades as the satellite approaches the noon and midnight positions.

At least two possible methods of yaw computation may be performed, the "T-B" method and the "A-B" method. Figure 7.2.1-1 shows the sun sensor geometry for either method. For the T-B method the yaw angle is calculated from:

$$\psi = \frac{1}{\cos B} (T - T_O + \phi \sin B)$$

where: ψ = calculated yaw angle
ϕ = roll angle (from earth sensor)
T = sun elevation (from T-B sun sensor)

T_O = Nominal sun elevation angle, either calculated on board or transmitted via telemetry.

B = Sun azimuth angle, obtained from the sun sensor with cos B, sin B calculated on board, or cos B, sin B transmitted via telemetry.

This method has the advantage that T_O and B vary slowly and a single telemetry update during a stationkeeping maneouver is adequate to maintain accuracy. The accuracy obtained with this method may be obtained from:

$$\Delta\psi \approx \frac{1}{\cos B} (\Delta T + \Delta T_O) + \Delta\phi \tan B$$

where $\Delta\psi$ = error in yaw measurement

ΔT = error in sun elevation measurement

ΔT_O = error in computation of nominal sun elevation angle

$\Delta\phi$ = error in measured roll angle

67/CHW/13

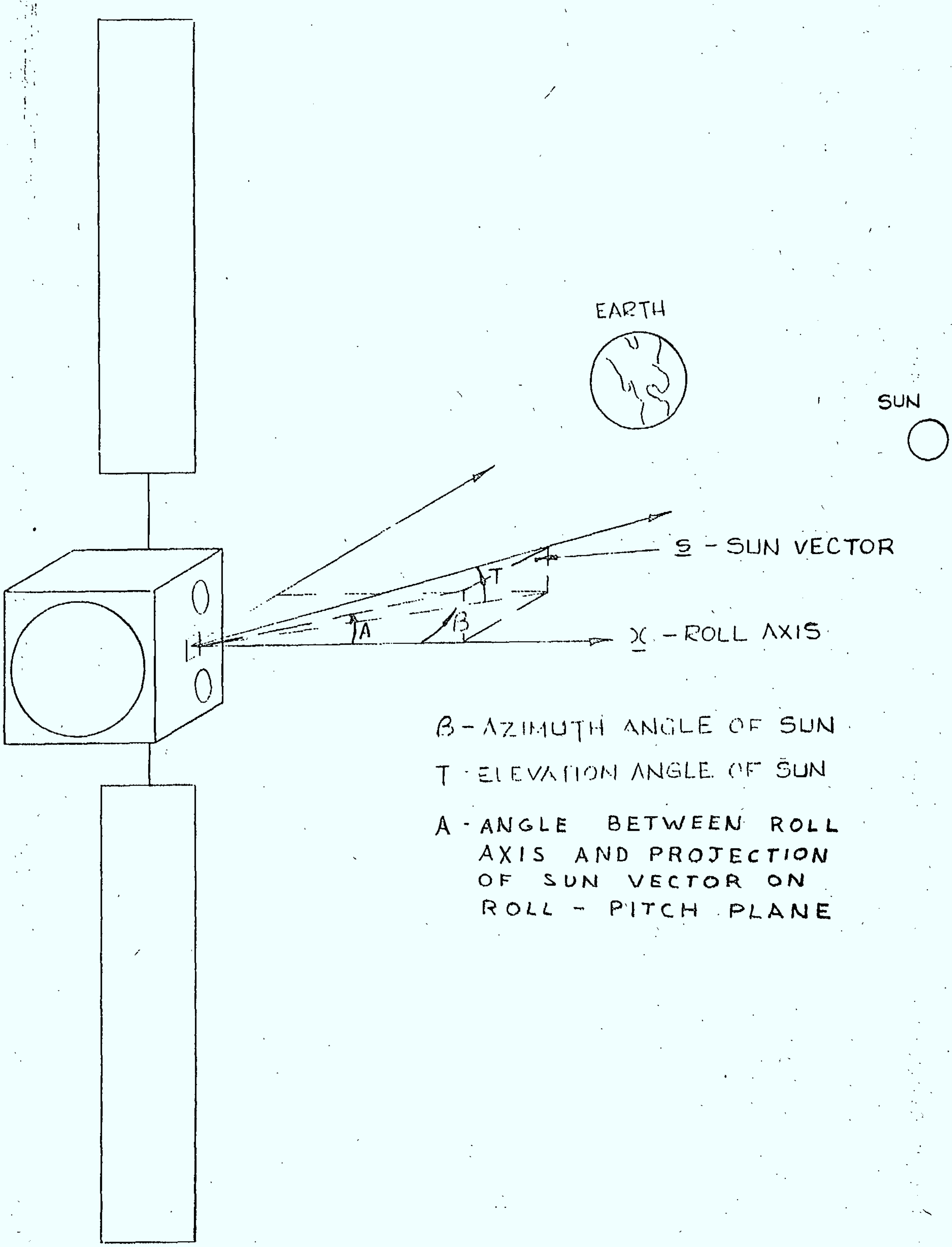

FIG. 7.2.1-1 SUN SENSOR GEOMETRY

This error relation is plotted in Figure 7.2.1-2. It will be noted that as B approaches 90° (noon or midnight position) the yaw measurement error grows without bound, and in general this technique of yaw measurement cannot be used within ± 30° of these two singular points.

For the A-B method, the yaw angle may be calculated from:

$$\psi = A - A_o + \tan B \cos A_o \, (\phi \cos A_o - \theta \sin A_o)$$

A = angle between the roll axis and the projection of the sun vector on the roll-pitch plane (from A-B sun sensor).

A_o = nominal value of A.

θ = pitch angle (from earth sensor).

B, ϕ = as defined previously.

It is noted that considerably more computation is required for this method and the angle A_o is rapidly varying. As with the T-B method, the accuracy using the A-B method degrades rapidly near noon and midnight.

7.2.2 Filling the Gap Inertially

The yaw sensing gap near noon and midnight may be filled using a rate integrating or strapdown gyro system. One such implementation is shown in Figure 7.2.2-1, where the sun sensor is used only at the dawn and evening terminator to correct for gyro drift. This implementation uses the gyro throughout the orbit as the basic continuous yaw sensor.

Since gyros tend to have a relatively short lifetime a continuous inertial yaw gyro sensor is probably not viable for the zero or low momentum control systems. However, for a biased momentum system, where yaw sensing is only required intermittently during stationkeeping maneouvres, a yaw gyro can

6/CHW/14

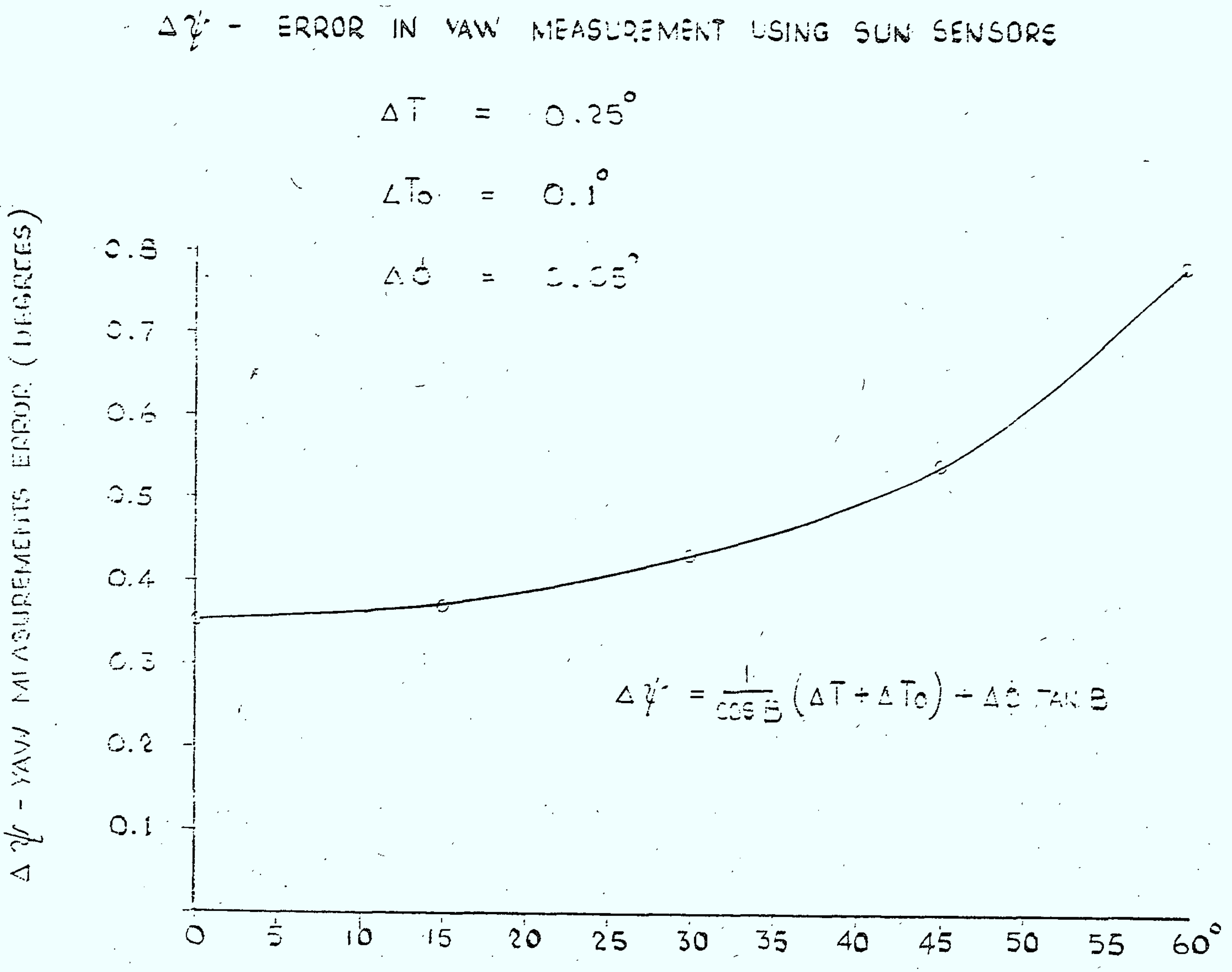

FIG. 7.2.1-2 B - AZIMUTH ANGLE (DEGREES)

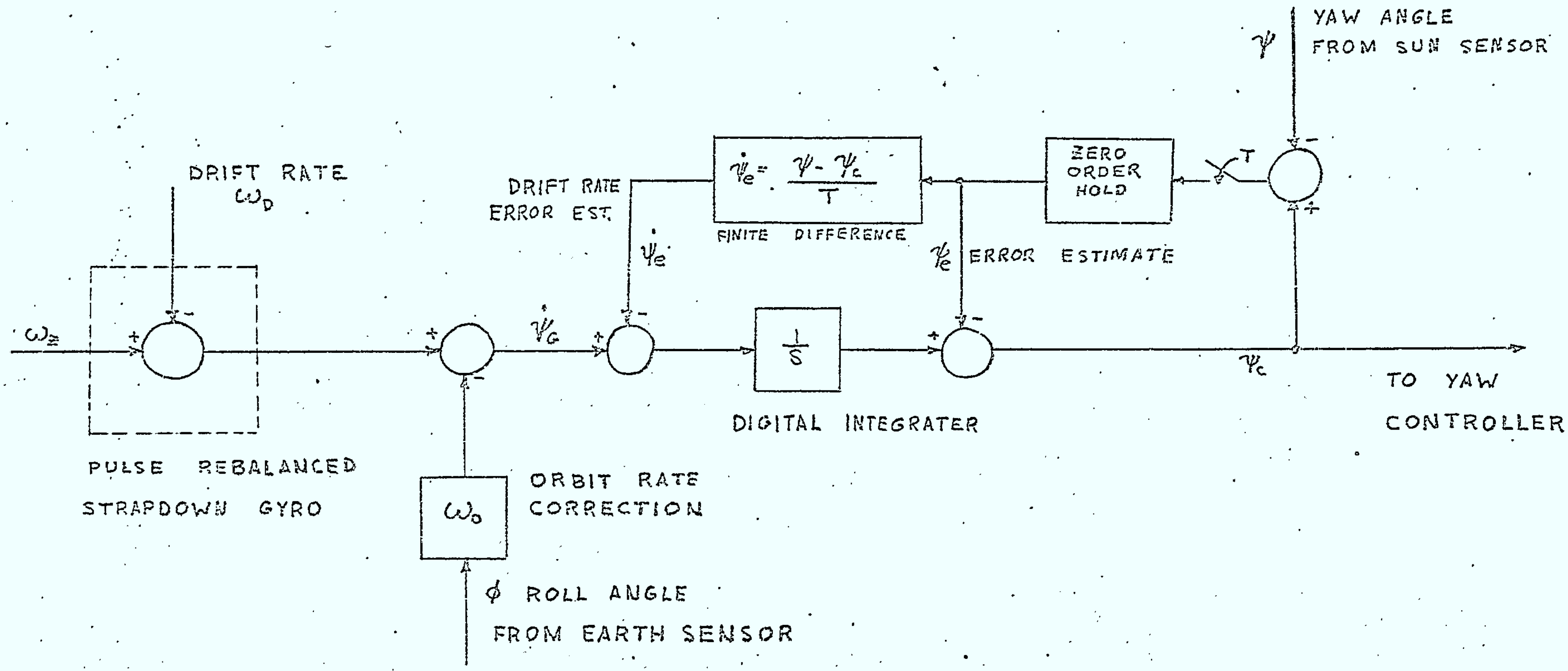

FIG 7.2.2-1 YAW GYRO PLUS SUN SENSOR YAW SENSING SYSTEM

be a viable sensor. In fact, it is only during the solstice seasons that yaw sensing would be required during the sun sensor gap. With a 21 day orbit adjust cycle, and ± 60° field-of-view sun sensor, the yaw gyro would be required for only 6 days per year, at the most. This amounts to less than 900 hours and 36 start-stop cycles in a 6 year mission, well within the lifetime of standard gyros.

7.2.3 Polaris As A Yaw Reference

Polaris, the North star, provides a direct reference for continuous yaw measurement using a star tracker. Star trackers, though providing a means for very accurate yaw sensing, are relatively heavy instruments which can lose lock on the reference star when reflective particles pass through the field-of-view or when reflections from the spacecraft solar arrays enter the tracker telescope. In addition, coordinate transformations are required to correct for the relative motion between polaris and the earth spin axis as well as the orbit normal. Consequently, for most applications under consideration, star trackers have not proved to be viable yaw sensors.

7.2.4 The Two Spacecraft Method

A potential means of yaw sensing which perhaps has not received sufficient study is the use of two (or more) satellites in the same orbit, each satellite using the other as yaw reference source. Each satellite would contain a microwave beacon and microwave sensor. Direct and continuous yaw measurement could result from such a configuration.

7.2.5 The Microwave Attitude Sensing System

The Microwave Attitude Sensing System (MASS) which was conceived and partially developed by the Communications Research Centre, provides a very attractive means for sensing yaw. Two methods of yaw sensing have been considered. One method often referred to as "MECO" (Monopulse and Earth Sensor Combination) employs an earth sensor which measures roll and pitch errors with respect to the

6/CHW/15

earth's centre at the sub-satellite point, and the MASS which measures similar orthogonal angles with respect to a beacon at a point on the earth separated from the sub-satellite point. A rotation about the yaw axis results in different outputs from the two sensors so that after some computation, the yaw angle may be calculated. Accuracies better than 1° may be obtained with this method, though two different sensors, each redundant for a long term mission, are required.

The other method employs a MASS which measures polarization angle (POLANG). With a beacon operating near 14 GHz, Faraday rotation through the atmosphere is sufficiently small that yaw accuracies better than 0.5° can apparently be obtained. The use of MASS with POLANG would result in a single sensor capable of measuring continuously roll, pitch and yaw thus making this a very attractive sensing system.

7.3 The Effect of Intermittent Yaw Sensing on Stationkeeping

During orbit inclination correction of a 3-axis satellite, significant perturbation torques may be generated due to misalignment of the thrust vector and migration of the spacecraft centre of mass. Biased momentum control systems contain wheels which are generally sized to accommodate the torques induced by solar pressure, and cannot maintain a yaw accuracy during the orbit maneuvers, and yaw sensors must be employed.

As shown in para 7.2.1 a sun sensor can provide yaw information only intermittently. This part time capability of sun sensors can often be matched to inclination correction operations with little or no penalty in fuel consumption.

The orbit inclination and nodal position can conveniently be represented in terms of the orbit normal vector. The Luni-Solar perturbations tend to precess this vector toward the first point of aries. Optimum re-orientation of this vector requires that inclination thrusting occur at the nodes. During the solstice seasons, the orbit nodes occur within the sun sensor gap. With a $\pm$ 60° field-of-view sun sensor, this sensor gap and inclination control gap exists for 60 days at each solstice. Since the maximum precession rate is nearly 0.003° per day, a total of 0.18° ($\pm$ 0.09°) precession will occur during the gap period. Thus, if the inclination control requirements are greater than $\pm$ 0.09°, optimum inclination control can be achieved, using the sun sensor.

With more stringent inclination control, the orbit adjust periods must be shorter than 60 days. Even in this case however, sun sensors alone may still be used for yaw control with the orbit adjustment during the solstice periods performed at off nodal points with some penalty in fuel consumption. These off nodal adjustments may be optimized to minimize fuel consumption. Figure 7.3-1 depicts an un-optimized adjustment sequence for 0.05° inclination control. Even in this case, the total ΔV penalty for a 6 year mission is about 30 ft/sec which for a 1000 lb. spacecraft is approximately 5 lb. of hydrazine fuel. More stringent inclination control will increase the fuel penalty in a non-linear manner.

POLAR PLOT OF ORBIT NORMAL DIRECTION

DRIFT RATE = .003° PER DAY TOWARD ♈

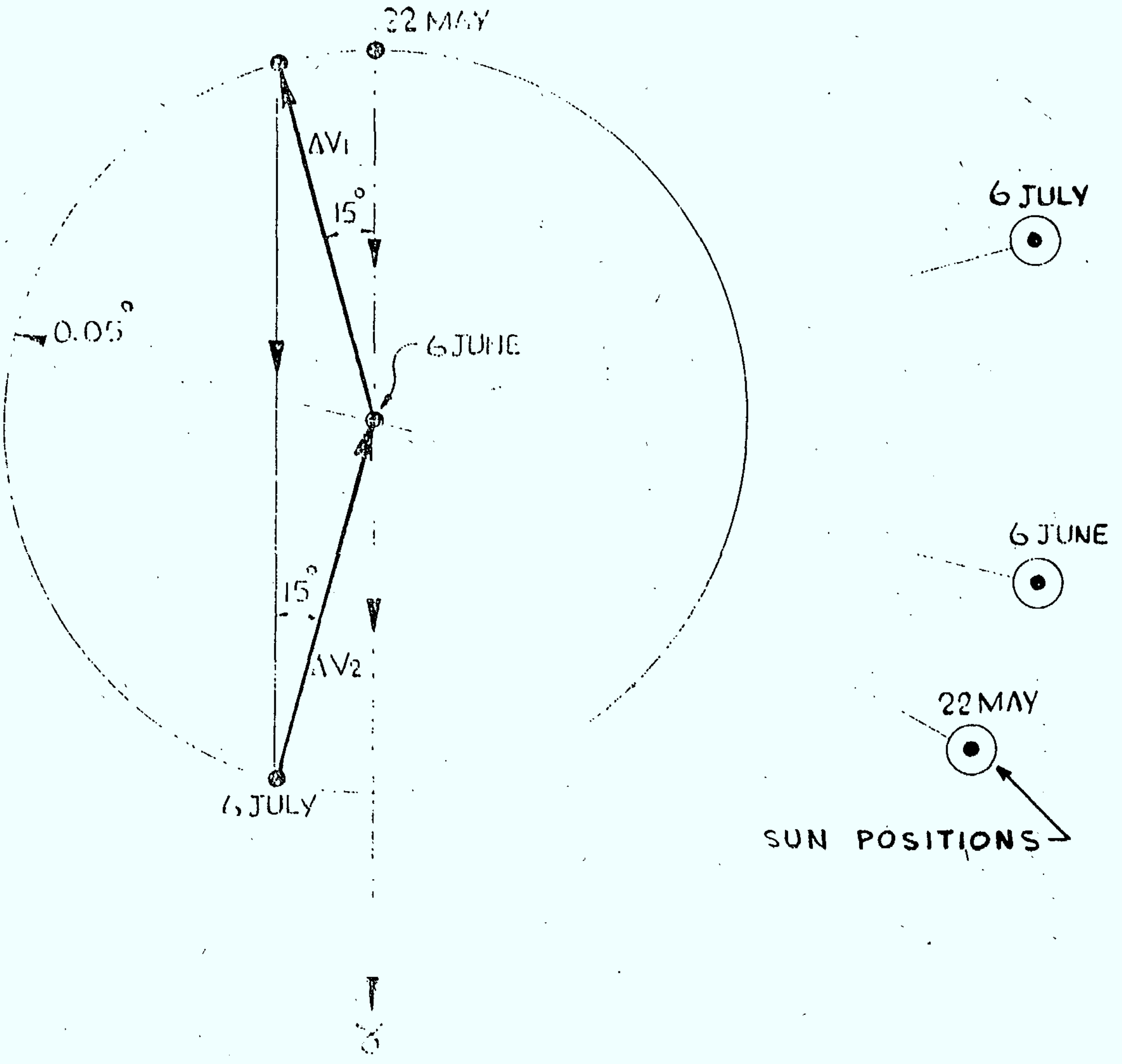

NON OPTIMAL STATION KEEPING PLAN FOR ±.05°

USING ± 60° FOV SUN SENSOR

FIG. 7.3-1

8.0 ATTITUDE CONTROL SYSTEM COMPONENTS

Physically, an Attitude Control System consists of a number of components (sensors and prime movers) configured about a central control unit. The component summary presented herein, is provided as background material for the system comparison of Section 9. More detailed component information is contained in the companion reports, references 5 and 6.

Typically a 3-axis spacecraft control system must provide control functions during three distinct mission phases:

(a) Spin stabilized phase

(b) Attitude Acquisition phase

(c) 3-axis attitude pointing phase

Only those components employed for the latter phase will be considered here.

8.1 Sensors

A variety of sensors have been employed within spacecraft attitude control systems. Yaw sensing techniques have been treated separately in Section 7.0 above and will not be repeated here. Roll and pitch sensors include thermal balance infrared horizon sensors scanning infrared horizon sensors and the microwave attitude sensor.

8.1.1 Thermal Balance Sensors

The thermal balance sensors employ a telescope which creates an image of the earth around which are placed eight equally spaced bolometers. At null attitude, all bolometers are equally irradiated. With an angular error, unequal irradiance occurs and with appropriate sums and difference of the electrical outputs, pitch and roll error signals are generated.

7/CBH/01

Only four bolometers are required to generate the output signal, the eight bolometers providing complete redundancy.

The accuracy attainable with these sensors is generally in the range .04° to 0.1°, at null including a relatively small noise component. With an offset angle of 0.5° the accuracy can degrade to 0.13°. A distinct advantage of these sensors is the relatively low weight of 8-10 lbs. for a highly reliable and completely redundant unit.

8.1.2 Scanning Sensors

The scanning sensor employs a very narrow field-of-view, scanned through a large amplitude by means of an oscillating mirror. The infrared detector output is essentially a rectangular pulse with length proportional to the earth's chord. The angular difference between the pulse centroid and the mirror central position is the attitude error directly in the scan direction, and the chord length is proportional to attitude error in the cross-scan direction.

The scanning sensor accuracy is in the range 0.04° to 0.05° both at null and with an offset in the scan direction. The noise error component is larger for this sensor than for the thermal balance sensor. Two separate units are required for redundancy, with a total weight of 14 lbs.

8.1.3 The Microwave Sensors

The microwave sensor or MASS, referred to in Section 7.0, employs a single corrugated horn from which sum and difference signals are extracted. A very deep trough in the difference signal output at null attitude provides an accurate measure of attitude error when compared to the sum signal. Roll and pitch accuracies better than 0.02° are achievable. With the addition of polarization angle measurement (POLANG), the MASS may be used for continuous yaw measurement.

7/CBH/ 02

Operationally, a ground based beacon is required with this sensor, and in order to overcome a possible loss of beacon signal, it may be necessary to include an infrared sensor as backup.

The advantages of a microwave sensor are numerous, including:

a) Continuous measurement of all three attitude angles.

b) High accuracy.

c) Low noise.

d) No pitch bias required to correct for a change in longitude position.

e) Possible optimization of ground coverage through placement of the ground beacon.

8.2 Wheels

As previously indicated, wheels may be classified as medium momentum (momentum wheels) or low momentum (reaction wheels). Momentum wheels operate about a non-zero nominal momentum and reaction wheels about a nominal zero momentum. A large variety of conventional ball bearing wheels of various sizes have been space qualified and flight proven.

Though proven in space for minimum lengths of two to three years, doubt has been expressed in some quarters that ball bearing wheels can provide an eight year life. As a result, magnetic bearing wheels are under development. These wheels, with no mechanical wearout mechanism, should prove highly reliable and weight effective with redundancy required only in electronic components. It is expected that once flight proven, the magnetic bearing wheels will become a mainstay of attitude control systems.

7/CBH/03

8.3 Controllers

The heart of any attitude control system is the electronic control unit. Initially, most spacecraft control systems used analogue circuitry. With increasing accuracy and mission requirements, there has been a shift toward special purpose digital control units and recently general purpose digital computers are being employed.

8.3.1 Analogue Controllers

Analogue circuits employing operational amplifiers, non-linear circuit elements and passive components, have been used extensively for spacecraft control. Linear compensation networks such as low pass and bandpass filter as well as lead-lag and higher order compensation circuits are readily implemented in analogue form using analogue computer techniques. Special non-linear analogue circuits such as the pseudo-rate controller have been developed to provide lead (rate damping) compensation with pulsed outputs to thruster valves, all within one relatively simple circuit.

Though analogue control circuits have been widely employed, they are subject to errors due to environmental extremes and age. In addition, the circuit time constants required for spacecraft control are generally large, up to several hundred seconds not being unreasonable, resulting in the use of bulky components.

8.3.2 Special Purpose Digital Controller

To overcome some of the difficulties associated with analogue controllers, digital computation is now in general use. Two major types of implementation may be identified, the DDA (Digital Differential Analyzer) and the digital filter (Z-transform implementation).

8.3.2.1 The Digital Differential Analyzer (DDA)

The DDA may be considered as a direct digital equivalent to an analogue circuit where accumulators are used in place of analogue integrations.

The DDA may be used to compute virtually any transfer function using two basic elements, adders and storage registers. Combinations of these elements can provide digital integration and addition. The DDA integrator accepts a digital number as input and by successive addition in an accumulator (R register) at a specific sampling frequency (f_1), provides an output number corresponding to the integral of the input number. Scaling is accomplished by allowing the R register to overflow and accumulating a "one" in the output register (Z register) every time an overflow occurs.

As an example, figure 8.3.2.1-1 shows both the analogue and DDA implementation block diagrams for the solution of a first order lag:

$$\frac{Y_o}{y_i} = \frac{1}{\tau S+1}$$

which in differential equation form is

$$\tau \frac{dy_o}{dt} + y_o = y_i$$

The DDA implementation will result in

$$\frac{N_o}{N_i} = \frac{1}{\frac{N_e}{f_1} S+1}$$

where N_e is the R register overflow number.

In this case, the time constant τ is given by

$$\tau = \frac{N_e}{f_1}$$

The DDA implementation can produce ideal integrator transfer functions with long and accurate time constants. Non-linear control elements may be readily introduced through logic elements.

7/CBH/05

8.3.2.2 The Digital Filter

The second major type of implementation is the digital filter, synthesized through the bi-linear Z-tranform representation of a transfer function. This transformation may be obtained as a mapping of the Laplace transform variable:

$$S \rightarrow \frac{Z-1}{Z+1}$$

where $Z^{-1} = e^{-ST}$ may be considered an operator representing a delay of one sample period T. This tranformation will map frequencies ω into ω_p with

$$\omega_p = \tan \frac{\omega T}{2}$$

and will map time constants τ into τ_p with

$$\tau_p = \frac{1}{\tan \frac{T}{2\tau}}$$

The example first order lag tranforms into

$$\frac{y_o}{y_i} = \frac{1}{1+\tau S} \qquad \frac{1}{1+\tau_p \left(\frac{Z-1}{Z+1}\right)}$$

that is

$$y_o = \frac{1}{\tau_p+1}\, y_i + \frac{1}{\tau_p+1}\, y_i\, Z^{-1} + \left(\frac{\tau_p-1}{\tau_p+1}\right) y_o\, Z^{-1}$$

Thus, the digital filter operation consists of multiplying the present and past values of the input and output signals by a set of weights, and summing the result. A block diagram for the digital filter is shown in figure 8.3.2.2-1.

As for the DDA implementation, virtually any transfer function may be realized with a digital filter and non-linear control elements included through logic circuits.

7/CBH/06

8.3.3 The General Purpose Computer

The special purpose digital controllers considered above are generally hard wired, real time control units which are difficult to modify for incorporation of additional or different control functions. As well, where several control functions are implemented, duplication of arithmetic elements can result, particularly when sophisticated computational algorithm are used.

The present trend in attitude control system design is toward the use of a general purpose computer consisting of a central processor and memory under the control of a stored program. Such a computer affords great flexibility in the definition of control algorithms.

The results of a technology survey the state-of-the-art of on-board digital computers is given in reference 6. For the system trade-off (section 9.0 below) a general purpose computer has been assumed.

8.4 Torquers

For the application of external control torques, two major methods have been employed, electromagnets interacting with the earth's magnetic field, and mass expulsion thrusters. There is considerable debate at present regarding the effectiveness of magnetic torquers at synchronous altitude. This debate centres about the effect of daily magnetopause crossings. Reference 5 contains a relatively detailed discussion of magnet optimization and effectiveness to which the reader is referred for more information.

Virtually all attitude control systems employ thrusters, either as the primary control torquer or for wheel momentum desaturation. A major requirement for attitude control thrusters is an ability to provide very small impulses. Earlier designs achieved this by means of compressed gas feeding small valve controlled thrusters. More recently, space qualified mono-propellant hydrazine catalytic thrusters have been developed which can provide relatively small impulses with a much higher fuel efficiency as well as provide the non-attitude control thruster functions without duplication of tankage and plumbing. Further development of non-catalytic electothermal hydrazine thrusters has resulted in thruster impulses comparable to the compressed gas thruster with fuel efficiency equal to or greater than the catalytic thruster.

Other pulsed thruster systems under development include bi-propellant systems and electric propulsion units. These latter propulsion systems, through promising high fuel efficiencies, will not likely achieve flight qualification status for several years and the monopropellant system is assumed in the following section.

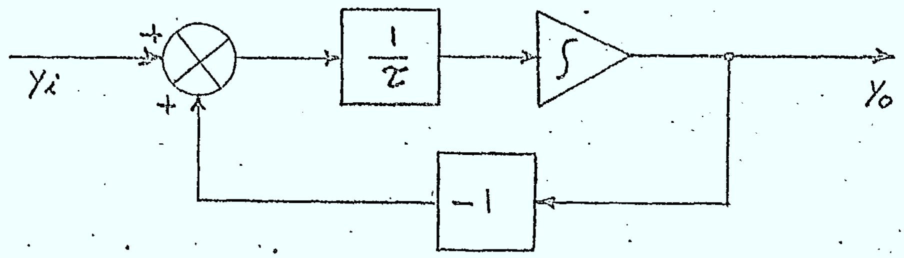

ANALOGUE BLOCK DIAGRAM

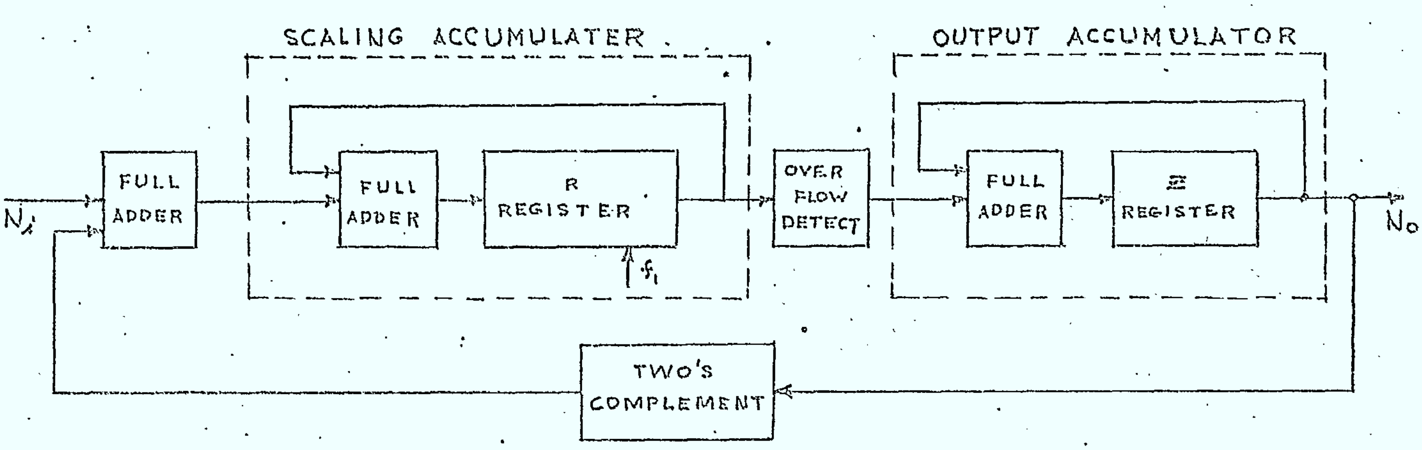

DDA BLOCK DIAGRAM

FIG. 8.3.2.1-1 FIRST ORDER LAG DDA IMPLEMENTATION

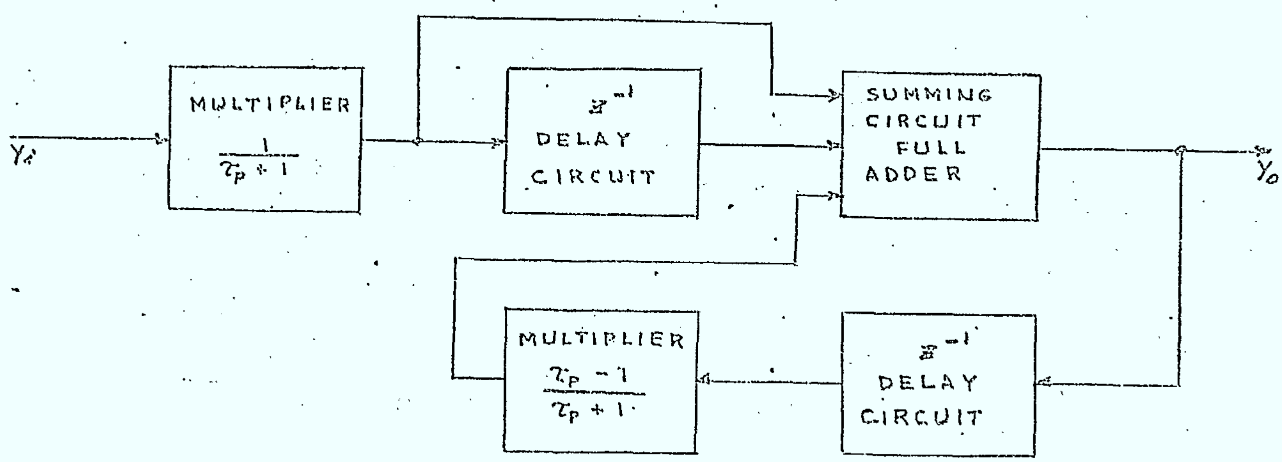

FIG. 8.3.2.2-1 FIRST ORDER LAG DIGITAL FILTER IMPLEMENTATION

9.0 TRADE STUDY OF ATTITUDE CONTROL SYSTEMS

For the purposes of a trade-off comparison of potential Attitude Control Systems, a performance specification has been prepared with parameters appropriate for the Multi-Purpose BUS Satellite. This specification is included as Appendix B.

The detailed parameters contained within the specification may change somewhat without substantially altering the conclusions reached herein.

This trade-off is based on information gathered as a result of CTS experience and recent vendor surveys, and reflects information available at SPAR at this time.

9.1 Identification of Major Trade Parameters

In order to arrive at a rational choice of candidate control systems it is necessary to quantify and compare a number of major parameters, including the following:

a) Accuracy

Both angular pointing accuracy as well as angular rate accuracy must be considered in light of specification requirements.

b) Power

Power consumption during the on-orbit phase requires the provision of sufficient solar array area and battery capacity to service the attitude control system. Power consumption may be expressed as a "power equivalent weight" by means of the following factors:

i) Array - 0.10 lb./watt
ii) Battery - 0.20 lb./watt

The battery power equivalent weight factor is based on the latest available information for space qualified batteries and the solar array factor is based on a straight line fit between an 835 watt and 625 watt (end of life) "rigid" array design. The total power equivalent weight factor is 0.3 lb./watt.

c) Weight

For most spacecraft, weight is a very important factor. For purposes of trade-off, the total weight should include not only the control system hardware weight, but also the RCS fuel weight required by the system, the weight of additional RCS engines required for system operation (as, for example, the offset engines required by Whecon), the power equivalent weight and any other overall weight impacts resulting from the system.

d) Reliability

A basic philosophy normally followed for extended life spacecraft is the elimination of potential single point failures, regardless of the system numerical reliability. This redundancy philosophy has significant weight impact, but has been followed for the candidate systems under consideration.

e) Cost

Cost is often considered to be as important as weight for comparison purposes. The cost data available for this trade-off must be considered preliminary since not all potential component vendors have been fully exercised. In addition, component costs are quite sensitive to program details. Consequently, the costs shown herein must be considered primarily for guidance purposes.

f) Risk

Certain components which are in a developmental stage represent potential risk areas for the system. These risk items are difficult to quantify other than perhaps with regard to development costs.

9.2 Baseline Variables

The independent baseline variables used for this trade study are as identified in Appendix B.

9.3 Candidate Systems

Three candidate control systems, a momentum bias system (Whecon), a reaction wheel system and a hybrid reaction wheel with thruster system are considered the most favourable candidate systems.

The momentum bias systems have been specifically configured such that yaw sensing on a continuous basis is not required. Until the introduction of the Microwave Attitude Sensing System, continuous yaw sensing has been difficult to accomplish for long life spacecraft. Of the various momentum bias schemes, the Whecon or fixed wheel with offset thruster system, has been chosen to satisfy the performance requirements with minimum cost, weight and maximum reliability.

The fixed wheel with ground command correction, though potentially providing the lightest, most reliable system, requires frequent ground correction and is, therefore, not considered sufficiently autonomous for an operational satellite. The remaining momentum bias schemes with additional reaction wheels or gymbals have been configured to provide additional performance features such as roll and yaw offset pointing and high resolution control. Such additional features are not required for the Multi-Purpose BUS Satellite and, for reasons of economy, weight and reliability, have not been considered as potential candidates.

It is suspected that the Whecon system, as originally conceived by Lockheed, has been used in classified missions, though probably of short duration. With modification included to limit nutation growth and thruster activity, the Whecon system was chosen for the CTS. Subsequently, Whecon (or equivalent) systems have been chosen for the FLEETSATCOM, RCA SATCOM, OTS and the Hughes 3-axis satellite.

A modification of the Whecon system proposed for the RCA SATCOM includes the use of electro-magnets interacting with the earth's magnetic field, both to compensate for secular disturbance torques through current loops in the solar arrays and to provide vernier control with pulsed magnets. Independent trade studies conducted during definition of the CTS control system, as well as TRW studies (reference 5), would indicate that any fuel weight savings using this approach would marginally effect total system weight. In addition, there is disagreement as to the frequency of magneto-pause crossings at synchronous altitude which could adversely effect the magnet system utility. Because of the unknown factors, the marginal performance benefit, increased complexity and a requirement for frequent (approximately once per week) ground calibration and magnet adjustment, the magnet system has not been included with the candidate Whecon system.

Low momentum or reaction wheel systems have been used in the past for various spacecraft missions. General Electric, in particular, has quite an extensive background with these systems and is, in fact, using a three reaction wheel system for the Japanese BSE. The major advantages of these systems is the very fine pointing and rate accuracy attainable as well as the ability to perform offset pointing or other manoeuvres. A major disadvantage is the requirement for continuous yaw sensing, which for the BSE is accomplished with a Microwave Attitude Sensor (MASS) plus earth sensor combination, as discussed in Section 7.0 above. With the addition of a polarization angle measurement (POLANG) to the MASS, the earth sensor may be dispensed with, resulting in a weight attractive sensor system.

The zero momentum system, utilizing control thrusters about each of the control axes, is not a viable alternative for the Multi-Purpose BUS Satellite. The rather large but purely periodic pitch disturbance torque and small pitch inertia would result in a pitch control fuel consumption of approximately 60 lb. for six years. Since this major inefficiency occurs only about the pitch axis, the use of a pitch reaction wheel to absorb the periodic disturbance torques is a possible alternative. Thus, the hybrid zero/low momentum system using the MASS with POLANG has promise as an attractive control system and is included as one of the prime candidates.

9.3.1 Common System Components

Each of the candidate systems include a number of common components, used for the spin phase, acquisition and array tracking. These components, whose major parameters are listed in table 9.3.1-1, include the following:

a) Spinning Horizon Sensor

This sensor, employing a narrow field-of-view infrared telescope, scans across the earth disk as the spacecraft rotates about its spin axis. The resulting earth scan signature provides a measure of the earth chord length. With two such sensors, one pointing 5^{o} above and the other 5^{o} below the spacecraft equatorial plane, a measure of the angle between the spin vector and the earth line is obtained from the difference between the two sensor chord length outputs.

b) Spinning Sun Sensor

The spinning sun sensor provides two outputs:

i) A sun pulse generated as the sun passes through a plane containing the spacecraft spin axis. This sun pulse is used to phase thruster pulses during precession manoeuvres.

ii) Angle between the spin vector and the sun line. This angle and the angle to the earth line together determine the spacecraft spin axis direction.

c) Array Track Sun Sensor

This sensor, with a relatively narrow fan shaped field-of-view, is mounted on the solar array and used to provide automatic array sun tracking and initialize a clock driven array tracking operation.

d) Acquisition Sun Sensors

These sensors, consisting of clusters of analogue "eyes", provide a complete spherical field-of-view allowing attitude acquisition to occur from any spacecraft orientation.

e) Nutation Damper

The nutation damper, consisting of a closed tube partially filled with mercury, is aligned along the spin axis and mounted near the perifery of the spacecraft. Passive nutation damping occurs as a result of energy dissipation through surface waves and sloshing of the mercury within the tube.

f) Control Electronics

The control unit considered here consists of redundant programmable computers and an interface box.

The electronics unit is included as a common component since the candidate control systems will have little impact on the major parameters for this unit.

9.3.2 The Whecon System

A block diagram of the candidate Whecon system is shown in figure 9.3.2-1. The pointing accuracy of this system will be $\pm0.14^\circ$ in roll and pitch and $\pm1^\circ$ in yaw. Rate accuracy would be approximately ±0.003 deg./sec. In addition to the common components, the candidate Whecon system includes components whose major parameters are listed in table 9.3.2-1, as follows:

a) Horizon Sensor

In order to meet the pitch slew requirement without accuracy degradation, a scanning infra-red horizon sensor is assumed for measurement of roll and pitch angles. Since the East-West stationkeeping accuracy is $\pm0.05^\circ$, earth chord length changes resulting from altitude variation will be of the order $\pm0.005^\circ$ thus allowing the CTS sensor to be used without modification. This sensor employs a single scanning field-of-view with chord length comparison to a pre-set nominal chord length providing cross-scan angle calculation. Two sensors would be employed for redundancy and to eliminate sun interference effects. One sensor would scan 5° above the earth equator in an east-west direction and the other would scan 5° below the equator.

b) Momentum Wheel

In order to meet the yaw pointing accuracy requirement a wheel of 15 ft.lb.sec. capacity is assumed. With conventional ball bearing wheels, redundant units will be required to meet a six to eight year life requirement. The CTS momentum wheel with a slightly modified bearing configuration would be used. As an alternative, a magnetic suspension wheel may be considered. Since the bearing wearout mechanism is eliminated, only a single wheel need be used. The levitation system, electronics and drive motor would be completely redundant.

c) Yaw Sun Sensor

Two digital sun sensor heads measuring the "vertical" (elevation) and "parallel" (slant azimuth) components of the sun line will provide a yaw angle measurement during all periods during which north-south stationkeeping must be performed. The vertical sensor, which is the "T-B" sensor discussed in 7.2.1 above, provides yaw angles within ±30^o of the sun line. The parallel sensor is an identical head, rotated through 90^o, and will fill the gap during solstice seasons, (but not equinox seasons), thus eliminating a requirement for a rate integrating gyro. This sensor complement will allow orbit inclination control to ±0.05^o.

9.3.3 The Reaction Wheel System

The reaction wheel system requires yaw sensing on a continuous basis. The use of sun sensors with rate integrating gyros is not considered sufficiently reliable for a six to eight year mission. Thus, the MASS with earth sensor or MASS with POLANG are the only alternatives apparent at this time. In addition, the MASS with earth sensor combination is not considered a weight effective combination. Thus, only the MASS with POLANG will be considered. The reaction wheel system will include the common components as well as the following:

a) MASS with POLANG

Since this sensor is not yet developed, only estimates of weight and power can be considered. The presently developed non-redundant MASS without POLANG weighs 8 lbs. and requires 10 watts. It is estimated that a redundant MASS with POLANG would weigh 16.8 lbs. and require 12 watts of power.

b) Reaction Wheels

Conventional ball bearing reaction wheels of 1.5 ft.lb.sec. capacity weigh 8 lbs. with a power requirement of 4.5 watts each. With four skewed wheels, three operational at any time, the total reaction wheel assembly weight would be 32 lbs. and would require 13.5 watts power.

Magnetic bearing reaction wheels of 1.5 ft.lb. capacity would weigh 11 lbs. each and require 1 watt. Only three wheels would be required.

A block diagram of the reaction wheel system is shown in Figure 9.3.3-1. The accuracy of this system will be 0.14° in roll and pitch, and 0.6° in yaw with rate control probably an order of magnitude better than the Whecon system although analysis will be required to justify this claim.

9.3.4 A Hybrid System

Due to simplicity and extensive flight background, an all gas zero momentum system has considerable merit. However, for the present configuration, gas control about pitch would impose a serious weight penalty due to the small moment of inertia and large periodic torque. A hybrid system consisting of a pitch reaction wheel and thruster control about roll and yaw is worthy of consideration. In this case only two conventional bearing reaction wheels or a single magnetic bearing wheel would be required. Attitude sensing would be obtained with the MASS as in the reaction wheel system.

Pointing accuracy for this system would be ±0.14° in pitch, ±0.16° in roll and ±0.7° in yaw. Rate accuracy would be similar to the Whecon system. The component major parameters for this system are presented in table 9.3.4-1.

9.4 Trade Study Matrix

Table 9.4-1 is a summary of the major parameters for each of the candidate systems. It is apparent that the reaction wheel system has little to offer over the Whecon or Hybrid systems. The following salient features may be identified:

a) The use of magnetic bearing wheels results in a significant weight saving over conventional bearing wheels as well as an increased system reliability. The additional cost for a magnetic bearing wheel has a small effect on total subsystem recurring costs since non-redundant wheels may be used.

b) The development of the Micro-Wave Attitude Sensing System with POLANG would allow use of the Hybrid system which is the lightest of all the candidate systems. If, in addition, the magnetic bearing reaction wheel is considered, the resulting Hybrid system is very attractive. This system is worthy of additional study. In particular, an optimization of the RCS interface could result in further total weight reductions.

c) It has been suggested that the ground beacon required for MASS, even if redundant, cannot be considered sufficiently reliable to exclude a backup sensing capability. This would imply not only redundant infrared horizon sensors would be required, but the yaw sun sensor and integrating rate gyro would also be necessary to provide a three-axis backup sensing system. The additional weight of 20 lb. for this backup capability would likely exclude a Hybrid system from consideration.

TABLE 9.3.1-1

COMMON CONTROL SYSTEM COMPONENTS

	Component	Weight (lb)	On-Orbit Power (Watts)	Mission Reliability	ROM COST Non-Recurring	ROM COST Recurring (per S/C)
a)	Spinning Horizon Sensor	3.0	-	0.998	-	88K
b)	Spinning Sun Sensor	1.84	-	0.998	-	42K
c)	Array Track Sun Sensor	0.52	0.1	0.996	-	24K
d)	Acquisition Sun Sensor	0.36	-	0.999	-	12K
e)	Nutation Damper	0.9	-	0.9999	-	15K
f)	Control Electronics	18.0*	15.0*	0.96*	800K	600K
g)	Bracketry	1.5*	-	-	10K	10K
	Totals	26.12	15.1	0.96 (On-Orbit Reliability)	810K	791K

*Estimated Quantities

SPAR-R.664

WHECON ATTITUDE CONTROL SYSTEM

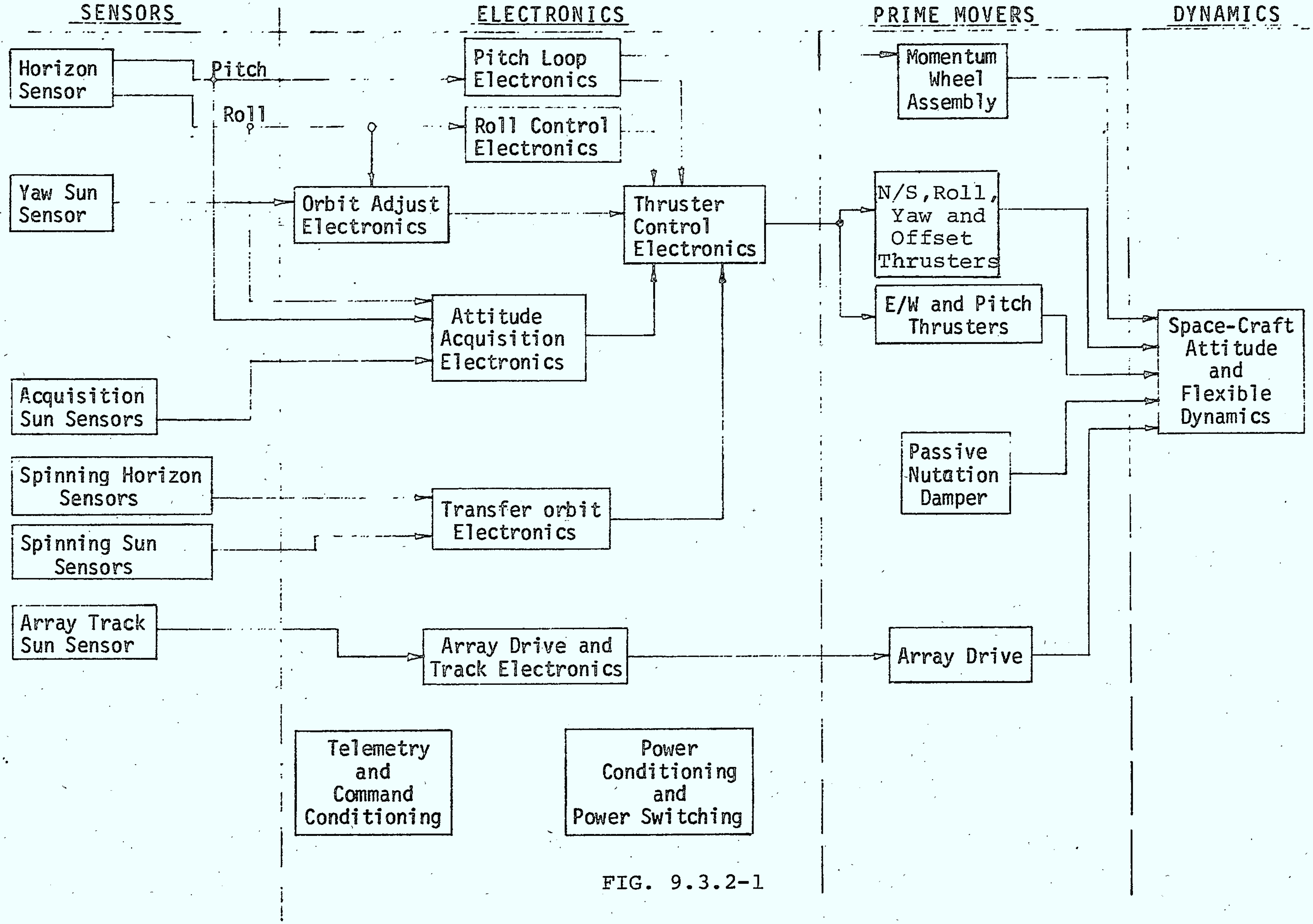

FIG. 9.3.2-1

SPAR-R.664

TABLE 9.3.2-1

WHECON SYSTEM COMPONENTS

Component	Weight (lb)	On-Orbit Power (Watts)	On-Orbit Reliability	Cost ($K) Non-Recurring	Cost ($K) Recurring
a) Horizon Sensor	12.0	4.5	0.988	-	275
b) Momentum Wheel					
- Conventional Bearing	34.0	15.0	0.978	133	132
- Magnetic Bearing	24.5	2.5	0.995	450	120
c) Yaw Sun Sensor	4.0	1.0	0.990	100	50
d) Common Components	26.12	15.1	0.960	810	791
Totals:					
- Conventional Wheel	76.12	45.6	0.918	1,043	1,248
- Magnetic	66.62	23.1	0.934	1,360	1,236
Weight Equivalent Power:					
- Conventional Wheel	13.68				
- Magnetic Wheel	6.33				
RCS Weight:					
- Offset Thrusters	3.0				
- Fuel (6 years)	9.0				

Total Weight - Conventional Wheel 101.8 lb.
- Magnetic Wheel 84.95 lb.

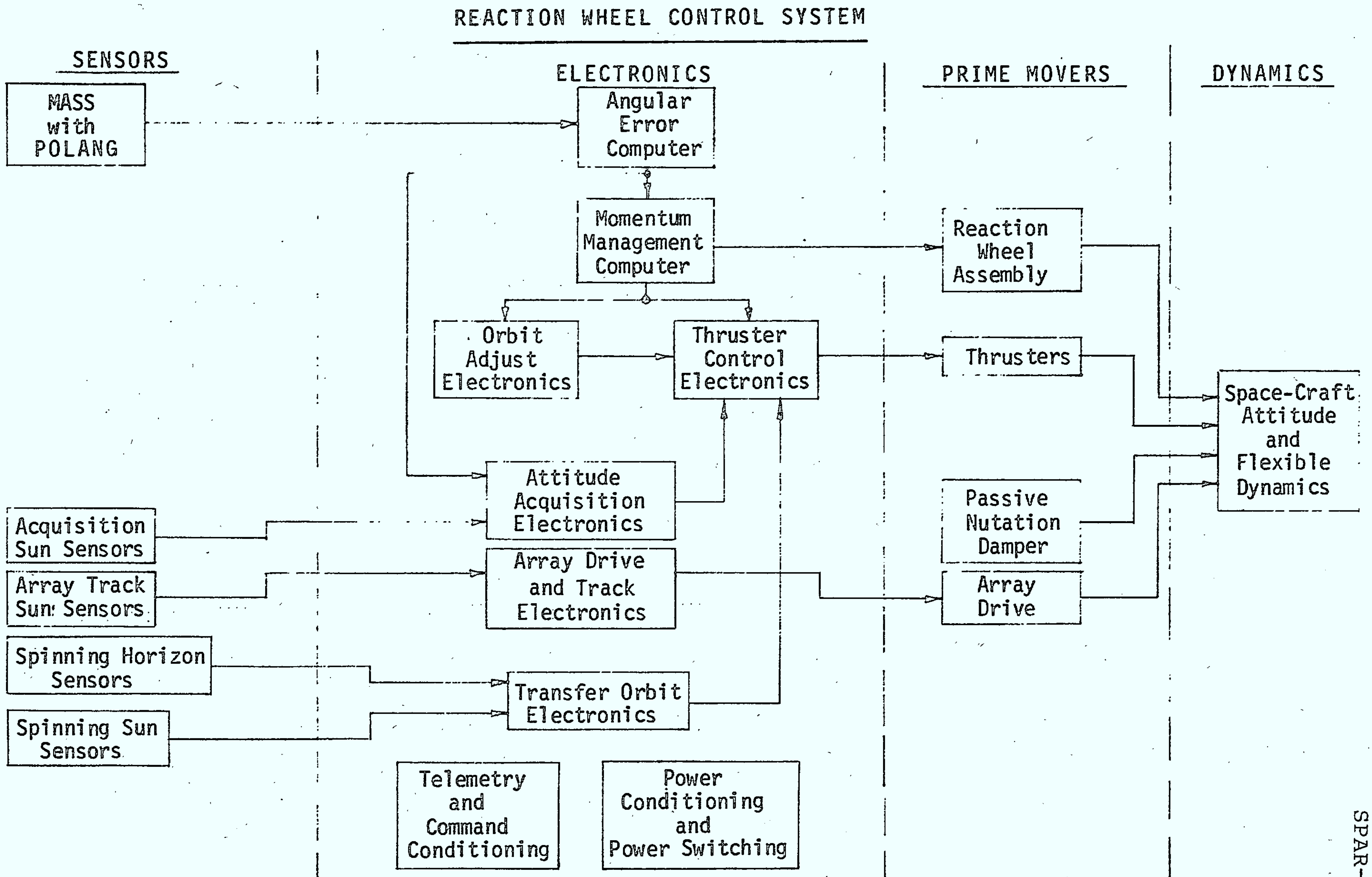
REACTION WHEEL CONTROL SYSTEM
SENSORS
ELECTRONICS
PRIME MOVERS
DYNAMICS
MASS with POLANG
Angular Error Computer
Momentum Management Computer
Reaction Wheel Assembly
Orbit Adjust Electronics
Thruster Control Electronics
Thrusters
Space-Craft Attitude and Flexible Dynamics
Attitude Acquisition Electronics
Acquisition Sun Sensors
Passive Nutation Damper
Array Drive and Track Electronics
Array Track Sun Sensors
Array Drive
Spinning Horizon Sensors
Transfer Orbit Electronics
Spinning Sun Sensors
Telemetry and Command Conditioning
Power Conditioning and Power Switching

FIG. 9.3.3-1

TABLE 9.3.3-1

REACTION WHEEL SYSTEM COMPONENTS

Component	Weight (lb)	On-Orbit Power (Watts)	Mission Reliability	ROM COSTS Non-Recurring	ROM COSTS Recurring (per S/C)
a) MASS (with POLANG)	16.8	12.0	0.985	600K	400K
b) Reaction Wheels					
- Conventional Bearings	32.0	13.5	0.970	-	300K
- Magnetic Bearings	33.0	3.0	0.985	300K	300K
c) Common Components	26.12	15.1	0.96	810K	791K
Totals:					
- Conventional Wheel	74.92	40.6	0.917	1,410K	1,491K
- Magnetic Wheel	75.92	30.1	0.931	1,710K	1,491K
Weight Equivalent Power:					
- Conventional Wheel	12.18				
- Magnetic Wheel	9.03				
RCS Fuel (6 years)	4.0				

Total weight - Conventional Wheel 91.10
- Magnetic Wheel 88.95

TABLE 9.3.4-1

HYBRID SYSTEM COMPONENTS

Component	Weight (lb)	On-Orbit Power (Watts)	Mission Reliability	ROM COST Non-Recurring	ROM COST Recurring (per S/c)
a) MASS (with POLANG)	16.8	12.0	0.985	600K	400K
b) Reaction Wheels					
- Conventional Bearings	16.0	9.0	0.978	-	150K
- Magnetic Bearings	11.0	1.0	0.995	300K	100K
c) Common Components	26.12	15.1	0.96	810K	791K
Totals:					
- Conventional Wheels	58.92	36.1	0.925	1,410K	1,341K
- Magnetic Wheels	53.92	28.1	0.941	1,710K	1,291K
Weight Equivalent Power:					
- Conventional Wheels	10.83				
- Magnetic Wheels	8.43				
RCS Fuel (6 years)	12.0				
Total Weight - Conventional Wheels		81.75			
- Magnetic Wheels		74.35			

TABLE 9.4-1

ACS SYSTEM TRADE MATRIX

System / Major Parameter	WHECON		REACTION WHEEL		HYBRID	
	Conventional Bearing Wheel	Magnetic Bearing Wheel	Conventional Bearing Wheel	Magnetic Bearing Wheel	Conventional Bearing Wheel	Magnetic Bearing Wheel
Subsystem Weight	76.12	66.62	74.92	75.92	58.92	53.92
Total Weight	101.8	84.95	91.10	88.95	81.75	74.35
On-Orbit Reliability (6 years)	.918	.934	0.917	0.931	0.925	0.941
Component Costs ($,000)						
- Non-Recurring	1,043	1,360	1,410	1,710	1,410	1,710
- Recurring (per S/c)	1,248	1,236	1,491	1,491	1,341	1,291

10.0 REFERENCES

1. H.J. Dougherty, K.L. Lebsock, J.J. Rodden, Attitude Stabilization of Synchronous Communications Satellites Employing Narrow Beam Antennas, AIAA 3rd Communications Satellite Systems Conference, Los Angeles, Calif., April 1970.

2. H.J. Dougherty, E.D. Scott, J.J. Rodden, Analysis and Design of WHECON - An Attitude Control Concept, AIAA 2nd Communications Satellite Systems Conference, San Francisco, Calif., April 1968.

3. M.G. Lyons, K.L. Lebsock, E.D. Scott, Double Gimballed Reaction Wheel Attitude Control System for High Altitude Communciations Satellites, AIAA Guidance, Control and Flight Mechanics Conference, Hostra University, Hempstead, New York, August 1971.

4. H.L. Mork, Synthesis and Design of a Gimballed Reaction Wheel Attitude Stabilization Package (GRASP), AIAA Guidance, Control, and Flight Mechanics Conference, Hofstra University, Hempstead, New York, August 1971.

5. SPAR-R.666, Technology Survey of Critical ACS Components for the Multi-Purpose UHF Satellite Project, SPAR Aerospace Products Limited, April, 1975.

6. SPAR-R.665, Technology Survey of On-Board Programmable Digital Computers for Satellite Attitude Control Applications, SPAR Aerospace Products Limited, April, 1975.

7/CGC/59

APPENDIX A

INTERACTION OF FLEXIBLE SOLAR PANELS WITH ATTITUDE CONTROL SYSTEMS

3/CHW/27

INTERACTION OF FLEXIBLE SOLAR PANELS WITH ATTITUDE CONTROL SYSTEMS

A-1.0 INTRODUCTION

Elastic behaviour of a spacecraft structure is usually considered during the design of a spacecraft control system and the possibility of severe control system/flexible structure interaction is usually foreseen. Less severe interaction may go undetected, however, but may still be of such magnitude as to result in a possible failure of the vehicle to complete all or part of its mission. Thus, the control system designer must be aware of the numerous and subtle ways in which a control system and flexible structure may interact.

One of the typical three-axis controlled synchronous satellite is shown in Figure 1. Two "flexible" extendible solar panels will be deployed in synchronous orbit to generate electrical power. The attitude control system is located within the main body which is considered to be "rigid".

Assuming the structural flexibility is linear and non-dissipative, the natural motion (with zero control and disturbance torques) is a superposition of an infinite number of sinusoidal oscillations. Each of these "modes" of oscillation is specified by its modal "shape" (or space dependence of the deflection) and the modal "frequency" of oscillation. Mathematically, this behaviour is characterized by an eigenvalue problem in which the eigenvalues and their associated eigenvectors correspond to the modal frequencies and shapes, respectively. Usually, only the first N (a finite number) modes need to be considered since the higher frequency oscillations would be filtered out by the attitude sensors and higher modal gains tend to diminish with increasing modal number.

The purpose of this Appendix is to consider the effects of structural flexibility on spacecraft

3/CHW/28

attitude control systems. Some analysis has been performed in order to provide insight into several critical parameters such as modal frequency, damping ratio, modal gain and control loop gain as these parameters relate to system bandwidth, stability and performance.

37/CHW/79

A-2.0 ANALYSIS

Figure 2 shows the block diagram of a control loop with flexible body dynamics. A simplified mathematical model is shown in Figure 3. In this model, K represents the loop gain, G(s) the transfer function including attitude sensor and controller, and D(s) the spacecraft dynamics which consists of both rigid body dynamics ($1/IS^2$) and dominant first unconstrained mode $[K_1 + 1)S^2 + 2\delta_1\omega_1 S + \omega_1^2]/[S^2 + 2\delta_1\omega_1 S + \omega_1^2]$. It is apparent that if the modal gain is very small, i.e., $K_1 \to 0$ or if the structure is very stiff, i.e., $\omega_1 \to \infty$, the flexibility effect can be ignored. Otherwise, the flexibility effect must be carefully evaluated in order to achieve an effective control system.

Figure 4(a) shows a typical Bode plot (or open-loop frequency response plot) of an attitude control system without flexibility effect. Two control loop gains with K' >K result in two different crossover frequencies with $\omega_c{}^1 > \omega_c$. The crossover frequency ω_c is approximately equal to the system bandwidth ω_b which is defined to be the frequency where the closed-loop frequency response magnitude is a factor of $0.707 = 1/\sqrt{2}$ or -3 db of its zero frequency value, that is, if the input is a pure sine wave, then ω_b is the frequency where the output amplitude has been attenuated to 70.7 percent of the input amplitude. The bandwidth is related to speed of response, to the overall control system ability to reproduce an input signal, and to the ability of the system to reject unwanted noise or spurious disturbance anywhere in the system. Large values of ω_b correspond to fast response, and vice versa. The desirability for exact reproduction of rapidly changing inputs and for low bandwidth for maximum noise rejection are in basic conflict in the design of control systems. However, if the noise frequency spectrum is sufficiently higher than the input signal frequency spectrum, a satisfactory ω_b can be selected that meets both those objectives.

3/CHW/30

As shown in Figure 4(a), the crossover frequency ω_c or bandwidth ω_b increases with an increasing loop gain K. This results in a faster responding system but with reduced stability gain margin. Furthermore, since the sensor noise transmission is proportional to $KG(s)D(s)/[1 + KG(s)D(s)]$ and torque disturbance transmission depends on $D(s)/[1 + KG(s)D(s)]$, a higher loop gain means more sensor noise will be transmitted to the attitude pointing error but the torque disturbance transmission will be reduced.

If the flexible structure first modal frequency ω_1 is much higher than the control loop bandwidth ω_b, as shown in Figure 4(b), the structure flexibility will have almost no effect on the control system. If the modal frequency is near the system bandwidth, undesirable resonance may occur. If ω_1 is within ω_b as shown in Figure 4(c), it tends to destabilize the system. It is apparent from the above considerations that a sophisticated controller and proper simulation of flexibility are required.

Higher damping ratios associated with each mode tend to reduce the effects of flexibility since the complex zeroes and poles, which represent flexible body dynamics in the S-plane, move away from the imaginary axis toward the left-half S-plane resulting in exponentially damped oscillations. This adds stability margin to the control system.

A-3.0 CONCLUSIONS

In order to control the effects of one or more flexible appendages or solar panels, the following are recommended:

i) If possible, design the bandwidth of the control system to be lower than the lowest flexible panel modal frequency and separated from it by as large a margin as possible.

ii) Where practical, ensure that the damping ratio associated with each flexible mode is as large as possible. Artificial passive or active damping may be considered where control requirements are incompatable with flexible interaction requirements.

iii) Ensure the modal gain is as low as possible; that is, maintain the mass and moment arm of the flexible panel as small as possible in relation to the spacecraft's rigid body inertia.

iv) Maintain the control gain as high as possible, consistent with stability limitations, to minimize attitude error in the presence of environmental disturbance torques and perturbation torques resulting from orbit adjust thrusting.

v) In order to reduce the effects of flexibility in the control loop, choose the control bandwidth so that it excludes the structural modal frequencies. This may be achieved through natural stiffening of the structure, by artificially stiffening the structure through use of special inner control loops, through utilization of a low-pass filter within the control amplifier, or through the use of notch filters should the flexible frequencies be well defined.

3/CHW/32

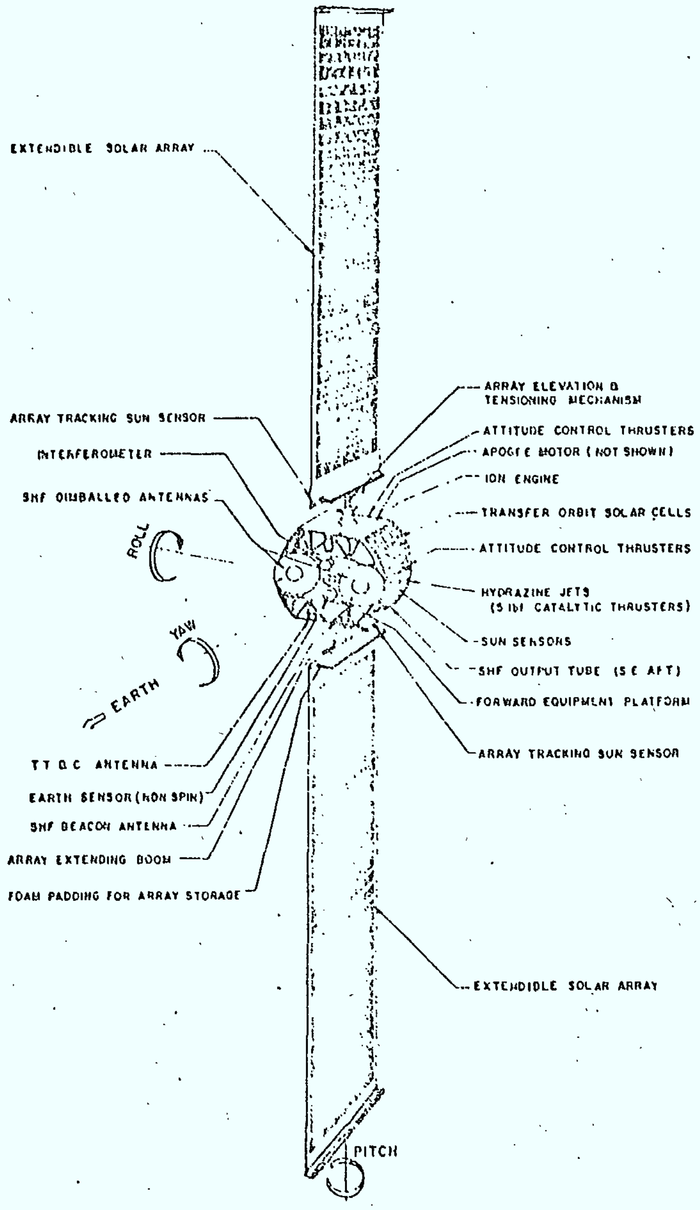

FIGURE 1 A THREE-AXIS CONTROLLED SATELLITE

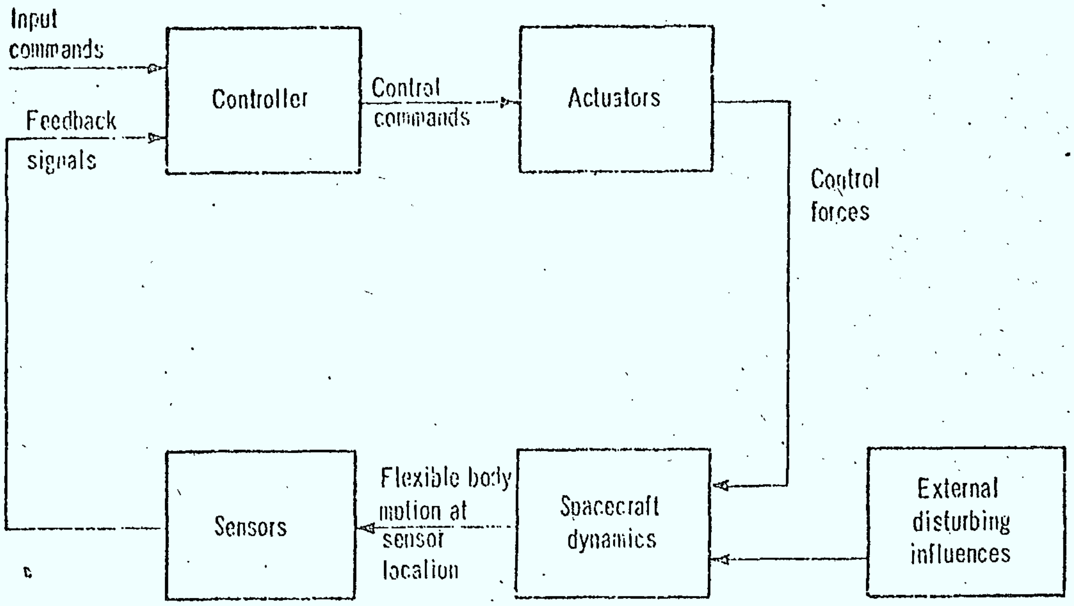

Figure 2 Block diagram of control loop with flexible body dynamics.

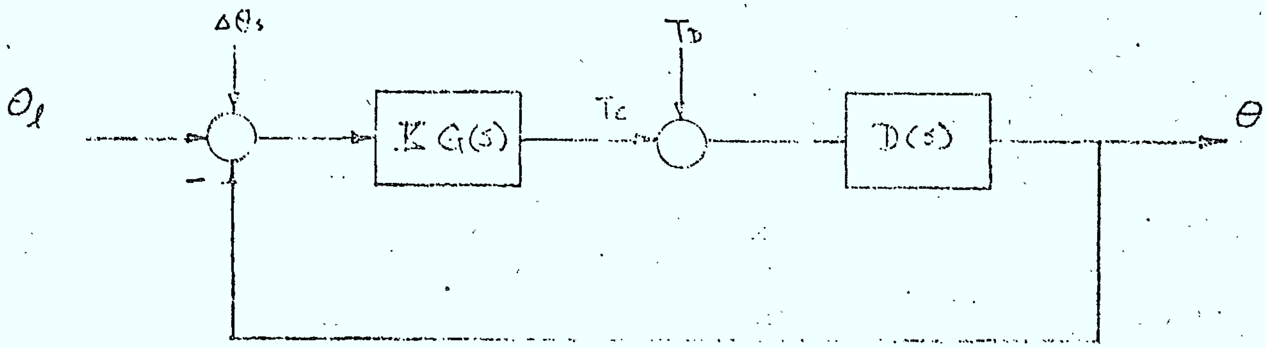

where K = control loop gain

$G(s)$ = sensor and controller

$$D(s) = \text{dynamics} = \frac{1}{Js^2}\left[\frac{(K+1)s^2 + 2\zeta_1\omega_1 s + \omega_1^2}{s^2 + 2\zeta_1\omega_1 s + \omega_1^2}\right]$$

FIGURE 3 CONTROL SYSTEM MATH. MODEL

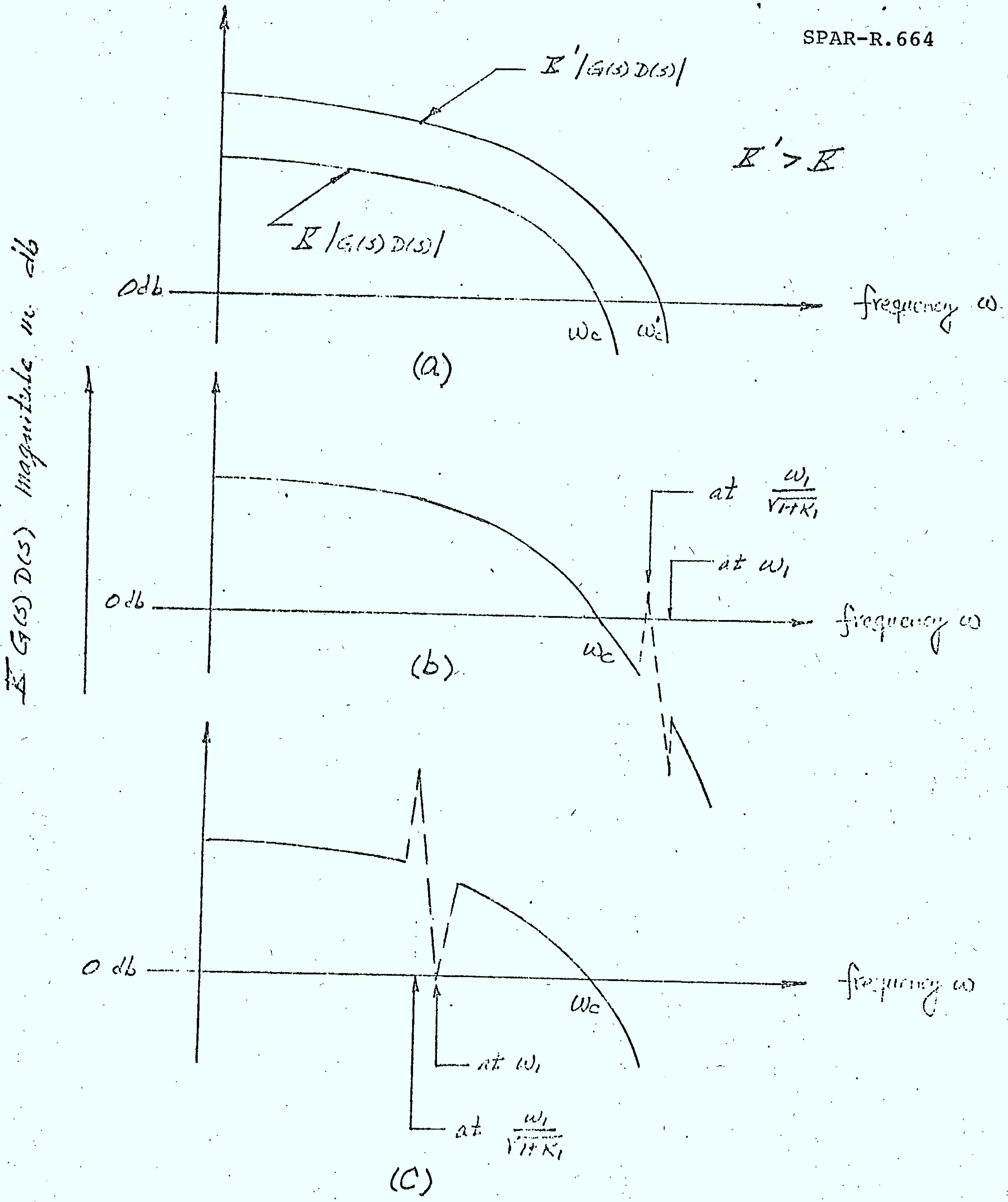

FIGURE 4 CONTROL SYSTEM BODE PLOT

APPENDIX B

PERFORMANCE SPECIFICATION

FOR AN

ATTITUDE CONTROL SUBSYSTEM

57CHW/53

TABLE OF CONTENTS

57/CHW/34

TABLE OF CONTENTS - Continued

1.0 SCOPE

1.1 General

This Specification establishes the requirements for the performance of a satellite Attitude Control Subsystem, hereinafter referred to as the ACS. The ACS will form a subsystem of the Multi-Purpose Bus (MPB) Satellite to be used in a geostationary equatorial orbit with several possible compliments of communication payloads.

1.2 Function

The ACS shall provide functions required on-board for the stabilization and control of spacecraft attitude throughout the transfer orbit, apogee injection, attitude acquisition, station acquisition, stationkeeping and on-orbit operation phases. During these phases two basic spacecraft configurations are employed. Following separation from the launch vehicle third stage, the spacecraft will be spin stabilized, with favourable moment of inertia ratios, until the start of the attitude acquisition phase. During the attitude acquisition phase the spacecraft will be transferred from this spinning configuration to a non-spinning three axis stabilized configuration, which will be maintained for the duration of on-orbit operation.

The primary functions of the ACS during these various phases are:

a) To provide sufficient attitude information and access to attitude control actuation so that ground control can implement attitude stabilization and control of the spacecraft during the transfer orbit and apogee injection.

b) To provide autonomous stabilization and control during the attitude acquisition phase with a minimum of ground control support to enable the spacecraft to be transferred from

3/CHW/36

the spin stabilized configuration to a three axis stabilized configuration with the solar arrays deployed.

c) To provide autonomous three-axis attitude stabilization and control during the on-orbit operation phase, with a minimum of ground support.

d) To provide autonomous three-axis attitude stabilization and control during orbit adjust operations.

e) To provide autonomous sun pointing control for the solar array subsystem.

2.0 APPLICABLE DOCUMENTS

TBD.

3.0 REQUIREMENTS

3.1 Performance

3.1.1 Functional Characteristics

3.1.1.1 Spinning Phase

3.1.1.1.1 Spinning Phase Operation

During the transfer orbit and apogee injection, the spacecraft will be spinning about the yaw axis. The spacecraft angular momentum vector is nominally in the direction of the positive yaw axis. Following injection into transfer orbit, the spin axis attitude will be determined and the spacecraft precessed into the appropriate apogee motor firing attitude.

3.1.1.1.2 Spinning Phase Support Function

In order to enable appropriate attitude stabilization and control during the spinning phases, the ACS will provide ground control with the following support functions:

a) A sun reference pulse when the sun passes through the spacecraft roll-yaw plane, for spin rate monitoring.

b) The sun line position relative to the spacecraft spin axis.

c) The earth line position relative to the spacecraft spin axis.

d) Timing and execution of trains of axial high thrust engine pulses (of specified number and duty cycle) on command for spin axis orientation control. The sun reference pulse will be used for timing individual pulses.

e) Passive damping of spin axis nutation.

3/CHW/39

3.1.1.1.3 Spin Rate

The ACS shall meet the performance requirement specified herein with a spacecraft spin rate of 60 ± 6 RPM about the yaw axis.

3.1.1.1.4 Attitude and Earth Radius

The ACS shall meet the performance requirements specified herein at an altitude of 19,323 ±10 nautical miles above the earth's surface whose radius is 3,444 nautical miles.

3.1.1.1.5 Sun Reference Pulse Accuracy

The three sigma angular error between the sun reference pulse and the sun trailing edge shall be ± 0.12° when the sun line lies in the roll-pitch plane.

3.1.1.1.6 Sun Elevation Accuracy

The three sigma sun elevation accuracy shall be less than ± 0.27 degrees.

3.1.1.1.7 Earth Chord Length Accuracy

The three sigma earth chord length accuracy shall be ± 0.12 degrees.

3.1.1.1.8 Axial Thruster Pulse Timing Accuracy

Thruster electrical pulse centroid and pulse width accuracy shall be equivalent to ± 1.0° three sigma or less.

3.1.1.1.9 Nutation Damper Time Constant

The nutation damper time constant shall not exceed 30 minutes.

3.1.1.2 Attitude Acquisition Phase

The attitude acquisition phase extends from the initiation of despin to the transfer of control to the on-orbit three axis control system.

3.1.1.2.1 Attitude Acquisition Operation

The attitude acquisition operation will include a sequence of manoeuvres performed to obtain the following orientation of the reference axes:

a) Yaw axis pointing at the geometric centre of the earth.

b) Pitch axis pointing along the southerly orbit normal.

c) Roll axis pointing along the tangential orbit velocity vector.

The attitude acquisition operations will include the following manoeuvres:

a) Despin
b) Sun acquisition
c) Solar array deployment
d) Earth acquisition
e) Transfer to on-orbit three-axis control.

The attitude acquisition manoeuvres will be performed autonomously upon initiation by ground command.

3.1.1.2.2 Acquisition Duration

The total time to complete the acquisition manoeuvres shall not exceed 3.5 hours.

3.1.1.2.3 Launch Window Constraint

There shall be no time of year limitation on launch (launch on any day of the year) due to the chosen attitude acquisition control system.

3.1.1.3 Station Acquisition

The ACS shall provide three-axis attitude control during longitude station acquisition where east-west stationkeeping thrusters are used.

3/CHW/41

3.1.1.4 Sun Hold Station Acquisition

In the event that earth acquisition cannot occur from the initial longitude station, the ACS will maintain control of the sun line along the spacecraft roll axis to allow a station change with east-west stationkeeping thrusters.

3.1.1.5 On-Orbit Three Axis Attitude Control

Following station acquisition the ACS will provide autonomous three-axis attitude control.

3.1.1.5.1 Attitude Error Budget

The spacecraft boresight error budget will consist of the following three sigma error contribution:

a) Roll and Pitch

i)	Antenna boresight alignment	±0.05°
ii)	Spacecraft thermal and vibration induced distortion	±0.02°
iii)	Attitude sensor alignment	±0.005°
iv)	ACS control error	±0.14°
	RSS Total	±0.15°

b) Yaw

i)	Antenna boresight alignment	±0.15°
ii)	Spacecraft thermal and vibration induced distortion	±0.1°
iii)	ACS component alignment	±0.1°
iv)	ACS Control Error	±1.08°
	RSS Total	1.1°

3.1.1.5.2 Attitude Control System Pointing Error

The attitude control system pointing error shall be $\pm$ 0.14° in roll and pitch and $\pm$ 1.08° in yaw, where these errors include sensor noise, bias and dynamic control errors, but exclude alignment errors, thermal and vibration induced distortions and antenna boresight alignment.

As a design goal, during periods of no orbit adjust thruster activity, the ACS pointing error in roll and pitch shall be $\pm$ 0.1°.

3.1.1.5.3 Attitude Rate Error

In order to accommodate attitude rate sensitive payloads, the attitude rates shall not exceed the following three sigma limits during periods of no-orbit adjust thrusting.

a) Roll and pitch TBD deg/sec
b) Yaw TBD deg/sec

3.1.1.6 Station Keeping

3.1.1.6.1 Station Keeping Operation

The ACS shall provide autonomous three-axis control during orbit adjust thrusting.

3.1.1.6.2 Station Keeping Support Function

The ACS shall provide timing and execution of station keeping low thrust engines (of specified thrust duration) upon initiation by ground command.

3.1.1.6.3 Station Keeping Limits

The RSS sum of the east-west and north/south stationkeeping limits will be:

$$\left[(0.1)^2 + (0.1)^2\right]^{1/2} = 0.1414 \quad \text{degrees.}$$

As a design goal, the RSS sum will be

$$\left[(0.05)^2 + (0.05)^2\right] = 0.0707 \quad \text{degrees}$$

3.1.1.6.4 Station Keeping Cycle

As a design goal, the ACS shall provide three-axis control with a 21 day stationkeeping cycle.

3.1.1.7 Solar Array Tracking

The ACS shall provide solar array sun pointing control to within an azimuth error of $\pm$ 1.0 degree.

3.1.1.8 Station Change Requirement

The ACS shall be capable of performing a pitch slew manoeuvre, on command, in order to maintain three-axis attitude control during and following a change in longitudinal station.

3.1.1.9 Spacecraft Dynamic Environment

The ACS shall be capable of meeting the performance requirements of this Specification with the dynamic environments defined in the subparagraphs below.

3/CHW/44

3.1.1.9.1 Mass Properties

3.1.1.9.1.1 Spin Phase Mass Properties

During the mission spinning phase the roll, pitch and yaw moments of inertia will be respectively:

$I_{xx} = 155$ slug ft^2

$I_{yy} = 175$ slug ft^2

$I_{zz} = 182$ slug ft^2

3.1.1.9.1.2 On-Orbit Orbit Phase Mass Properties

In the deployed configuration the roll, pitch and yaw moments of inertia will be respectively:

$I_{xx} = 800$ slug ft^2

$I_{yy} = 250$ slug ft^2

$I_{zz} = 830$ slug ft^2

3.1.1.9.1.3 Solar Array Mass Properties

The total weight of the deployable portion of the solar arrays will be 90 lb. The distance between the solar array centre of mass, which will lie on the yaw axis, will be 15 inches. The moments of inertia of the deployable portion of the solar array subsystem about its centre of mass will be:

$I_{xx} = 650$ slug ft^2

$I_{yy} = 4$ slug ft^2

$I_{zz} = 650$ slug ft^2

3.1.1.9.2 Flexible Appendage Properties

The spacecraft will include flexible solar arrays mounted in a north-south configuration, and flexible antennas with a boresight contained within the yaw pitch plane and canted towards the north by up to 5.0 degrees.

3.1.1.9.2.1 Analytic Modelling of Flexible Appendages

An "unconstrained" modal decomposition of the flexible appendages may be assumed, including equivalent viscous damping. Only the first three flexible modes need be considered for analysis.

3.1.1.9.2.2 Solar Array Flexible Parameter

The solar array natural frequencies and gains will be as follows:

TABLE 1

SOLAR ARRAY FREQUENCIES AND GAINS

Mode	Range of Frequencies (Hz)	Range of Gains
First out-of-plane	0.1 - 0.4	4.0 - 8.0
Second out-of-plane	TBD	TBD
Third out-of-plane	TBD	TBD
First Torsional	0.1 - 0.4	0.01 - 0.02
Second Torsional	TBD	TBD
Third Torsional	TBD	TBD

3.1.1.9.2.3 Antenna Flexible Parameters

The antenna natural frequencies and gains will be as follows:

TABLE 2

ANTENNA FREQUENCIES AND GAINS

Mode	Range of Frequencies (Hz)	Range of Gains
First Bending	0.5 - 1.0	TBD
Second Bending	TBD	TBD
Third Bending	TBD	TBD
First Torsional	TBD	TBD
Second Torsional	TBD	TBD
Third Torsional	TBD	TBD

37CHW/46

3.1.1.9.2.4 Flexible Damping

The equivalent viscous damping ratio for all flexible modes will be greater than 0.05 percent.

3.1.1.9.3 Solar Perturbation Torque

The major perturbation torque will be due to solar radiation pressure and will have the following form:

a) Pitch Torque (micro ft. lb.)

$$T_p = 22 \cos^2 \theta_D \cos (\omega_o t)$$

b) Roll Torque (micro ft.lb.)

$$T_R = 8\sin(2\theta_D) + [3\cos^2\theta_D + 3\sin(2\theta_D)]\cos(\omega_o t)$$

c) Yaw Torque (micro ft.lb.)

$$T_Y = -[3\cos^2\theta_D + 3\sin(2\theta_D)]\sin(\omega_o t)$$

The variables θ_D, ω_o and t are defined as:

θ_D = sun declination angle

ω_o = orbit rate (7.29×10^{-5} rad/sec)

t = time (seconds)

3.1.1.10 Reaction Control Subsystem Interface

3.1.1.10.1 General

The Reaction Control Subsystem (RCS) High Thrust Engines (HTE) and Low Thrust Engines (LTE) will provide the means whereby external torques may be applied to the spacecraft as required by the ACS.

3.1.1.10.2 RCS LTE Configuration

The RCS LTE are grouped into two sets - primary and redundant. Each LTE is identified by resultant torque produced in the case of the attitude control LTE and by thrust direction in the case of the stationkeeping LTE (summarized in Table 3).

3.1.1.10.3 Moment Arms and Torque Polarity

The moment arm and torque polarity associated with each LTE is listed in Table 3.

TABLE 3

LTE THRUSTER IDENTIFICATION, MOMENT ARM AND TORQUE POLARITY

TBD

3/CHW/48

3.1.1.10.4 RCS Performance Parameters

The RCS LTE performance is defined as follows:

a) LTE Force - Steady State

The range of steady state thrust levels is TBD.

b) LTE Impulse Bit

The impulse bit per LTE during pulse operation will be TBD.

c) LTE Impulse Bit Repeatability

The repeatability from pulse to pulse for a given electrical on-time will be TBD for any LTE. Predictability between LTE's will be TBD.

3.1.2 Operability

3.1.2.1 Reliability

The subsystem will be designed to achieve a mission reliability not less than 0.9999 for 110 hours in transfer orbit, and as a design goal 0.89 during on-orbit operation with the environmental and life requirements detailed in this Specification. In order to achieve the on-orbit reliability, a high level of semi-conductor screening will be required.

3.1.2.2 Useful Life

The ACS will be capable of performing as specified for not less than six years in space following a maximum two years of prelaunch test and storage.

It will be a design goal to provide hardware capable of eight years life in space.

3/CHW/49

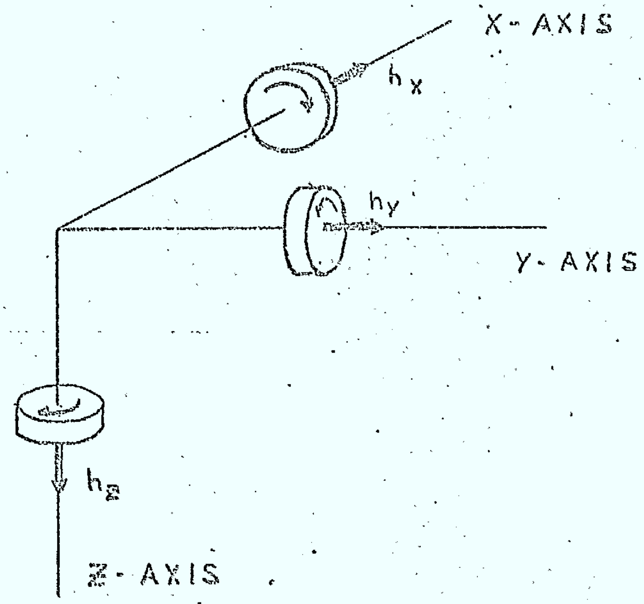

FIG. 5.1-1 BASIC THREE WHEEL CONFIGURATION

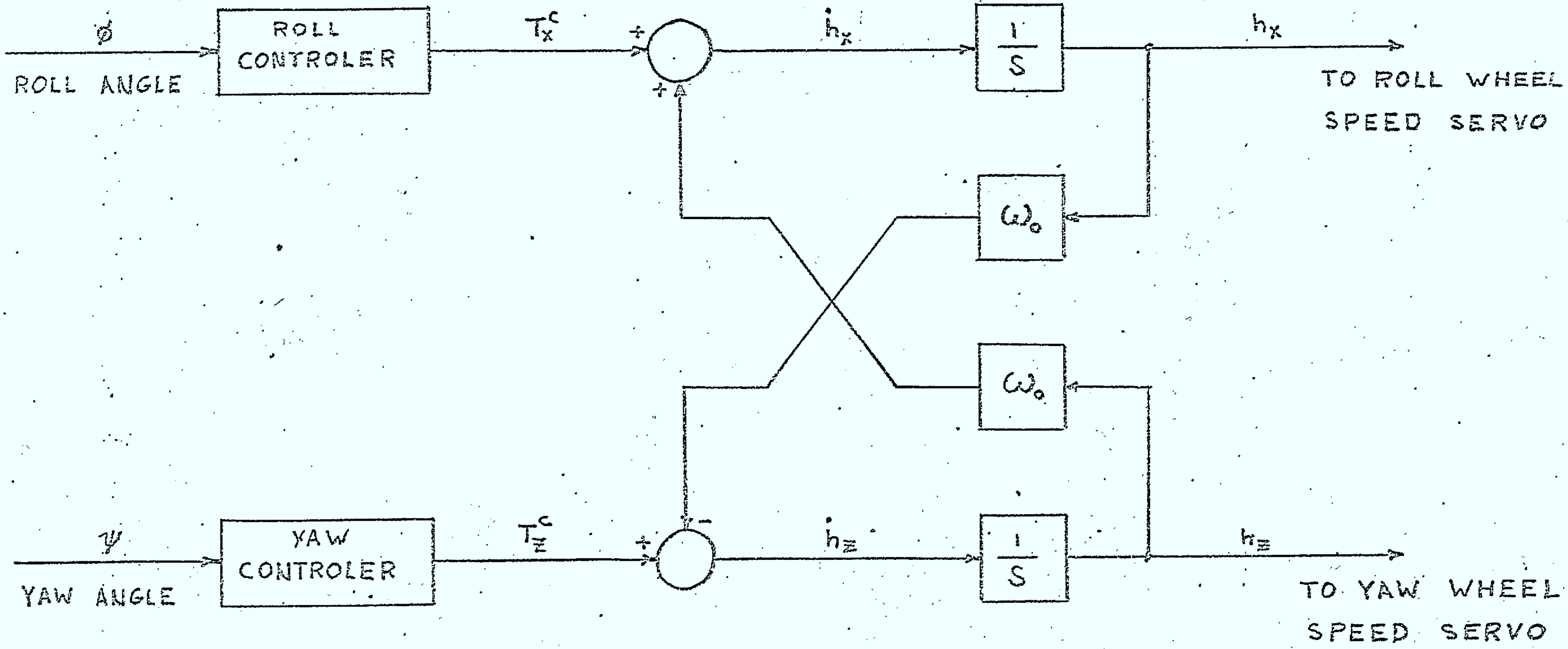

FIG 5.1-2 BLOCK DIAGRAM OF ROLL/YAW DECOUPLING

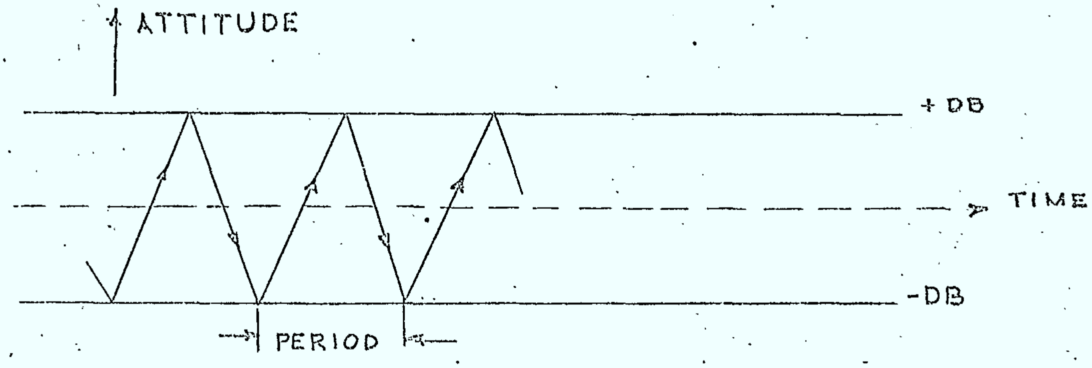

(a) TORQUE FREE LIMIT CYCLE MOTION

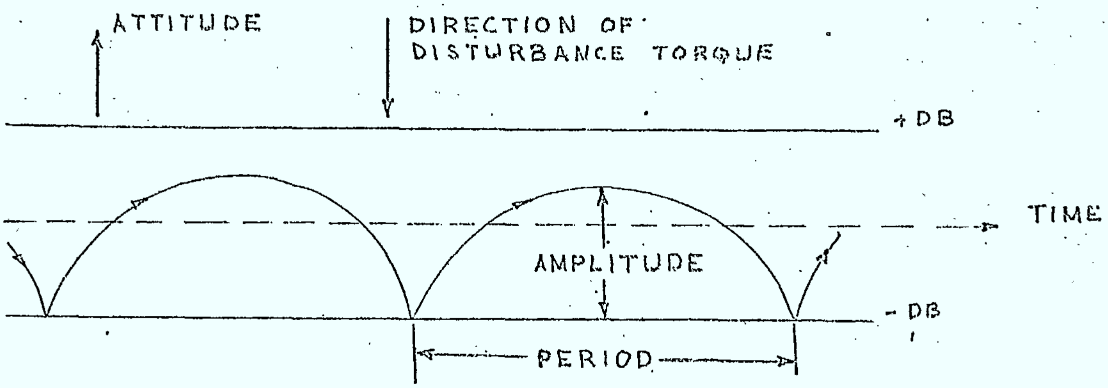

(b) SCALLOP MOTION WITH DISTURBANCE TORQUE

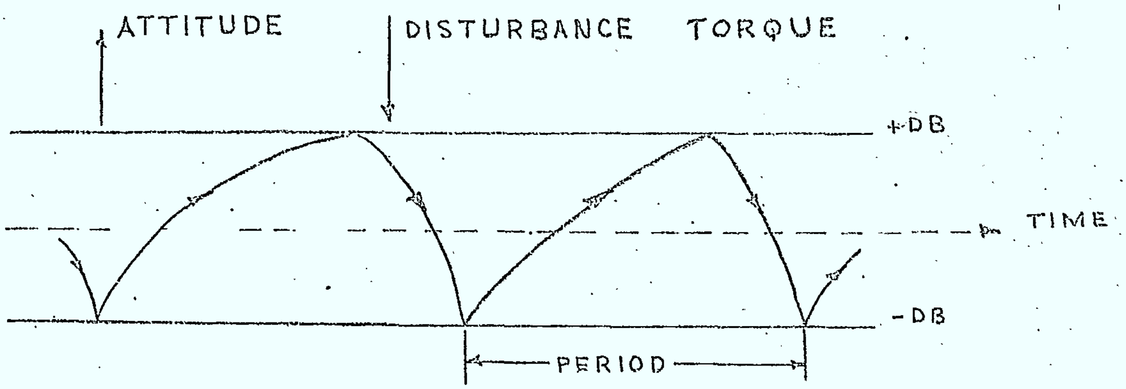

(c) LIMIT CYCLE MOTION WITH DISTURBANCE TORQUE

FIG 6.1-1 ZERO MOMENTUM LIMIT CYCLES

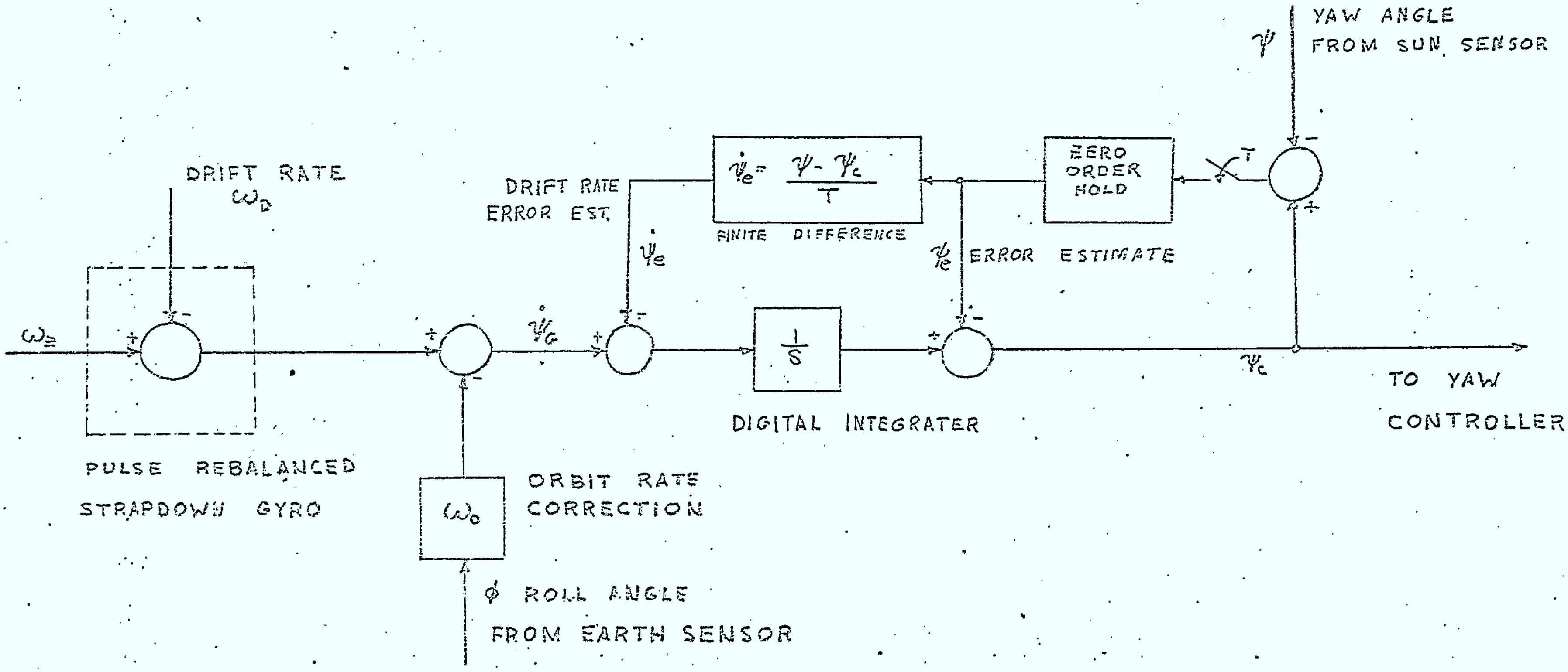

FIG 7.2.2-1 YAW GYRO PLUS SUN SENSOR YAW SENSING SYSTEM

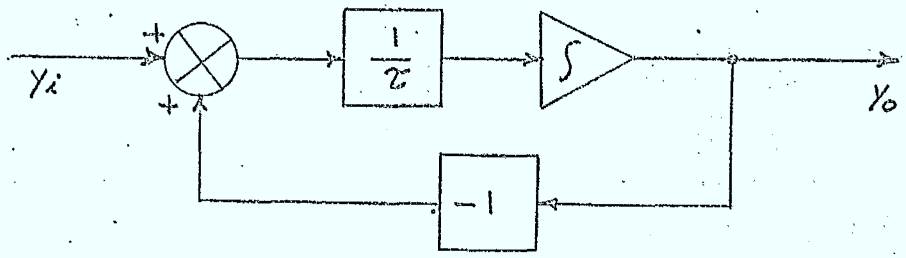

ANALOGUE BLOCK DIAGRAM

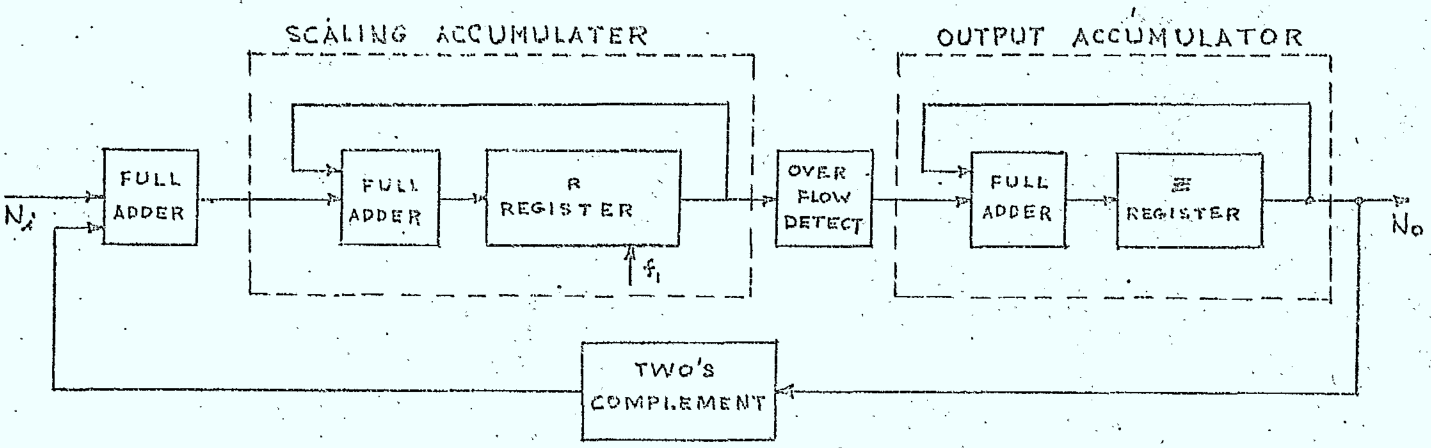

DDA BLOCK DIAGRAM

FIG. 8.3.2.1-1. FIRST ORDER LAG DDA IMPLEMENTATION

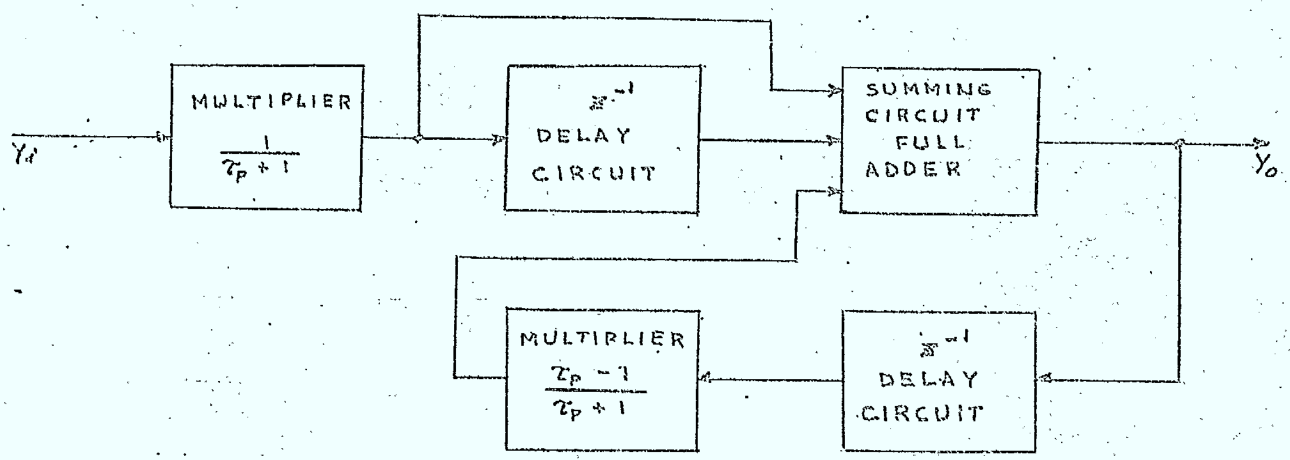

FIG. 8.3.2.2-1 FIRST ORDER LAG DIGITAL FILTER IMPLEMENTATION

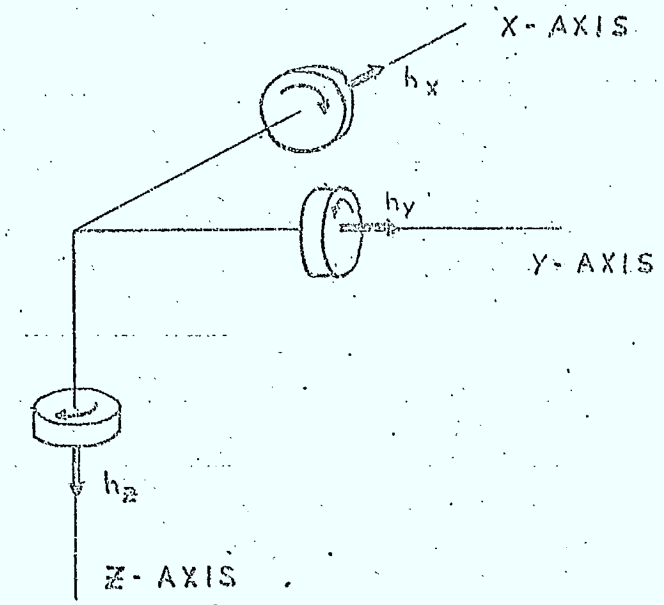

FIG. 5.1-1 BASIC THREE WHEEL CONFIGURATION

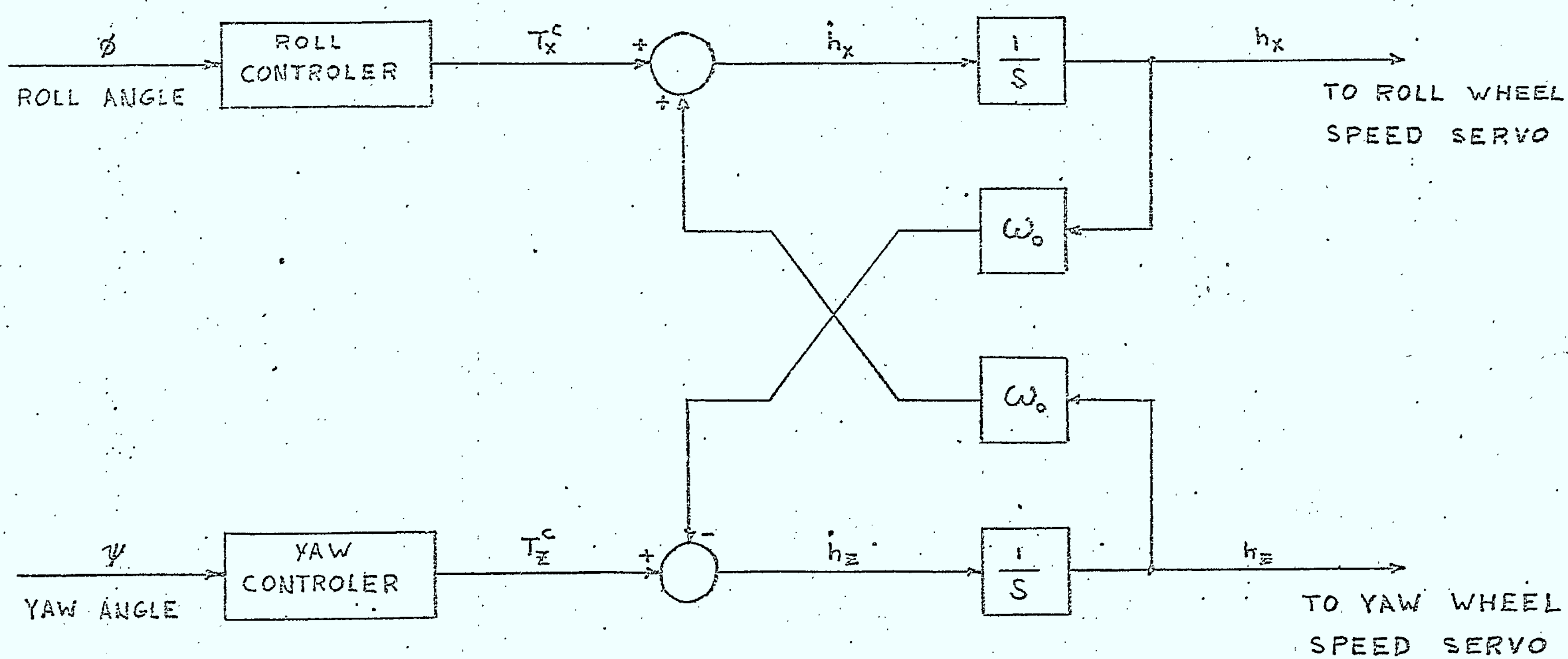

FIG 5.1-2 BLOCK DIAGRAM OF ROLL/YAW DECOUPLING

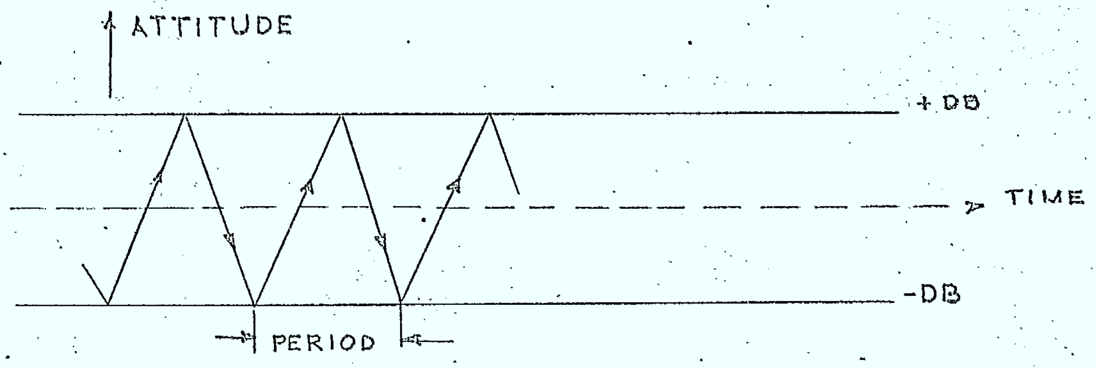

(a) TORQUE FREE LIMIT CYCLE MOTION

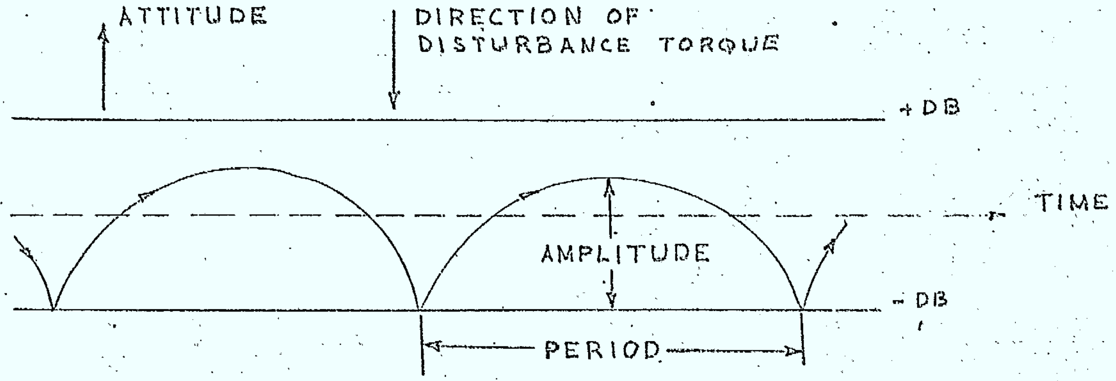

(b) SCALLOP MOTION WITH DISTURBANCE TORQUE

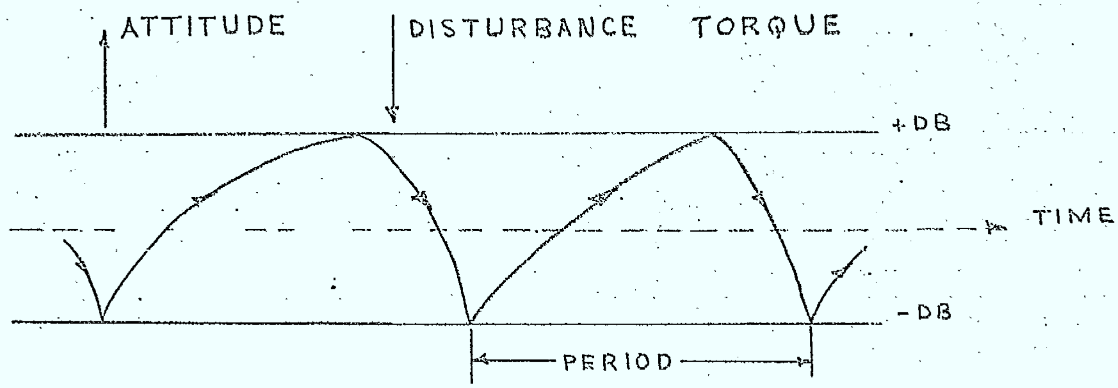

(c) LIMIT CYCLE MOTION WITH DISTURBANCE TORQUE

FIG. 6.1-1 ZERO MOMENTUM LIMIT CYCLES

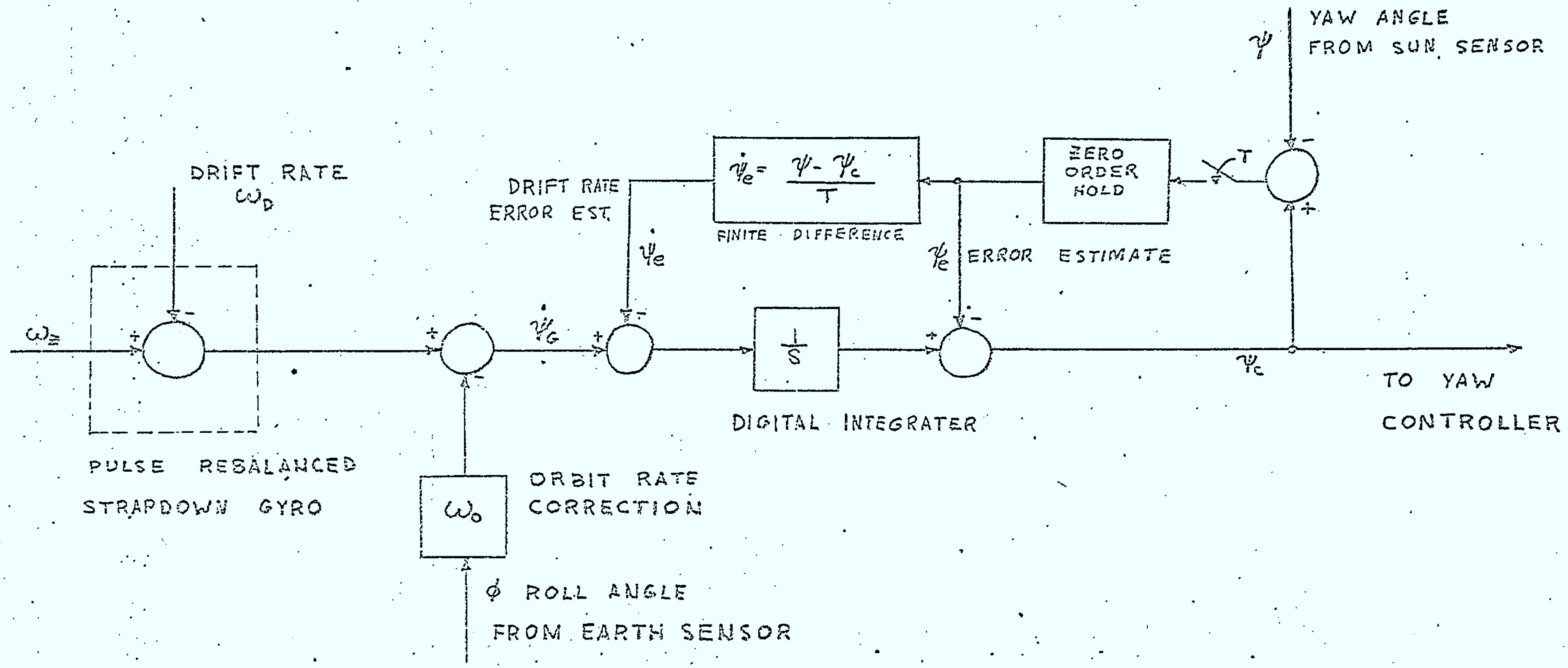

FIG 7.2.2-1 YAW GYRO PLUS SUN SENSOR YAW SENSING SYSTEM

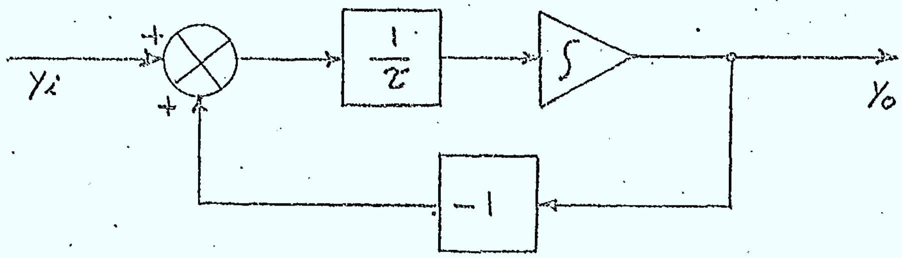

ANALOGUE BLOCK DIAGRAM

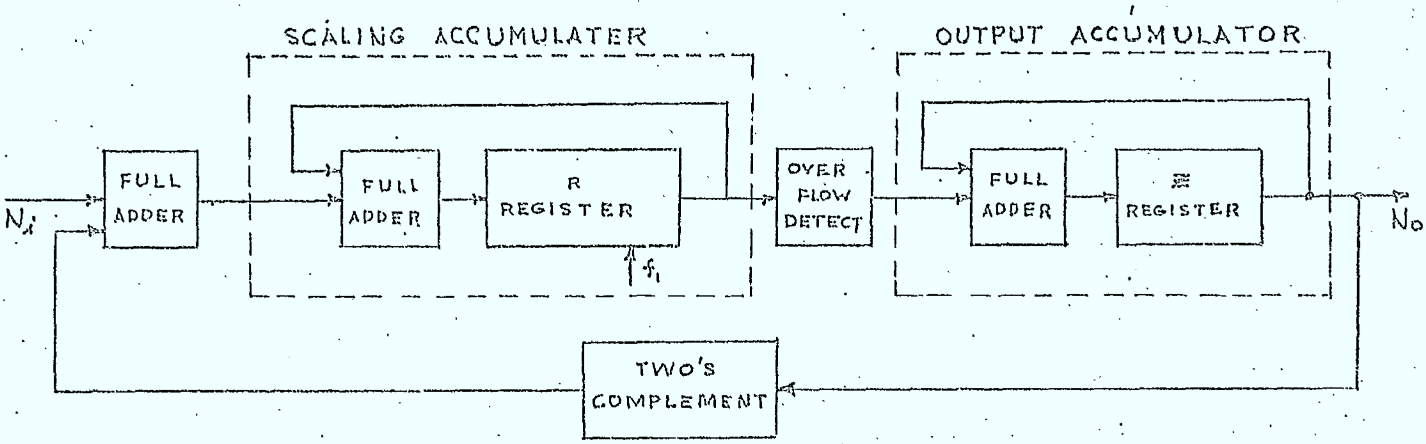

DDA BLOCK DIAGRAM

FIG. 8.3.2.1-1 FIRST ORDER LAG DDA IMPLEMENTATION

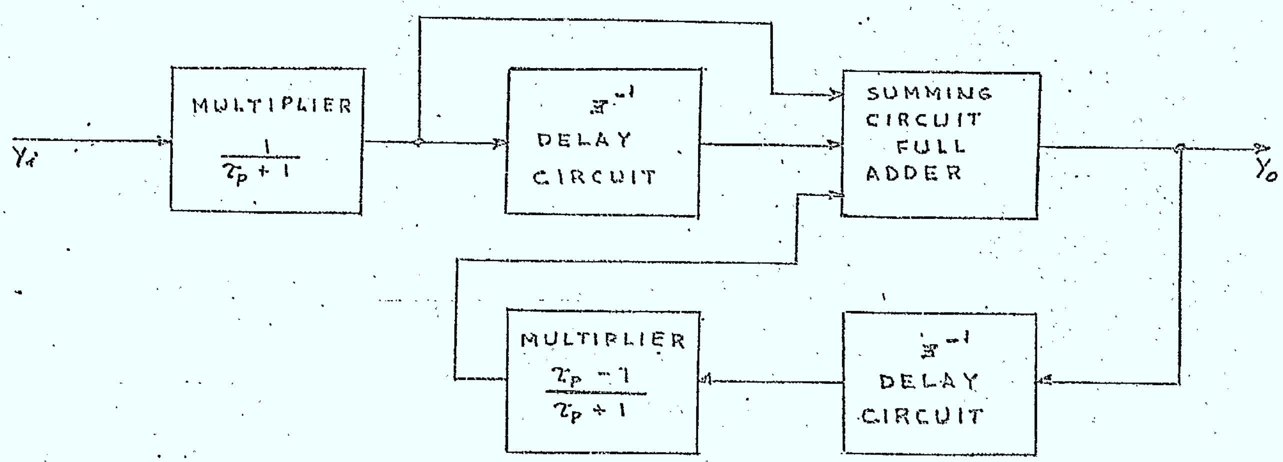

FIG. 8.3.2.2-1 FIRST ORDER LAG DIGITAL FILTER IMPLEMENTATION

CACC / CCAC
81841

STALEY, D.A.
Technology survey of attitude control techniques.

P
91
C655
S723
1975

DATE DUE
DATE DE RETOUR

LOWE-MARTIN No. 1137